Density Model for Bottlenose Dolphin (*Tursiops truncatus*) for the U.S. Gulf of Mexico: Supplementary Report

Duke University Marine Geospatial Ecology Lab*

Model Version 3.3 - 2015-10-07

Citation

When referencing our methodology or results generally, please cite our open-access article:

Roberts JJ, Best BD, Mannocci L, Fujioka E, Halpin PN, Palka DL, Garrison LP, Mullin KD, Cole TVN, Khan CB, McLellan WM, Pabst DA, Lockhart GG (2016) Habitat-based cetacean density models for the U.S. Atlantic and Gulf of Mexico. Scientific Reports 6: 22615. doi: 10.1038/srep22615

To reference this specific model or Supplementary Report, please cite:

Roberts JJ, Best BD, Mannocci L, Fujioka E, Halpin PN, Palka DL, Garrison LP, Mullin KD, Cole TVN, Khan CB, McLellan WM, Pabst DA, Lockhart GG (2015) Density Model for Bottlenose Dolphin (*Tursiops truncatus*) for the U.S. Gulf of Mexico Version 3.3, 2015-10-07, and Supplementary Report. Marine Geospatial Ecology Lab, Duke University, Durham, North Carolina.

Copyright and License

Revision History

Version	Date	Description of changes
1	2014-10-21	Initial version.
2	2014-11-13	Updated documentation. No changes to models.
3	2014-11-23	Removed CumVGPM180 predictor and refitted models. Updated documentation.
3.1	2015-02-02	Updated the documentation. No changes to the model.
3.2	2015-05-14	Added Ambiguous Sightings section of this report; it was mistakenly omitted. Updated calculation of CVs. Switched density rasters to logarithmic breaks. No changes to the model.
3.3	2015-10-07	Updated the documentation. No changes to the model.

*For questions, or to offer feedback about this model or report, please contact Jason Roberts (jason.roberts@duke.edu)

Survey Data

Survey	Period	Length (1000 km)	Hours	Sightings
SEFSC GOMEX92-96 Aerial Surveys	1992-1996	27	152	574
SEFSC Gulf of Mexico Shipboard Surveys, 2003-2009	2003-2009	19	1156	69
SEFSC GulfCet I Aerial Surveys	1992-1994	50	257	84
SEFSC GulfCet II Aerial Surveys	1996-1998	22	124	153
SEFSC GulfSCAT 2007 Aerial Surveys	2007-2007	18	95	330
SEFSC Oceanic CetShip Surveys	1992-2001	49	3102	267
SEFSC Shelf CetShip Surveys	1994-2001	10	707	372
Total		195	5593	1849

Table 2: Survey effort and sightings used in this model. Effort is tallied as the cumulative length of on-effort transects and hours the survey team was on effort. Sightings are the number of on-effort encounters of the modeled species for which a perpendicular sighting distance (PSD) was available. Off effort sightings and those without PSDs were omitted from the analysis.

Period	Length (1000 km)	Hours	Sightings
1992-2009	195	5592	1849
1998-2009	62	2679	733
% Lost	68	52	60

Table 3: Survey effort and on-effort sightings having perpendicular sighting distances. % Lost shows the percentage of effort or sightings lost by restricting the analysis to surveys performed in 1998 and later, the era in which remotely-sensed chlorophyll and derived productivity estimates are available. See Figure 1 for more information.

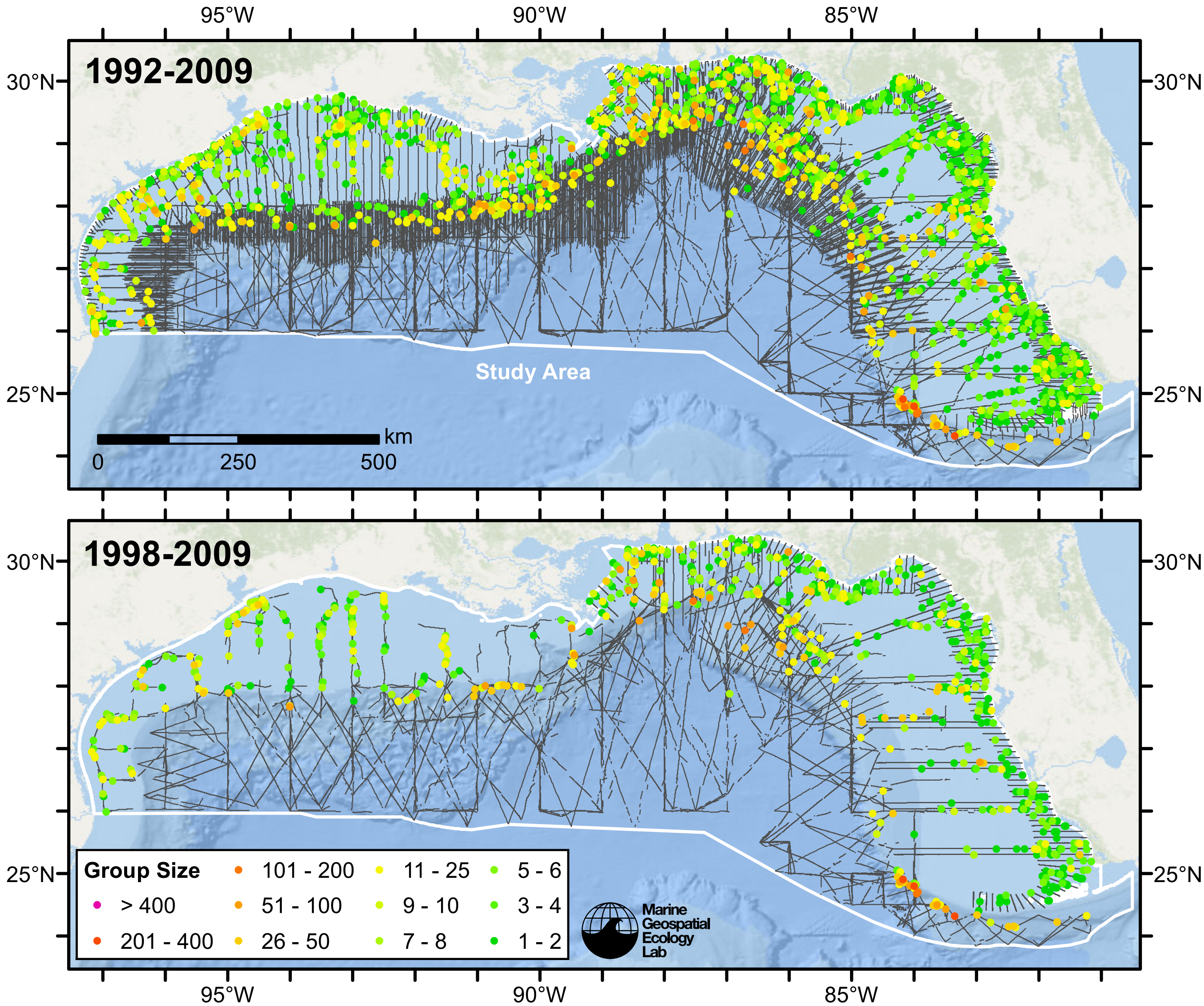

Figure 1: Bottlenose dolphin sightings and survey tracklines. The top map shows all surveys. The bottom map shows surveys performed in 1998 or later. the era in which remotely-sensed chlorophyll and derived productivity estimates are available. Models fitted to contemporaneous (day-of-sighting) estimates of those predictors only utilize these surveys. These maps illustrate the survey data lost in order to utilize those predictors. Models fitted to climatogical estimates of those predictors do not suffer this data loss.

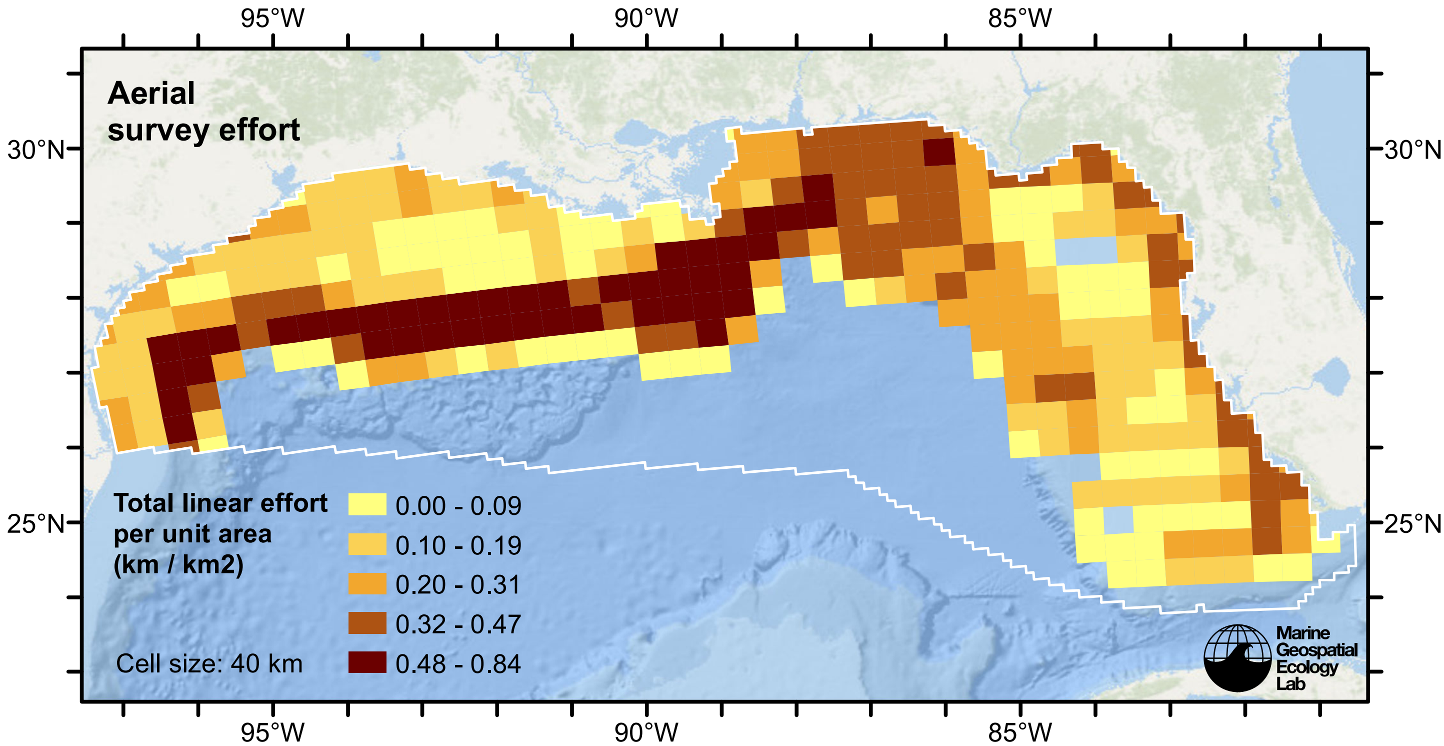

Figure 2: Aerial linear survey effort per unit area.

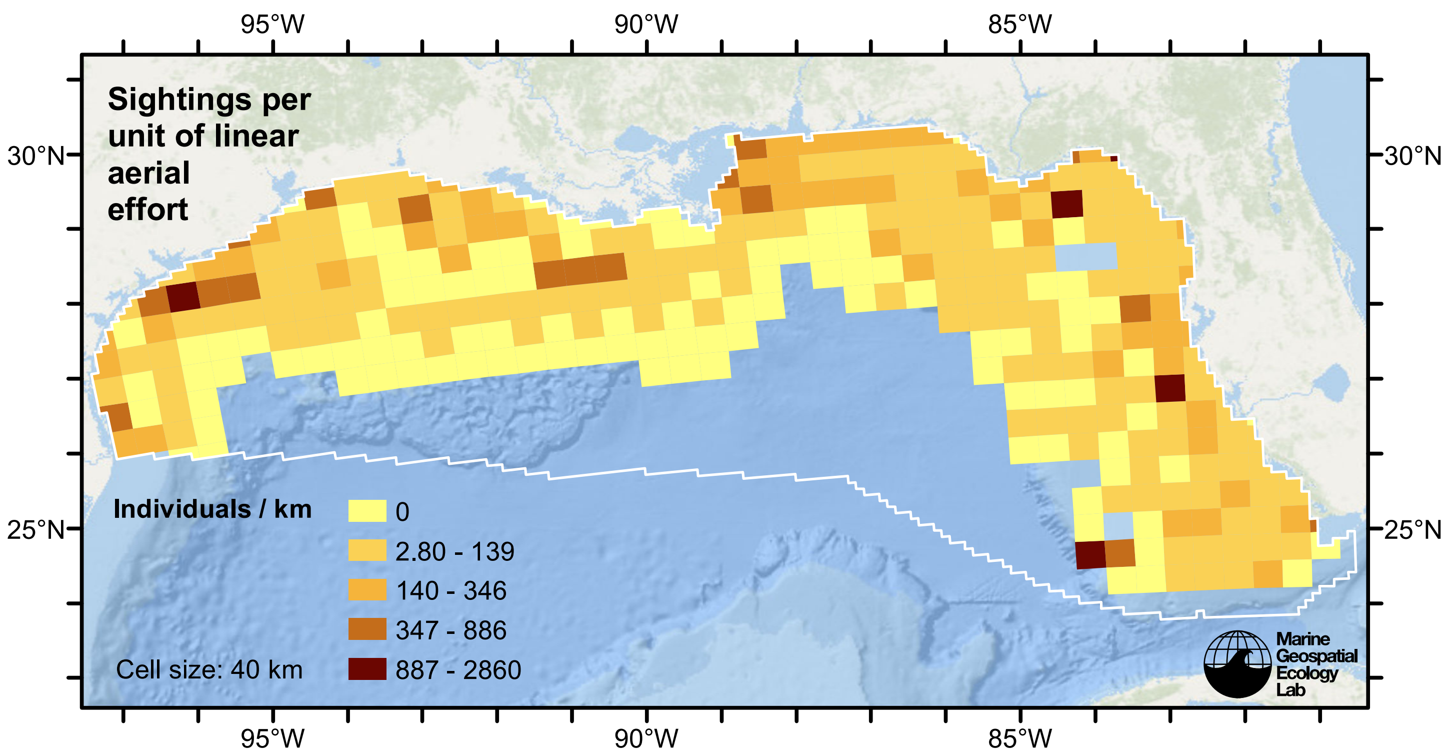

Figure 3: Bottlenose dolphin sightings per unit aerial linear survey effort.

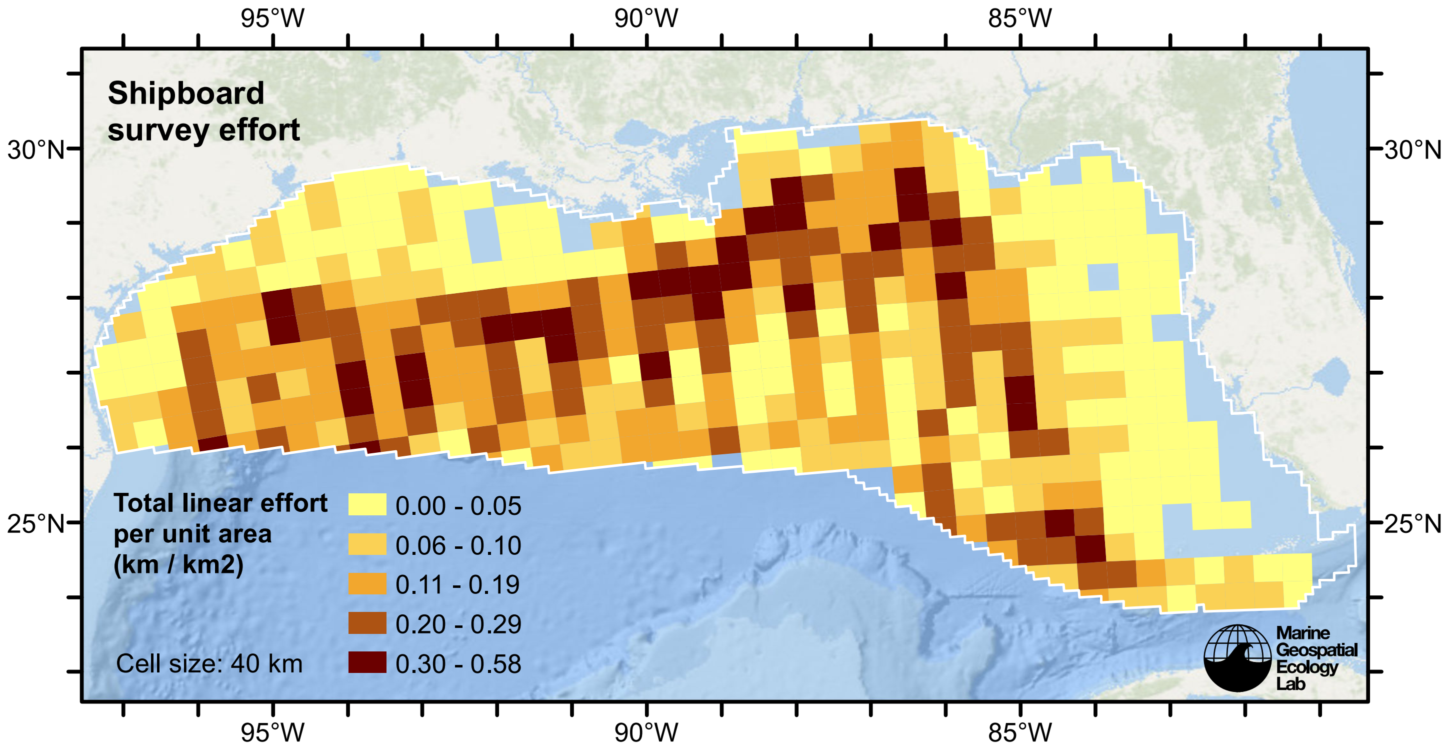

Figure 4: Shipboard linear survey effort per unit area.

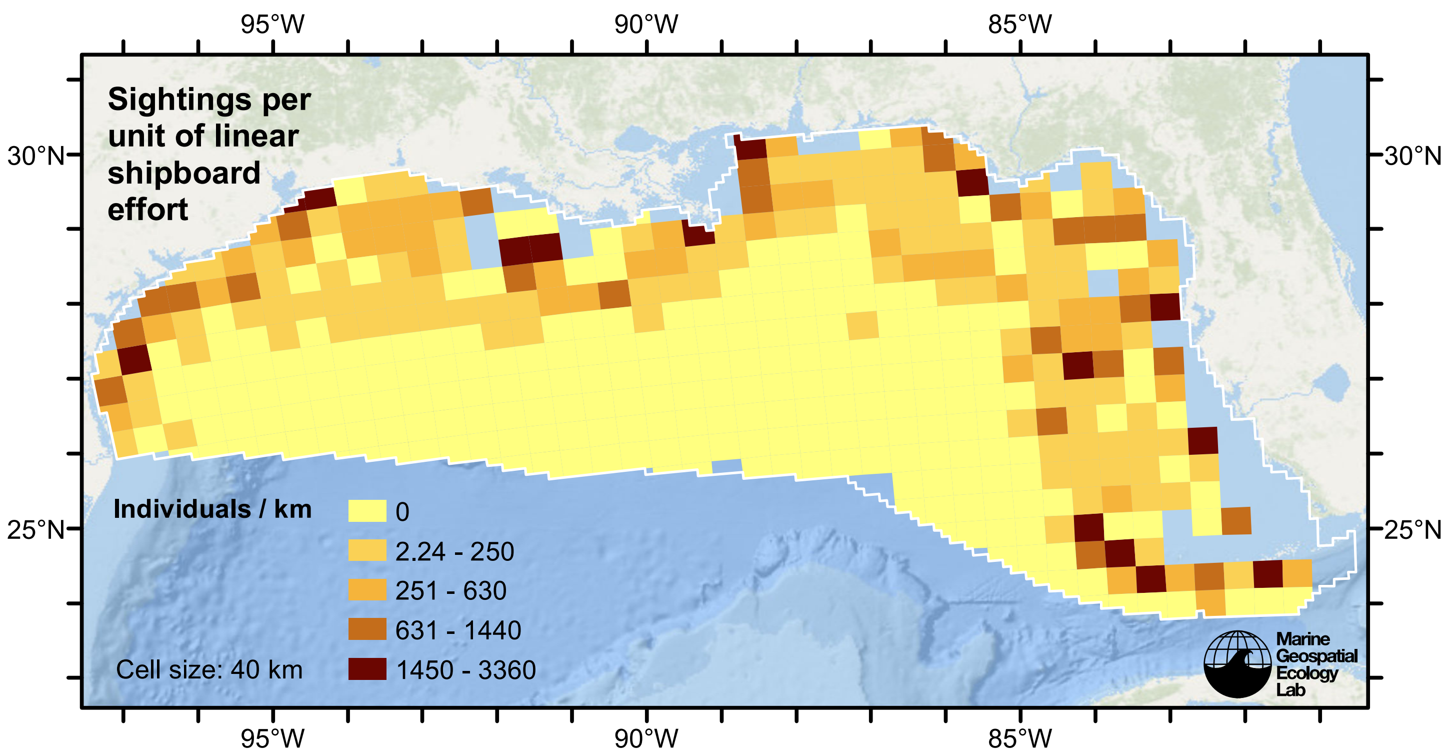

Figure 5: Bottlenose dolphin sightings per unit shipboard linear survey effort.

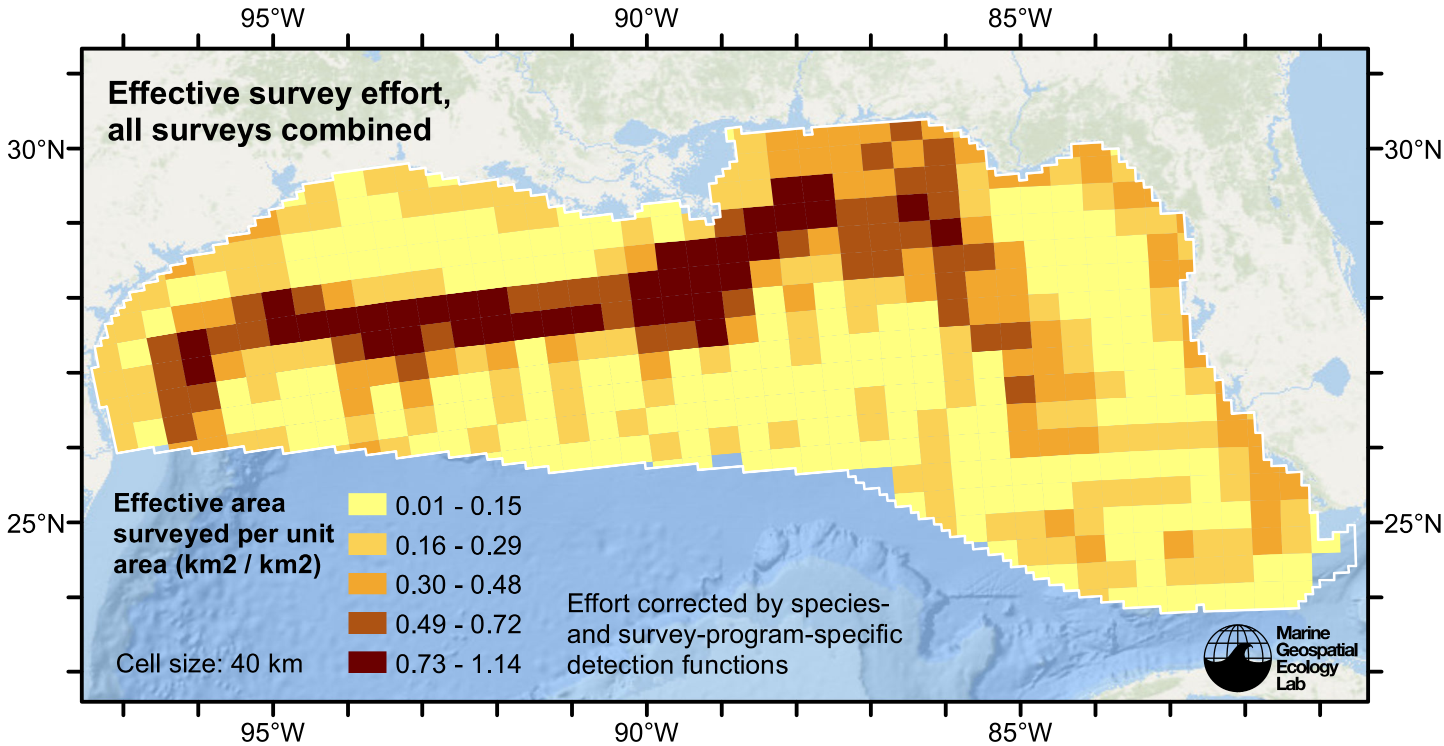

Figure 6: Effective survey effort per unit area, for all surveys combined. Here, effort is corrected by the species- and survey-program-specific detection functions used in fitting the density models.

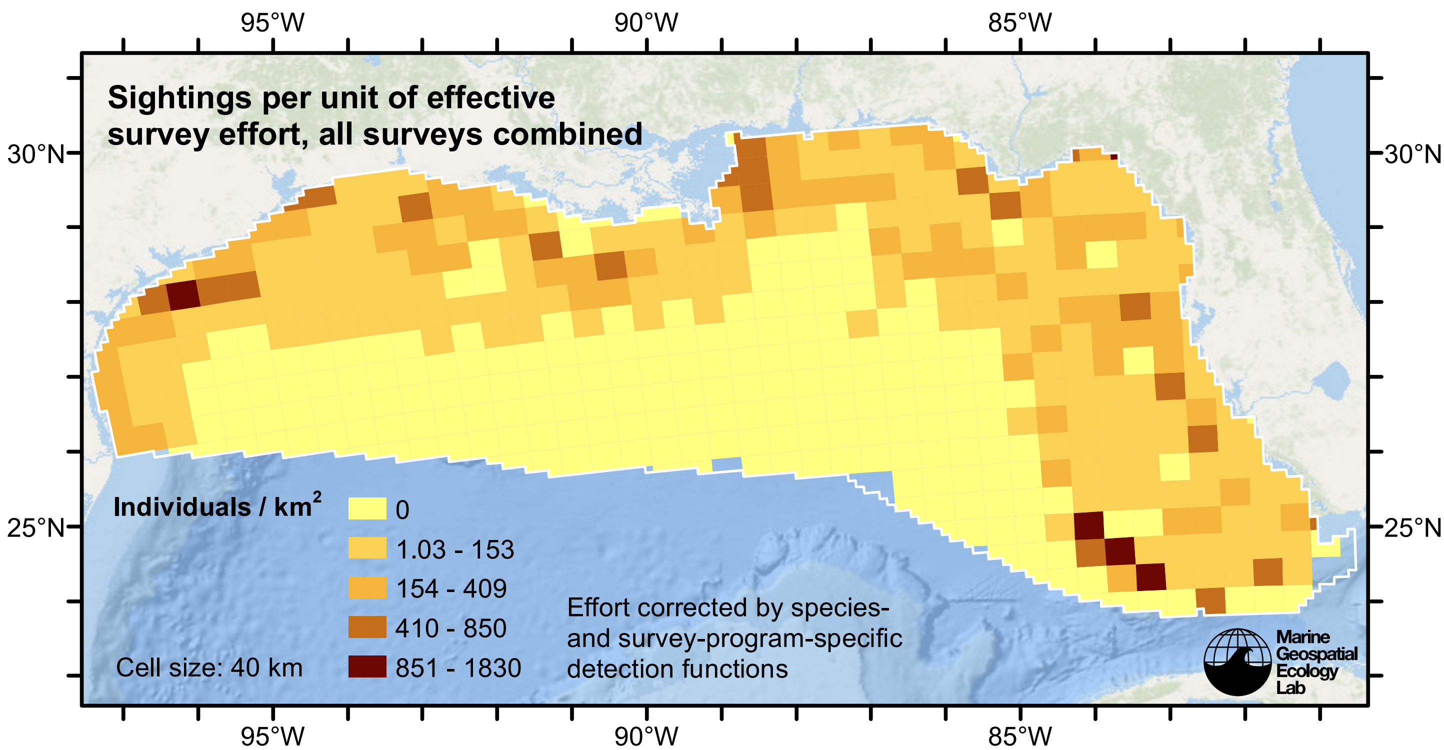

Figure 7: Bottlenose dolphin sightings per unit of effective survey effort, for all surveys combined. Here, effort is corrected by the species- and survey-program-specific detection functions used in fitting the density models.

Reclassification of Ambiguous Sightings

Observers occasionally experience difficulty identifying species, due to poor sighting conditions or phenotypic similarities between the possible choices. For example, observers may not always be able to distinguish fin whales from sei whales (Tim Cole, pers. comm.). When this happens, observers will report an ambiguous identification, such as “fin or sei whale”.

In our density models, we handled ambiguous identifications in three ways:

1. For sightings with very generic identifications such as “large whale”, we discarded the sightings. These sightings represented a clear minority when compared to those with definitive species identifications, but they are uncounted animals and our density models may therefore underestimate density to some degree.
2. For sightings of certain taxa in which a large majority of identifications were ambiguous (e.g. “Globicephala spp.”) rather than specific (e.g. “Globicephala melas” or “Globicephala macrorhynchus”), it was not tractable to model the individual species so we modeled the generic taxon instead.
3. For sightings that reported an ambiguous identification of two species (e.g. “fin or sei whale”) that are known to exhibit different habitat preferences or typically occur in different group sizes, and for which we had sufficient number of definitive sightings of both species, we fitted a predictive model that classified the ambiguous sightings into one species or the other.

This section describes how we utilized the third category of ambiguous sightings in the density models presented in this report.

For the predictive model, we used the cforest classifier (Hothorn et al. 2006), an elaboration of the classic random forest classifier (Breiman, 2001). First, we trained a binary classifier using the sightings that reported definitive species identifications (e.g. “fin whale” and “sei whale”). The training data included all on-effort sightings, not just those in the focal study area. We used the species ID as the response variable and oceanographic variables or group size as predictor variables, depending on the species. We used receiver operating characteristic (ROC) curve analysis to select a threshold for classifying the probabilistic predictions of species identifications made by the model into a binary result of one species or another; for the threshold, we selected the value that maximized the Youden index (see Perkins and Schisterman, 2006).

Then, for all sightings reporting the ambiguous identification, we reclassified the sighting as either one species or the other by processing the predictor values observed for that sighting through the fitted model. We then included the reclassified sightings in the detection functions and spatial models of density. The sightings reported elsewhere in this document incorporate both the definitive sightings and the reclassified sightings.

Reclassification of “Stenella frontalis/Tursiops truncatus” in the East Coast Region

Density Histograms

These plots show the per-species distribution of each predictor variable used in the reclassification model. When a variable exhibits a substantially different distribution for each species, it is a good candidate for classifying ambiguous sightings as one species or the other.

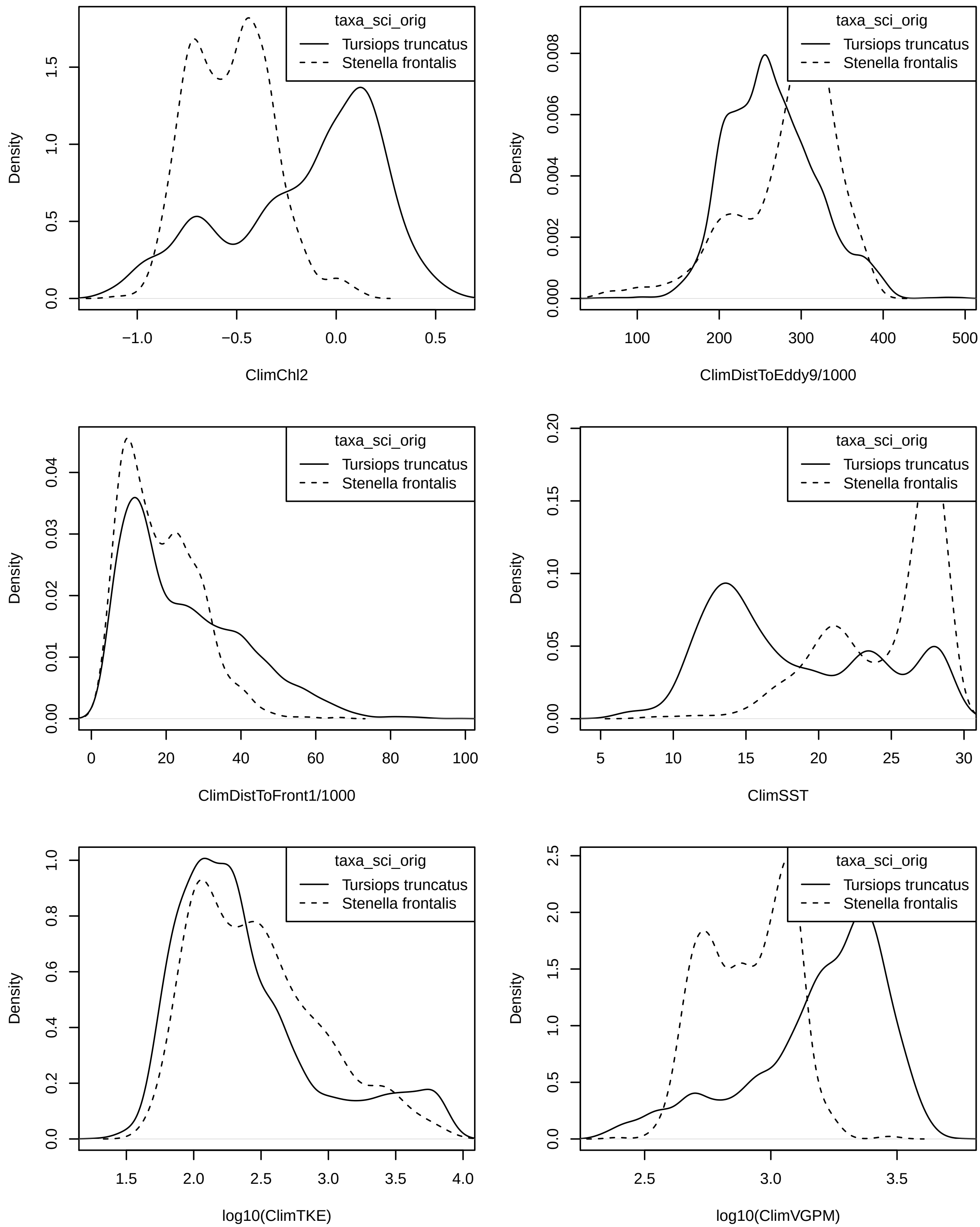
taxa_sci_orig
Tursiops truncatus
Stenella frontalis
Density
ClimChl2
ClimDistToEddy9/1000
ClimDistToFront1/1000
ClimSST
log10(ClimTKE)
log10(ClimVGPM)

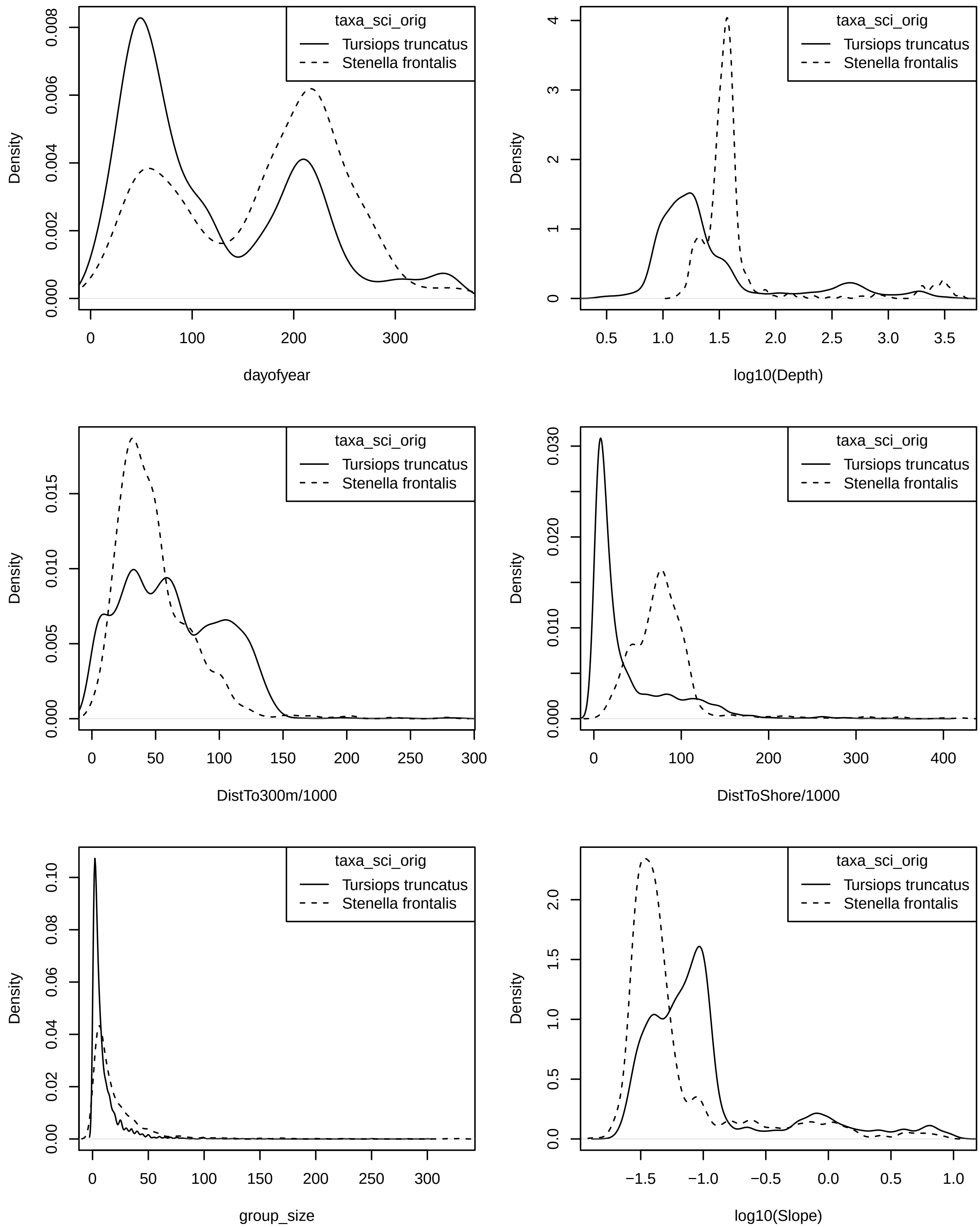

Statistical output

MODEL SUMMARY:

```
==============

     Random Forest using Conditional Inference Trees

Number of trees:  1000

Response:  factor(taxa_sci_orig)
Inputs:  group_size, dayofyear, Depth, Slope, DistToShore, DistTo300m, ClimSST, ClimDistToFront1, ClimChl2, Cl
Number of observations:  5265

Number of variables tried at each split: 5

Estimated predictor variable importance (conditional = FALSE):

                 Importance
ClimVGPM            0.02904
group_size          0.02416
ClimSST             0.02001
Slope               0.01773
DistToShore         0.01602
ClimChl2            0.01454
ClimTKE             0.01186
ClimDistToEddy9     0.01108
DistTo300m          0.00874
Depth               0.00641
ClimDistToFront1    0.00525
dayofyear           0.00353

MODEL PERFORMANCE SUMMARY:
==========================

Statistics calculated from the training data.

Area under the ROC curve (auc)           = 0.980
Mean cross-entropy (mxe)                 = 0.137
Precision-recall break-even point (prbe) = 0.966
Root-mean square error (rmse)            = 0.204

Cutoff selected by maximizing the Youden index = 0.838

Confusion matrix for that cutoff:

                              Actual Tursiops truncatus  Actual Stenella frontalis  Total
Predicted Tursiops truncatus                       4080                         47   4127
Predicted Stenella frontalis                        381                        757   1138
Total                                              4461                        804   5265

Model performance statistics for that cutoff:

Accuracy (acc)                                = 0.919
Error rate (err)                              = 0.081
Rate of positive predictions (rpp)            = 0.784
Rate of negative predictions (rnp)            = 0.216

True positive rate (tpr, or sensitivity)      = 0.915
False positive rate (fpr, or fallout)         = 0.058
True negative rate (tnr, or specificity)      = 0.942
False negative rate (fnr, or miss)            = 0.085
```

```
Positive prediction value (ppv, or precision) = 0.989
Negative prediction value (npv)               = 0.665
Prediction-conditioned fallout (pcfall)       = 0.011
Prediction-conditioned miss (pcmiss)          = 0.335

Matthews correlation coefficient (mcc)        = 0.748
Odds ratio (odds)                             = 172.478
SAR                                           = 0.701

Cohen's kappa (K)                             = 0.732
```

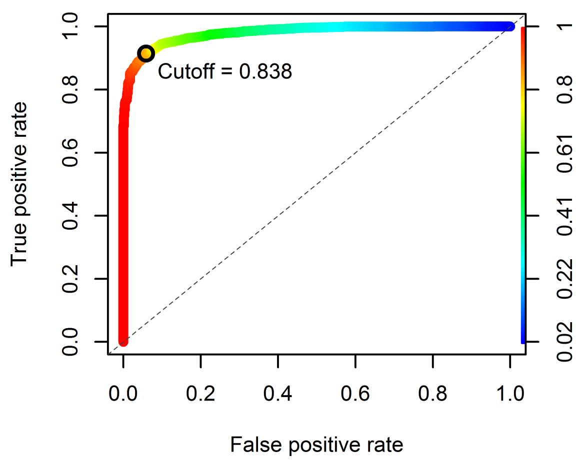

Figure 8: Receiver operating characteristic (ROC) curve illustrating the predictive performance of the model used to reclassify "Stenella frontalis/Tursiops truncatus" sightings into one species or the other.

Reclassifications Performed

Survey	Definitive T. truncatus Sightings	Definitive S. frontalis Sightings	Ambiguous Sightings	Reclassed to T. truncatus	Reclassed to S. frontalis
NEFSC Aerial Surveys	99	1	0	0	0
NEFSC North Atlantic Right Whale Sighting Survey	46	0	0	0	0
NEFSC Shipboard Surveys	184	16	0	0	0
NJDEP Aerial Surveys	92	0	0	0	0
NJDEP Shipboard Surveys	174	0	0	0	0
SEFSC Atlantic Shipboard Surveys	355	319	33	17	16
SEFSC Mid Atlantic Tursiops Aerial Surveys	693	101	20	11	9
SEFSC Southeast Cetacean Aerial Surveys	197	11	39	28	11
UNCW Cape Hatteras Navy Surveys	109	19	0	0	0
UNCW Early Marine Mammal Surveys	645	1	0	0	0
UNCW Jacksonville Navy Surveys	325	267	0	0	0

UNCW Onslow Navy Surveys	148	65	0	0	0
UNCW Right Whale Surveys	1847	5	0	0	0
Virginia Aquarium Aerial Surveys	67	0	0	0	0
Total	4981	805	92	56	36

Table 4: Counts of definitive sightings, ambiguous sightings, and what the ambiguous sightings were reclassified to. Note that this analysis was performed on all on-effort sightings, not just those in the focal study area. These counts may therefore be larger than those presented in the Survey Data section of this report, which are restricted to the focal study area.

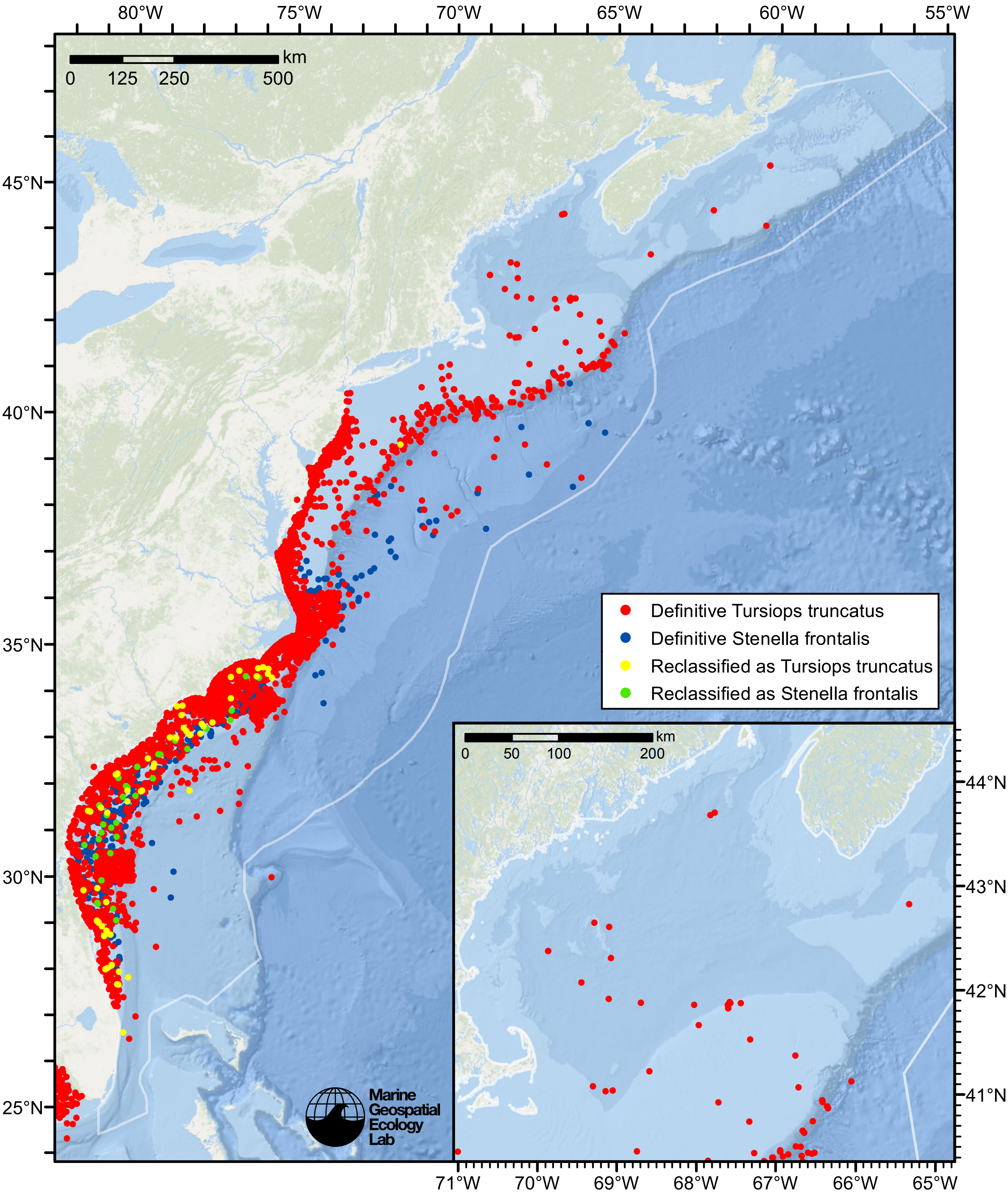

Figure 9: Definitive sightings used to train the model and ambiguous sightings reclassified by the model, by season.

Reclassification of “Stenella frontalis/Tursiops truncatus” in the Gulf of Mexico Region

Density Histograms

These plots show the per-species distribution of each predictor variable used in the reclassification model. When a variable exhibits a substantially different distribution for each species, it is a good candidate for classifying ambiguous sightings as one species or the other.

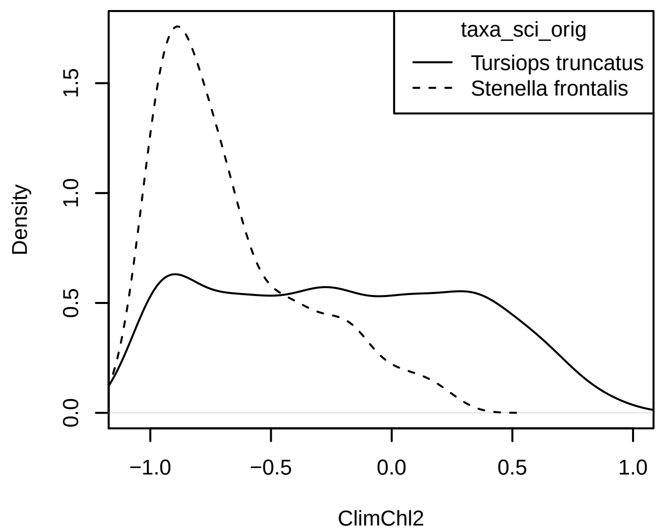

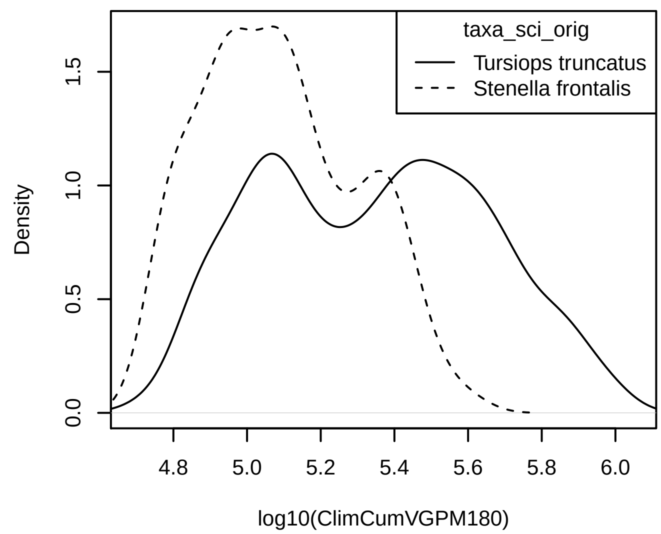

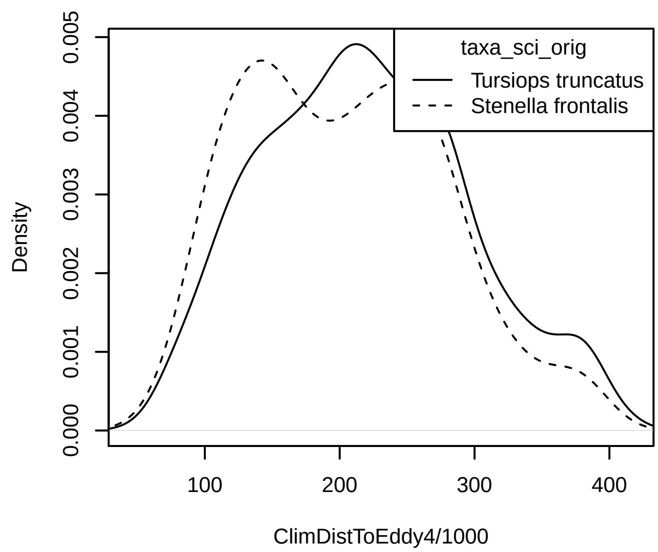

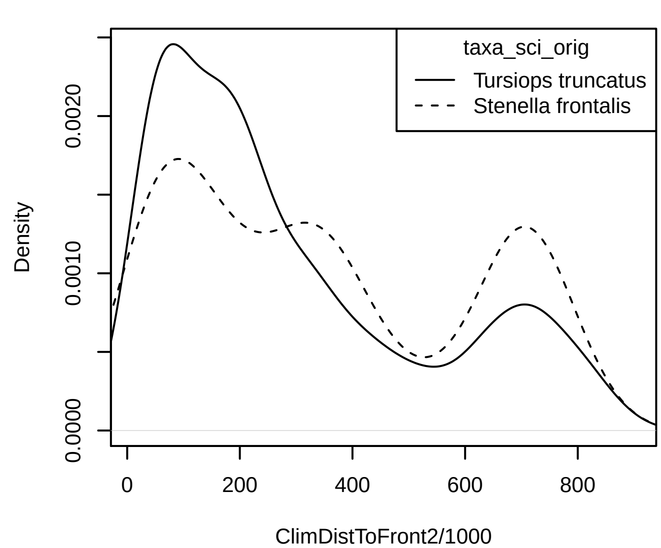

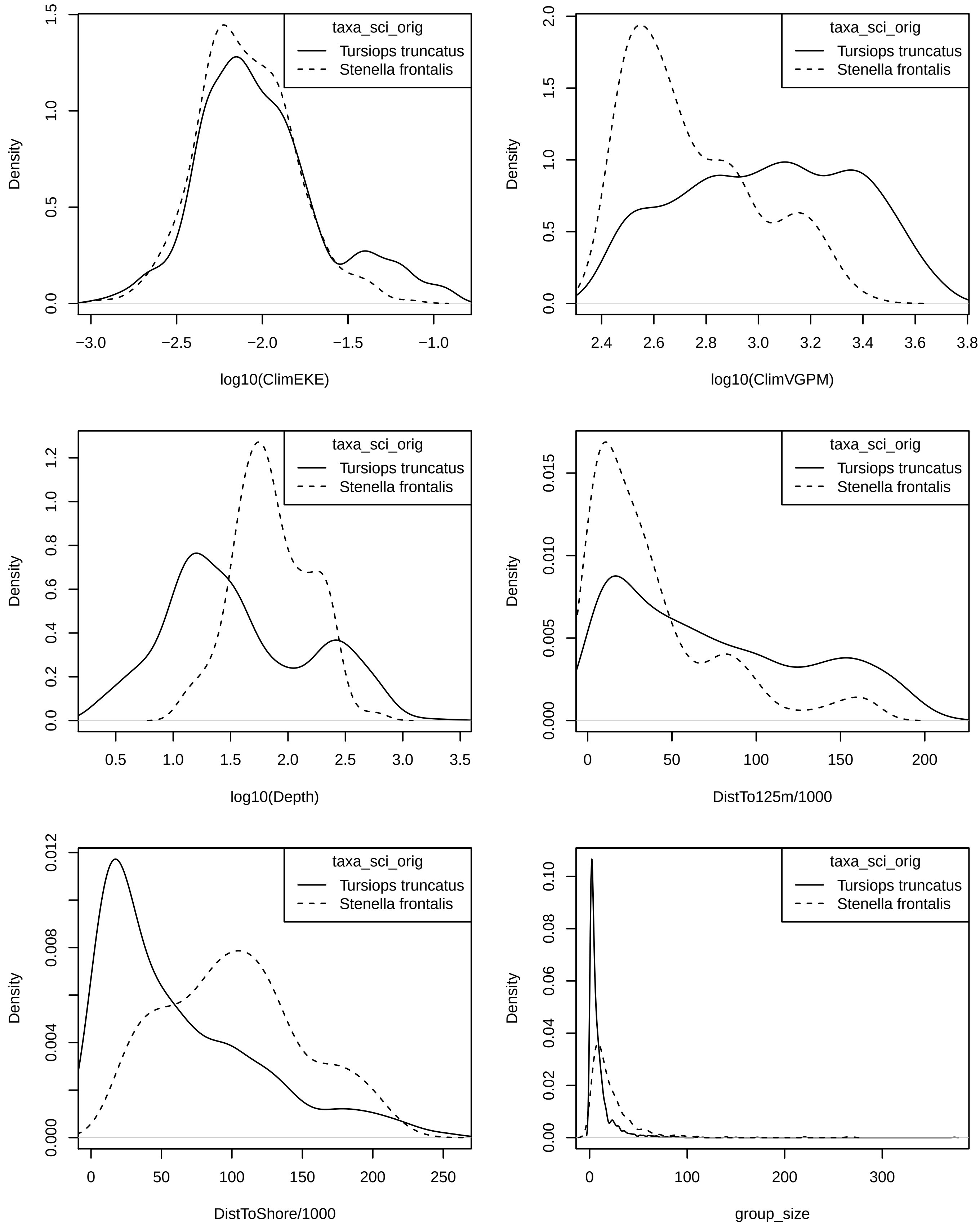
taxa_sci_orig
Tursiops truncatus
Stenella frontalis
Density
log10(ClimEKE)
log10(ClimVGPM)
log10(Depth)
DistTo125m/1000
DistToShore/1000
group_size

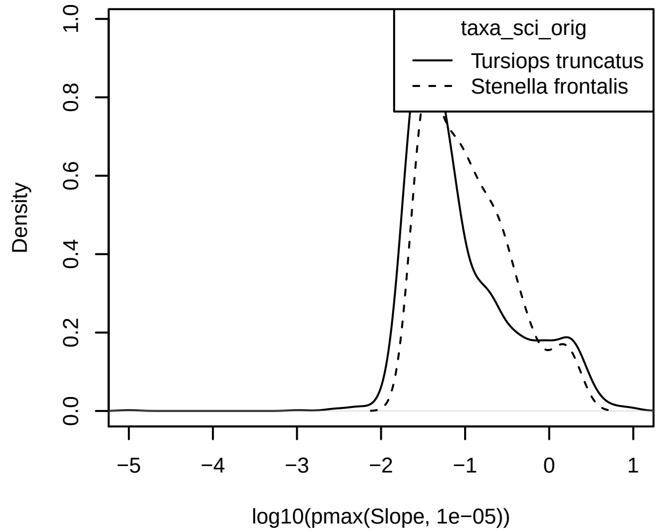

Statistical output

```
MODEL SUMMARY:
==============

     Random Forest using Conditional Inference Trees

Number of trees:  1000

Response:  factor(taxa_sci_orig)
Inputs:  group_size, ClimChl2, Depth, ClimVGPM, DistTo125m, ClimCumVGPM180, Slope, DistToShore, ClimEKE, ClimD
Number of observations:  1959

Number of variables tried at each split: 5

Estimated predictor variable importance (conditional = FALSE):

                 Importance
group_size          0.04073
ClimChl2            0.03281
Depth               0.02925
ClimVGPM            0.01694
ClimDistToEddy4     0.00976
ClimCumVGPM180      0.00798
Slope               0.00759
DistTo125m          0.00619
ClimEKE             0.00433
DistToShore         0.00361
ClimDistToFront2    0.00314

MODEL PERFORMANCE SUMMARY:
==========================

Statistics calculated from the training data.

Area under the ROC curve (auc)           = 0.961
Mean cross-entropy (mxe)                 = 0.193
Precision-recall break-even point (prbe) = 0.951
Root-mean square error (rmse)            = 0.247
```

```
Cutoff selected by maximizing the Youden index = 0.910

Confusion matrix for that cutoff:

                              Actual Tursiops truncatus  Actual Stenella frontalis  Total
Predicted Tursiops truncatus                       1388                         17   1405
Predicted Stenella frontalis                        256                        298    554
Total                                              1644                        315   1959

Model performance statistics for that cutoff:

Accuracy (acc)                                  = 0.861
Error rate (err)                                = 0.139
Rate of positive predictions (rpp)              = 0.717
Rate of negative predictions (rnp)              = 0.283

True positive rate (tpr, or sensitivity)        = 0.844
False positive rate (fpr, or fallout)           = 0.054
True negative rate (tnr, or specificity)        = 0.946
False negative rate (fnr, or miss)              = 0.156

Positive prediction value (ppv, or precision) = 0.988
Negative prediction value (npv)                 = 0.538
Prediction-conditioned fallout (pcfall)         = 0.012
Prediction-conditioned miss (pcmiss)            = 0.462

Matthews correlation coefficient (mcc)          = 0.645
Odds ratio (odds)                               = 95.042
SAR                                             = 0.690

Cohen's kappa (K)                               = 0.605
```

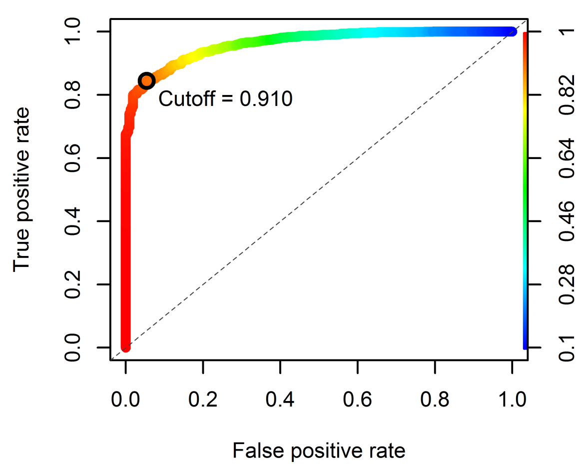

Figure 10: Receiver operating characteristic (ROC) curve illustrating the predictive performance of the model used to reclassify "Stenella frontalis/Tursiops truncatus" sightings into one species or the other.

Reclassifications Performed

Survey	Definitive T. truncatus Sightings	Definitive S. frontalis Sightings	Ambiguous Sightings	Reclassed to T. truncatus	Reclassed to S. frontalis
SEFSC Caribbean Shipboard Surveys	0	1	0	0	0
SEFSC GOMEX92-96 Aerial Surveys	608	21	19	15	4
SEFSC Gulf of Mexico Shipboard Surveys, 2003-2009	69	10	1	0	1
SEFSC GulfCet I Aerial Surveys	83	12	6	5	1
SEFSC GulfCet II Aerial Surveys	153	24	12	12	0
SEFSC GulfSCAT 2007 Aerial Surveys	327	15	5	5	0
SEFSC Oceanic CetShip Surveys	247	73	27	21	6
SEFSC Shelf CetShip Surveys	309	159	86	63	23
Total	1796	315	156	121	35

Table 5: Counts of definitive sightings, ambiguous sightings, and what the ambiguous sightings were reclassified to. Note that this analysis was performed on all on-effort sightings, not just those in the focal study area. These counts may therefore be larger than those presented in the Survey Data section of this report, which are restricted to the focal study area.

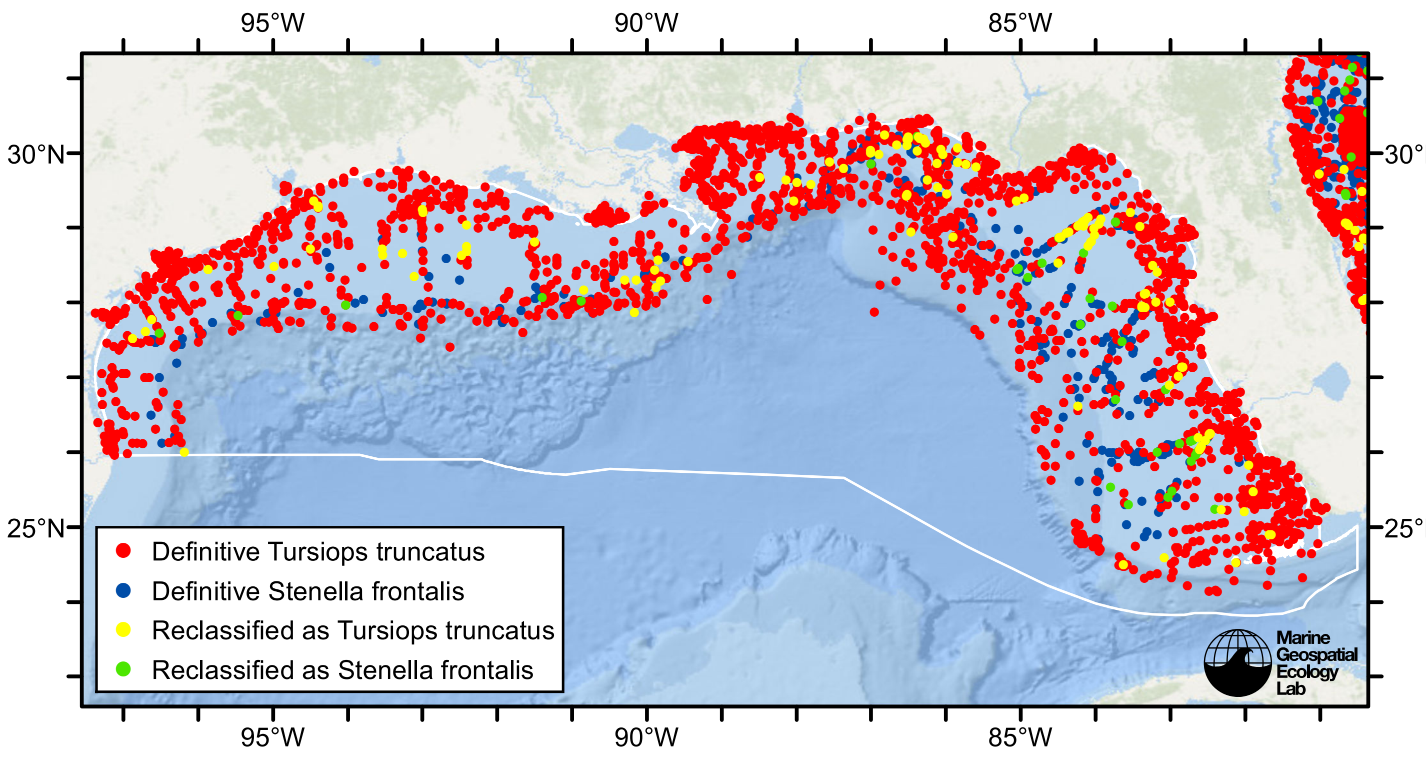

Figure 11: Definitive sightings used to train the model and ambiguous sightings reclassified by the model, by season.

Detection Functions

The detection hierarchy figures below show how sightings from multiple surveys were pooled to try to achieve Buckland et. al's (2001) recommendation that at least 60-80 sightings be used to fit a detection function. Leaf nodes, on the right, usually represent individual surveys, while the hierarchy to the left shows how they have been grouped according to how similar we believed the surveys were to each other in their detection performance.

At each node, the red or green number indicates the total number of sightings below that node in the hierarchy, and is colored green if 70 or more sightings were available, and red otherwise. If a grouping node has zero sightings–i.e. all of the surveys within it had zero sightings–it may be collapsed and shown as a leaf to save space.

Each histogram in the figure indicates a node where a detection function was fitted. The actual detection functions do not appear in this figure; they are presented in subsequent sections. The histogram shows the frequency of sightings by perpendicular sighting distance for all surveys contained by that node. Each survey (leaf node) recieves the detection function that is closest to it up the hierarchy. Thus, for common species, sufficient sightings may be available to fit detection functions deep in the hierarchy, with each function applying to only a few surveys, thereby allowing variability in detection performance between surveys to be addressed relatively finely. For rare species, so few sightings may be available that we have to pool many surveys together to try to meet Buckland's recommendation, and fit only a few coarse detection functions high in the hierarchy.

A blue Proxy Species tag indicates that so few sightings were available that, rather than ascend higher in the hierarchy to a point that we would pool grossly-incompatible surveys together, (e.g. shipboard surveys that used big-eye binoculars with those that used only naked eyes) we pooled sightings of similar species together instead. The list of species pooled is given in following sections.

Shipboard Surveys

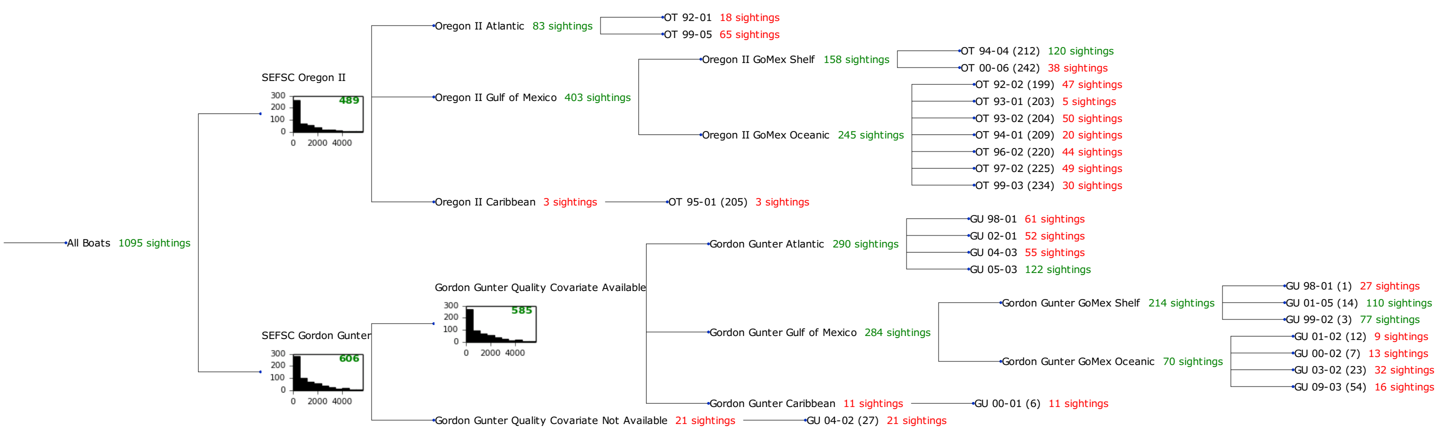

Figure 12: Detection hierarchy for shipboard surveys

SEFSC Oregon II

The sightings were right truncated at 4000m.

Covariate	Description
beaufort	Beaufort sea state.
quality	Survey-specific index of the quality of observation conditions, utilizing relevant factors other than Beaufort sea state (see methods).
size	Estimated size (number of individuals) of the sighted group.

Table 6: Covariates tested in candidate "multi-covariate distance sampling" (MCDS) detection functions.

Key	Adjustment	Order	Covariates	Succeeded	Δ AIC	Mean ESHW (m)
hr			beaufort, quality, size	Yes	0.00	423
hr			beaufort, size	Yes	1.81	410
hr			beaufort, quality	Yes	13.83	359
hr			beaufort	Yes	16.49	344
hr			quality, size	Yes	21.53	308
hr			size	Yes	26.51	276
hr			quality	Yes	34.43	265
hr				Yes	42.58	228
hr	poly	4		Yes	44.07	235
hn	cos	3		Yes	211.33	1112
hn	cos	2		Yes	220.06	1266
hn			beaufort, quality, size	Yes	252.47	1626
hn			beaufort, size	Yes	254.51	1631
hn			quality, size	Yes	264.40	1634
hn			size	Yes	268.82	1637
hn			beaufort, quality	Yes	272.47	1637
hn			beaufort	Yes	277.23	1641
hn			quality	Yes	280.46	1644
hn				Yes	287.10	1647
hn	herm	4		Yes	287.82	1643
hr	poly	2		No		

Table 7: Candidate detection functions for SEFSC Oregon II. The first one listed was selected for the density model.

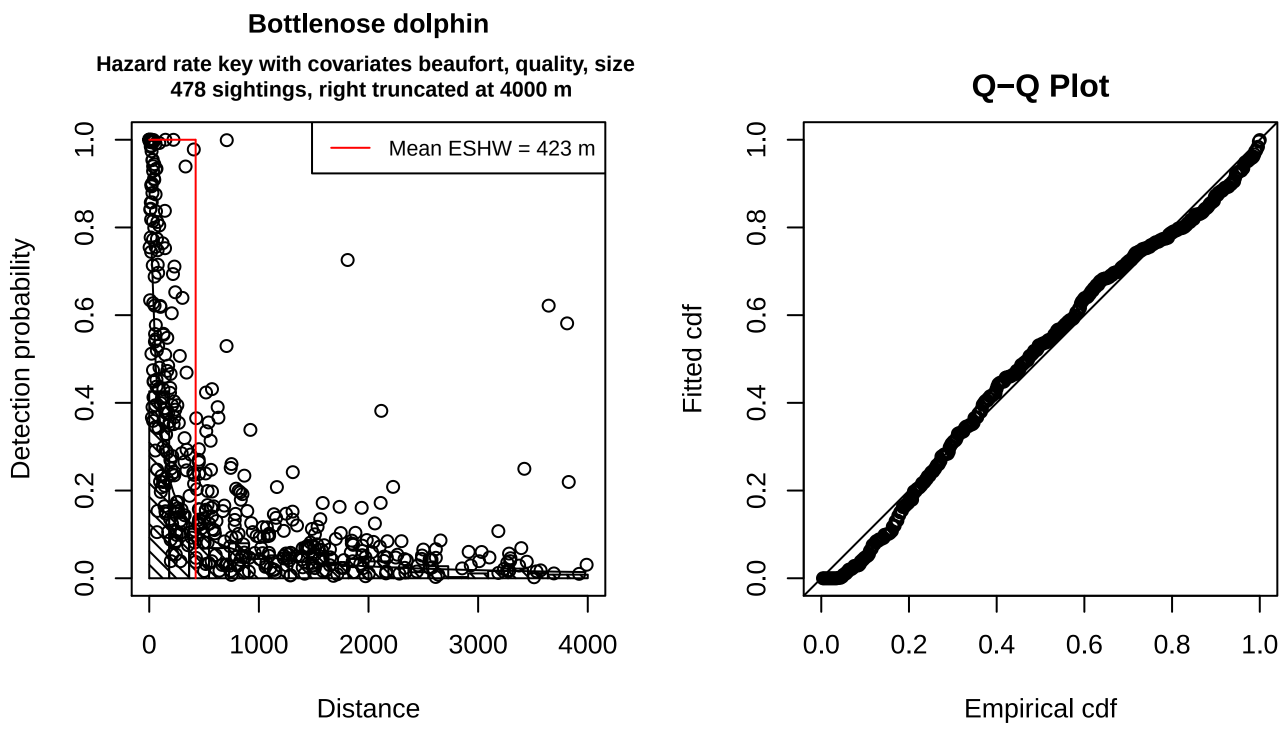

Figure 13: Detection function for SEFSC Oregon II that was selected for the density model

Statistical output for this detection function:

```
Summary for ds object
Number of observations :  478
Distance range         :  0  -  4000
AIC                    :  7262.16

Detection function:
 Hazard-rate key function

Detection function parameters
Scale Coefficients:
              estimate        se
(Intercept)  5.5026964 0.4212720
beaufort    -0.5435437 0.1033765
quality     -0.2515070 0.1252423
size         0.6785389 0.1649255

Shape parameters:
            estimate         se
(Intercept)        0 0.05338445

                       Estimate           SE        CV
Average p           5.977685e-02 7.429875e-03 0.1242935
N in covered region 7.996407e+03 1.058194e+03 0.1323337
```

Additional diagnostic plots:

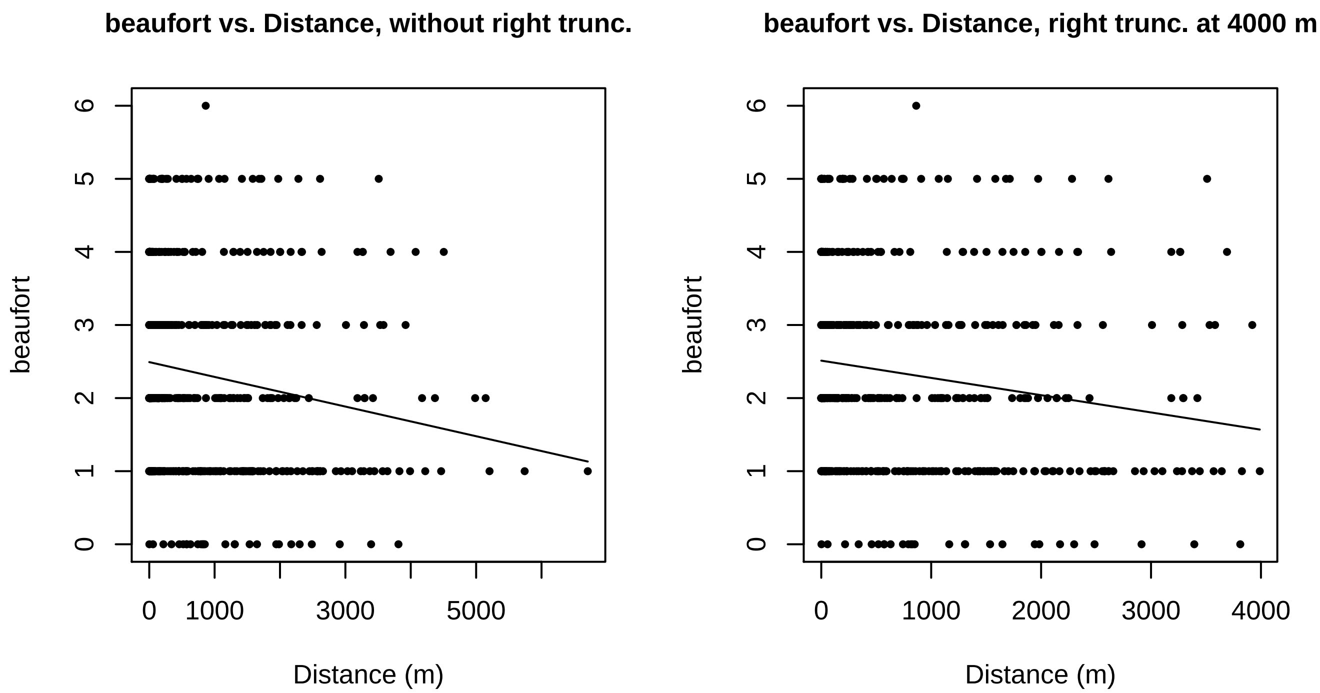

Figure 14: Scatterplots showing the relationship between Beaufort sea state and perpendicular sighting distance, for all sightings (left) and only those not right truncated (right). The line is a simple linear regression.

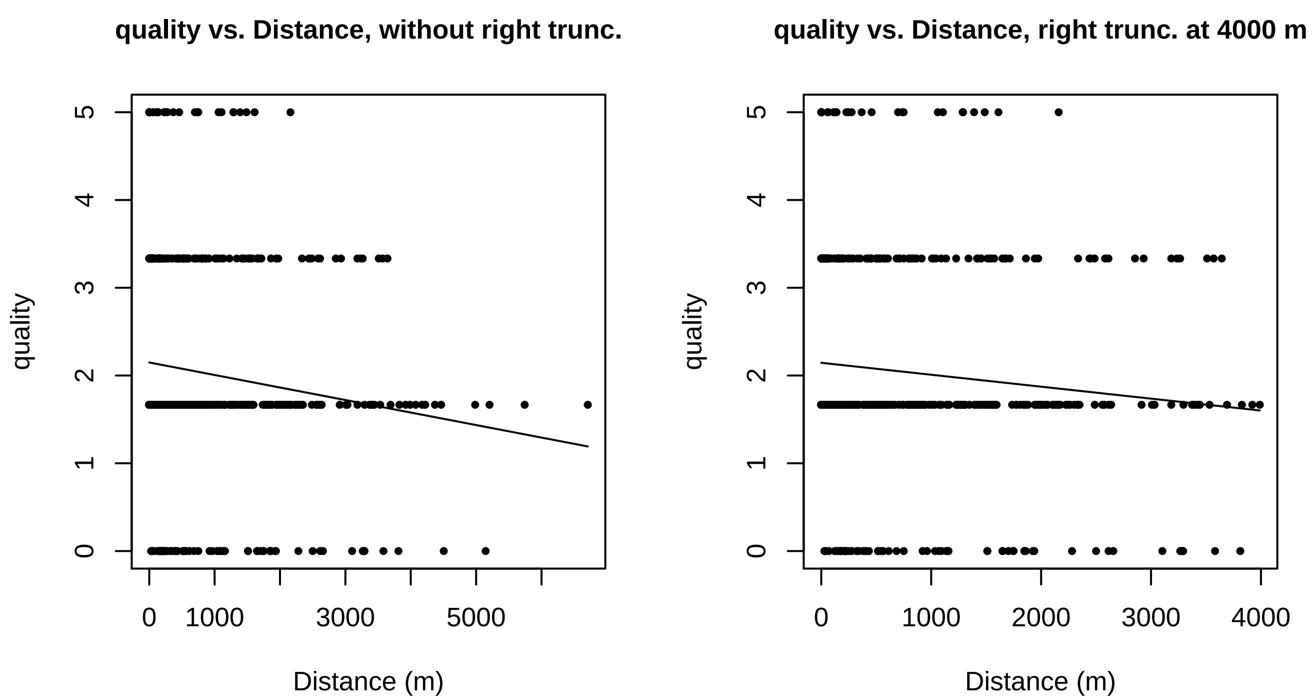

Figure 15: Scatterplots showing the relationship between the survey-specific index of the quality of observation conditions and perpendicular sighting distance, for all sightings (left) and only those not right truncated (right). Low values of the quality index correspond to better observation conditions. The line is a simple linear regression.

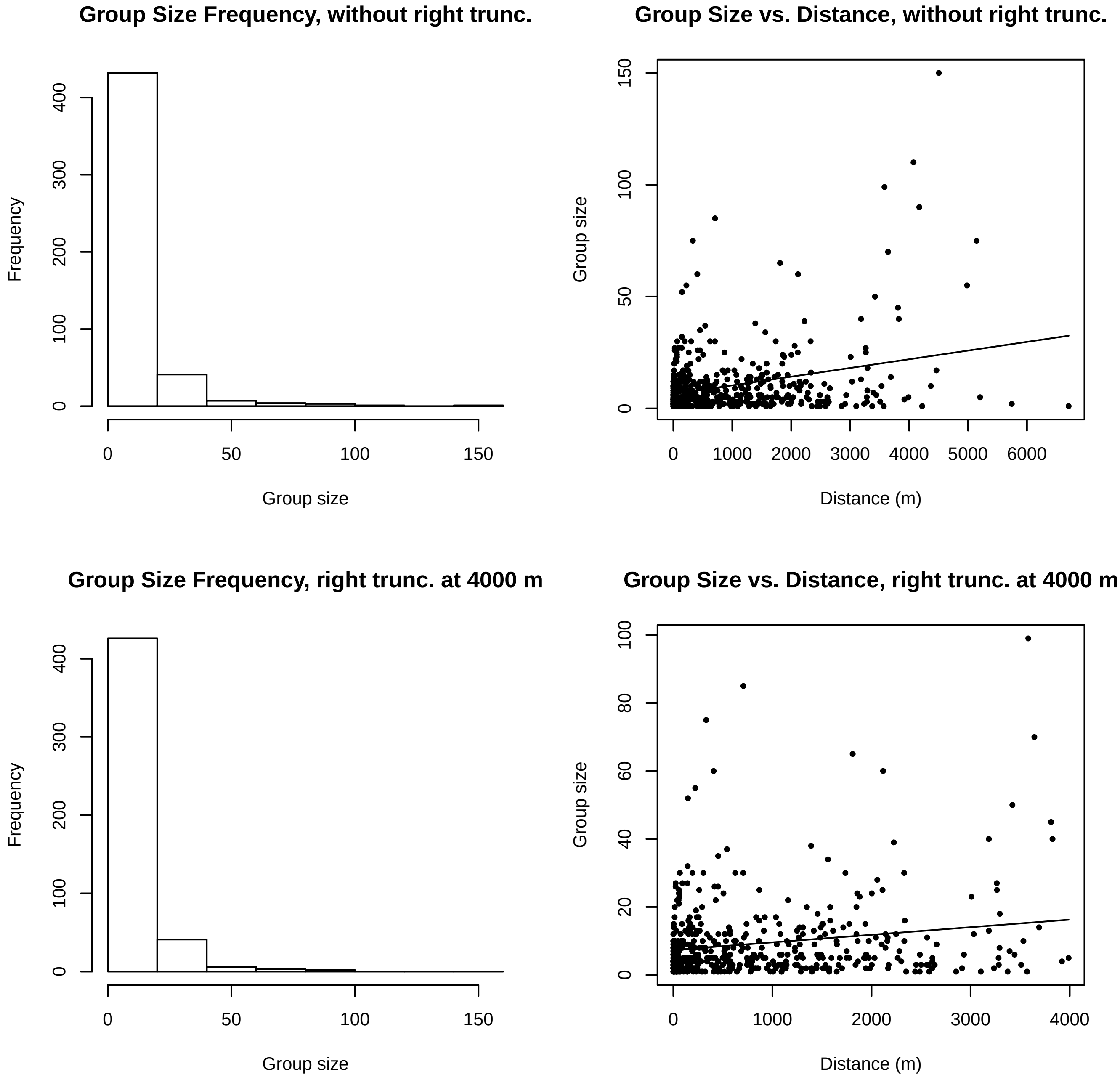

Figure 16: Histograms showing group size frequency and scatterplots showing the relationship between group size and perpendicular sighting distance, for all sightings (top row) and only those not right truncated (bottom row). In the scatterplot, the line is a simple linear regression.

SEFSC Gordon Gunter

The sightings were right truncated at 5000m.

Covariate	Description
beaufort	Beaufort sea state.
size	Estimated size (number of individuals) of the sighted group.

Table 8: Covariates tested in candidate “multi-covariate distance sampling” (MCDS) detection functions.

Key	Adjustment	Order	Covariates	Succeeded	Δ AIC	Mean ESHW (m)
hr			beaufort, size	Yes	0.00	1001
hr			beaufort	Yes	28.50	782
hr			size	Yes	66.30	673
hr	poly	2		Yes	92.72	501
hr				Yes	95.04	453
hn			beaufort, size	Yes	193.73	2018
hn	cos	3		Yes	210.72	1406
hn	cos	2		Yes	212.55	1574
hn			beaufort	Yes	233.58	1987
hn			size	Yes	251.49	2040
hn				Yes	279.81	1998
hn	herm	4		Yes	280.42	1995
hr	poly	4		No		

Table 9: Candidate detection functions for SEFSC Gordon Gunter. The first one listed was selected for the density model.

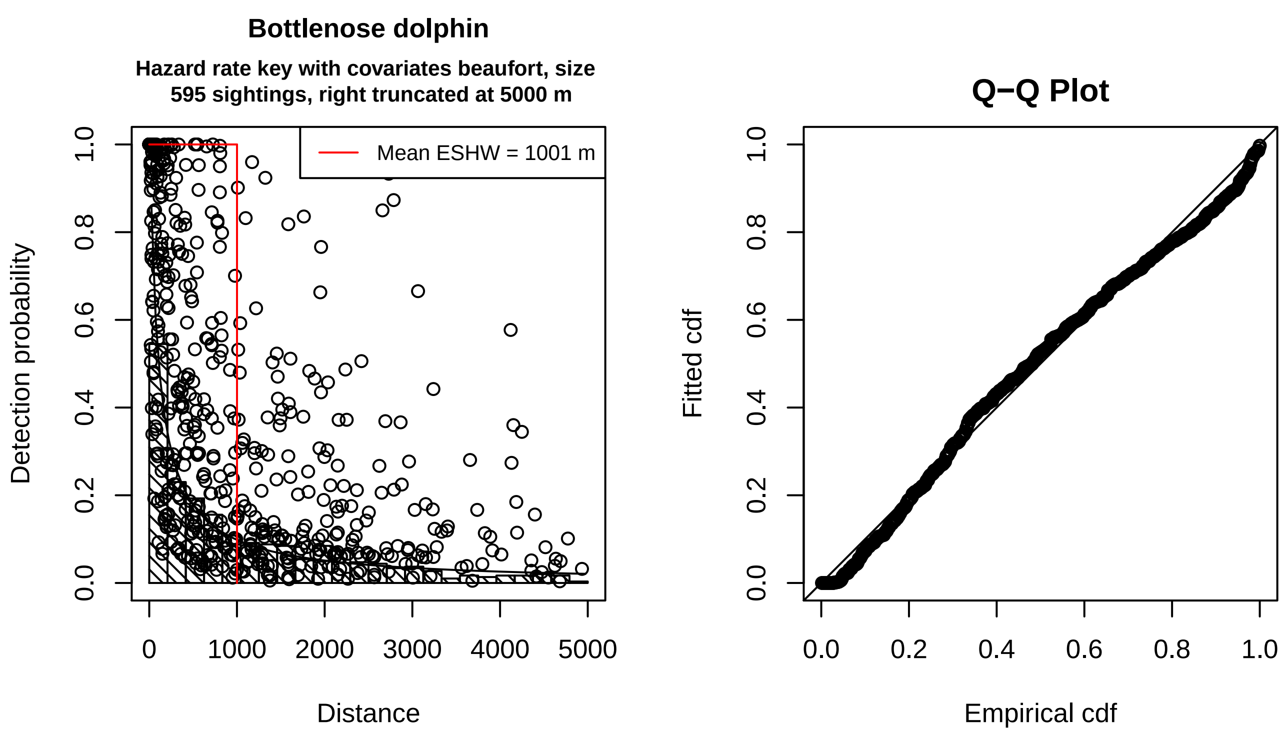

Figure 17: Detection function for SEFSC Gordon Gunter that was selected for the density model

Statistical output for this detection function:

```
Summary for ds object
```

```
Number of observations :  595
Distance range         :  0  -  5000
AIC                    :  9350.17

Detection function:
 Hazard-rate key function

Detection function parameters
Scale Coefficients:
              estimate        se
(Intercept)  6.9645860 0.2791044
beaufort    -0.8765275 0.0974669
size         1.2832927 0.2311812

Shape parameters:
             estimate         se
(Intercept) 0.1320332 0.05640665

                        Estimate           SE        CV
Average p              0.0839147   0.01106363 0.1318437
N in covered region 7090.5335680 980.38707905 0.1382670
```

Additional diagnostic plots:

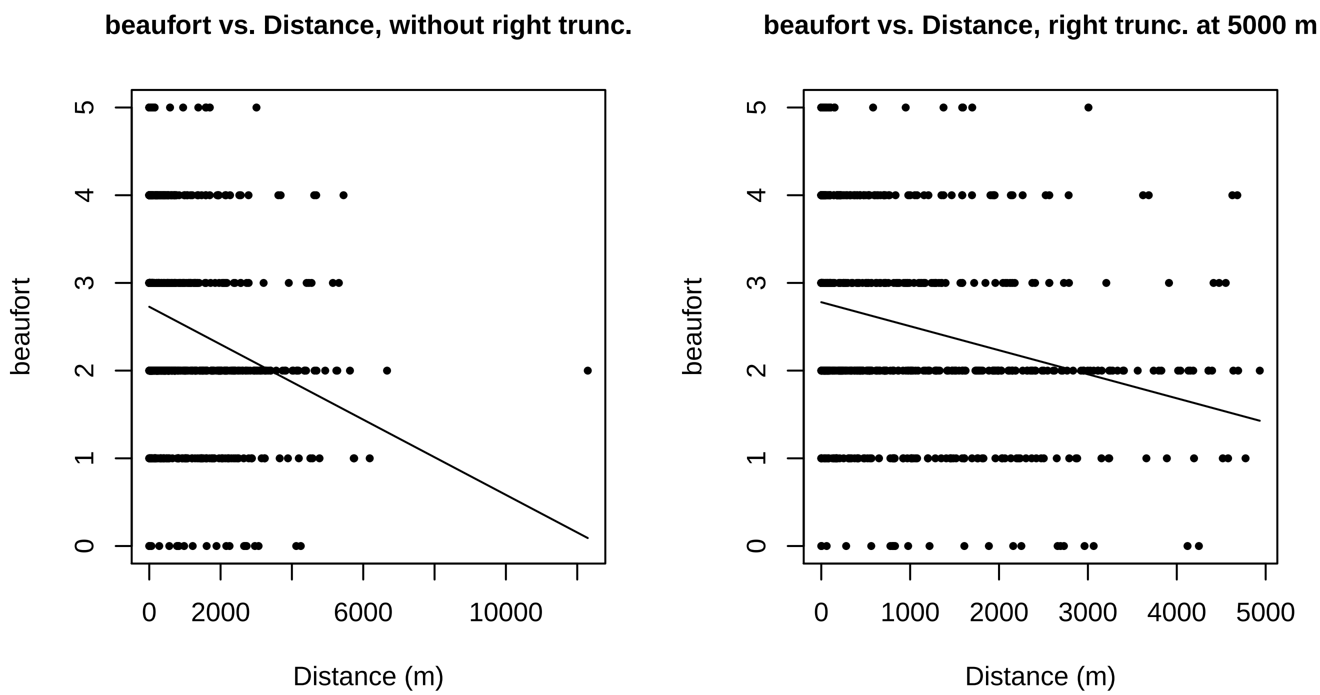

Figure 18: Scatterplots showing the relationship between Beaufort sea state and perpendicular sighting distance, for all sightings (left) and only those not right truncated (right). The line is a simple linear regression.

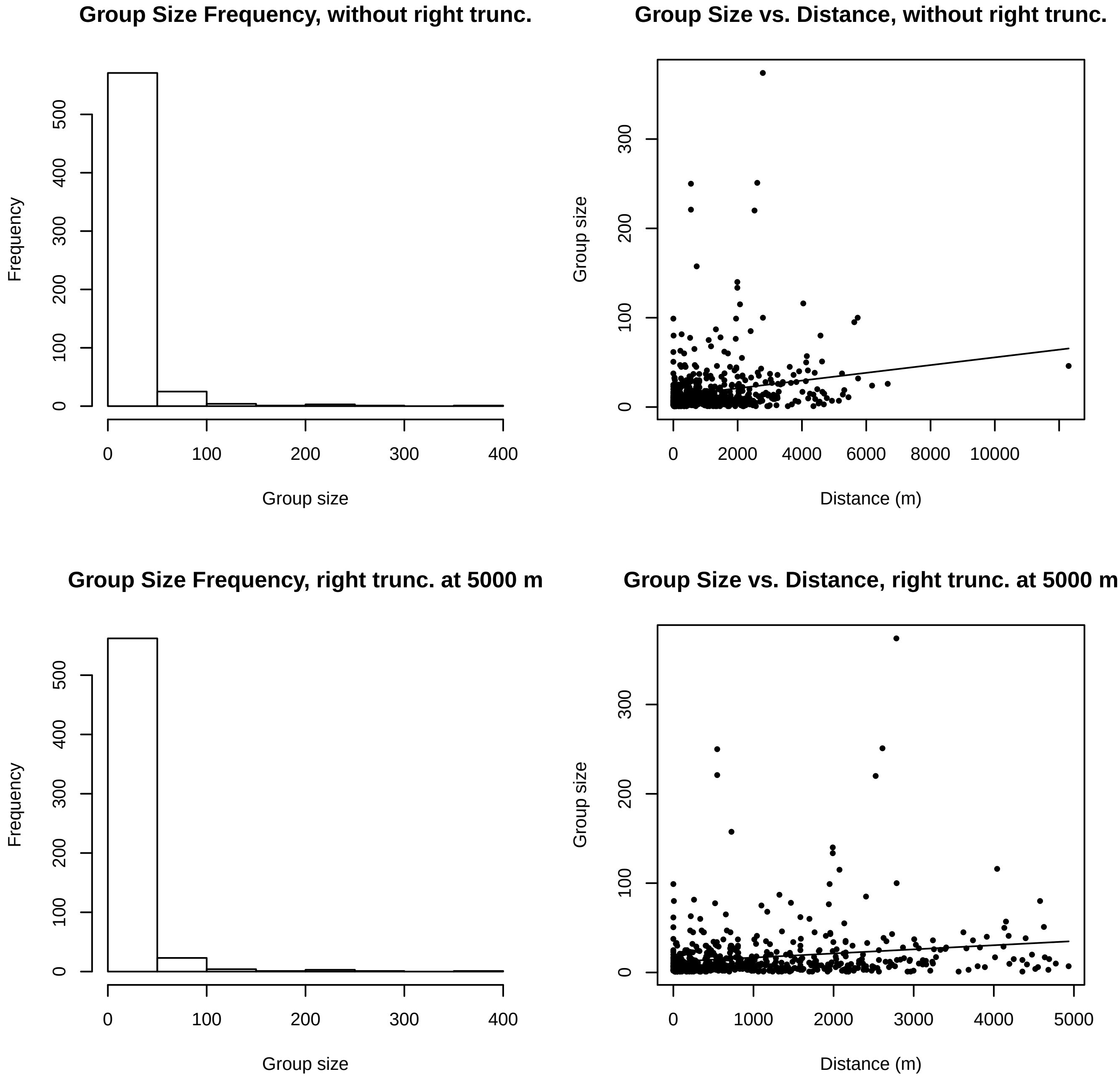

Figure 19: Histograms showing group size frequency and scatterplots showing the relationship between group size and perpendicular sighting distance, for all sightings (top row) and only those not right truncated (bottom row). In the scatterplot, the line is a simple linear regression.

Gordon Gunter Quality Covariate Available

The sightings were right truncated at 5000m.

Covariate	Description
beaufort	Beaufort sea state.
quality	Survey-specific index of the quality of observation conditions, utilizing relevant factors other than Beaufort sea state (see methods).
size	Estimated size (number of individuals) of the sighted group.

Table 10: Covariates tested in candidate "multi-covariate distance sampling" (MCDS) detection functions.

Key	Adjustment	Order	Covariates	Succeeded	Δ AIC	Mean ESHW (m)
hr			beaufort, quality, size	Yes	0.00	1057
hr			beaufort, size	Yes	0.92	1023
hr			beaufort	Yes	31.84	787
hr			beaufort, quality	Yes	32.40	800
hr			quality, size	Yes	42.91	762
hr			size	Yes	57.27	683
hr			quality	Yes	73.57	534
hr				Yes	88.09	463
hn			beaufort, size	Yes	176.57	2002
hn			beaufort, quality, size	Yes	178.52	2000
hn	cos	3		Yes	193.39	1400
hn	cos	2		Yes	197.63	1575
hn			beaufort	Yes	209.82	1976
hn			beaufort, quality	Yes	210.19	1977
hn			quality, size	Yes	231.81	2014
hn			size	Yes	234.23	2029
hn			quality	Yes	253.99	1988
hn				Yes	260.03	1989
hn	herm	4		Yes	260.74	1985
hr	poly	2		No		
hr	poly	4		No		

Table 11: Candidate detection functions for Gordon Gunter Quality Covariate Available. The first one listed was selected for the density model.

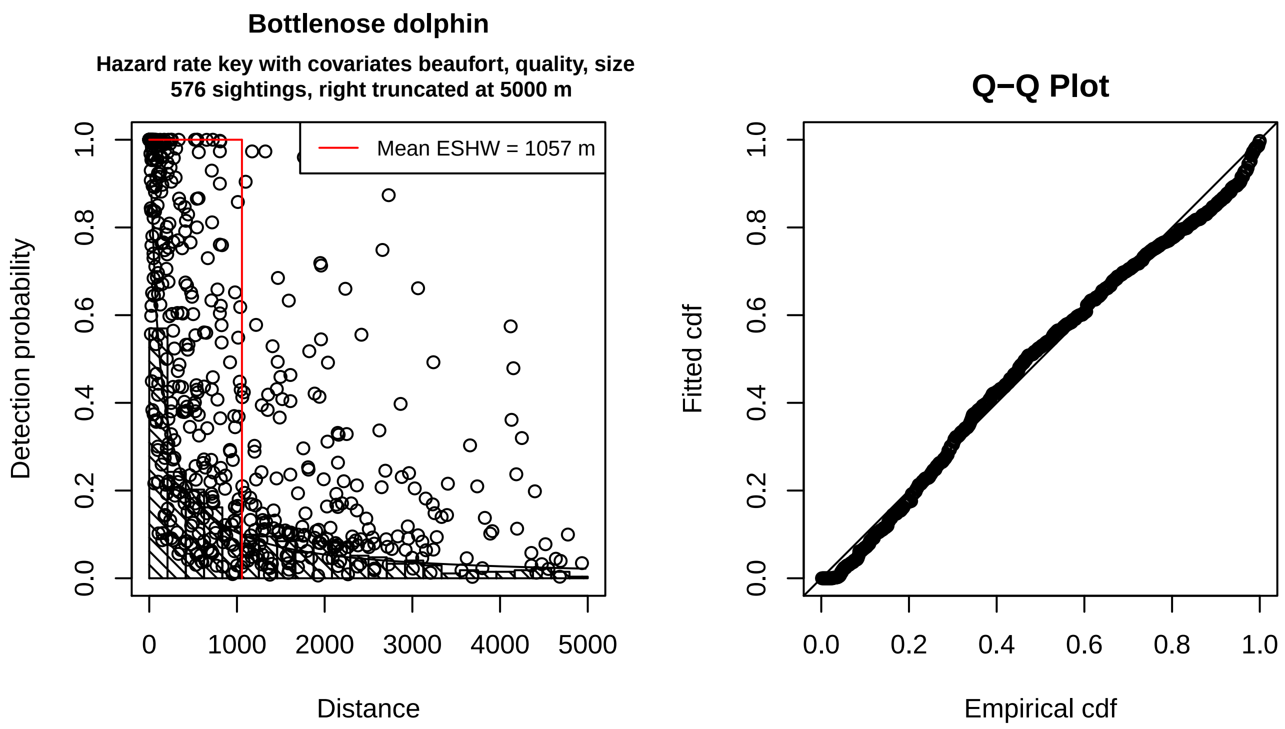

Figure 20: Detection function for Gordon Gunter Quality Covariate Available that was selected for the density model

Statistical output for this detection function:

```
Summary for ds object
Number of observations :  576
Distance range         :  0  -  5000
AIC                    :  9057.588

Detection function:
 Hazard-rate key function

Detection function parameters
Scale Coefficients:
              estimate         se
(Intercept)  7.1448192 0.29997342
beaufort    -0.7643044 0.10907324
quality     -0.1838412 0.09913961
size         1.4231059 0.26038370

Shape parameters:
             estimate         se
(Intercept) 0.1544527 0.05933841

                        Estimate           SE        CV
Average p            8.822243e-02   0.01197154 0.1356973
N in covered region 6.528952e+03 928.18022775 0.1421637
```

Additional diagnostic plots:

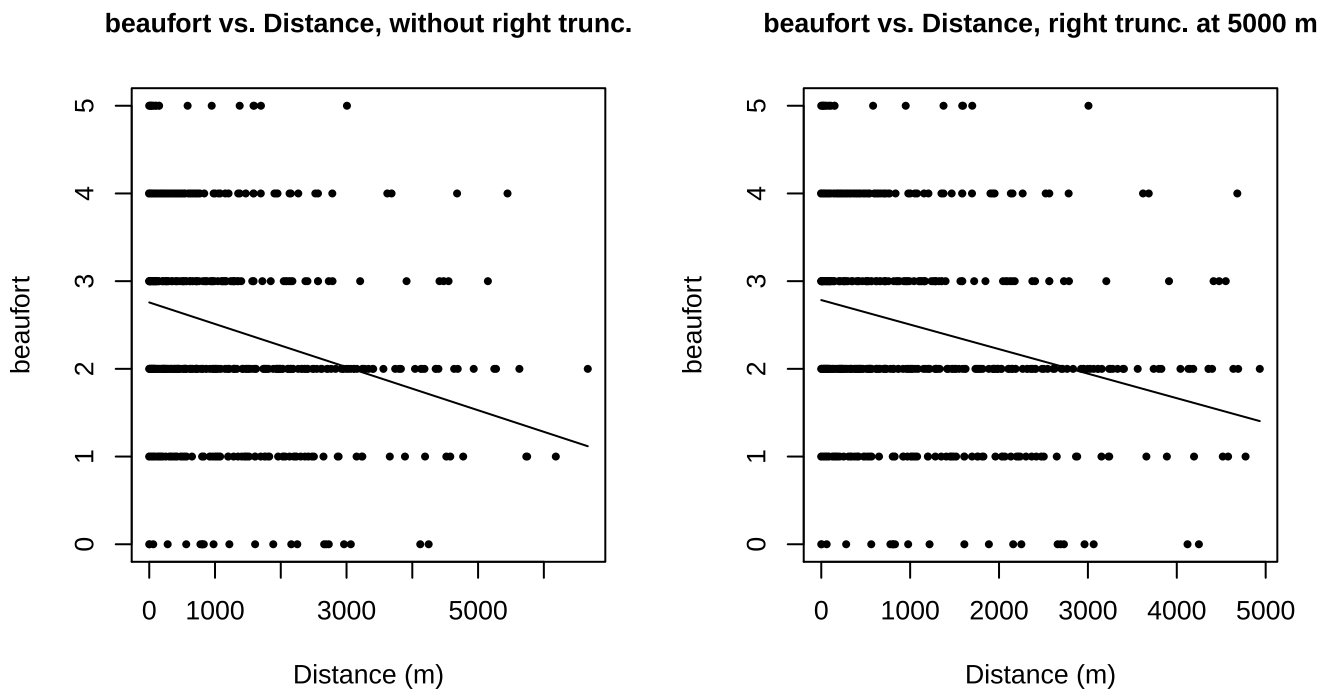

Figure 21: Scatterplots showing the relationship between Beaufort sea state and perpendicular sighting distance, for all sightings (left) and only those not right truncated (right). The line is a simple linear regression.

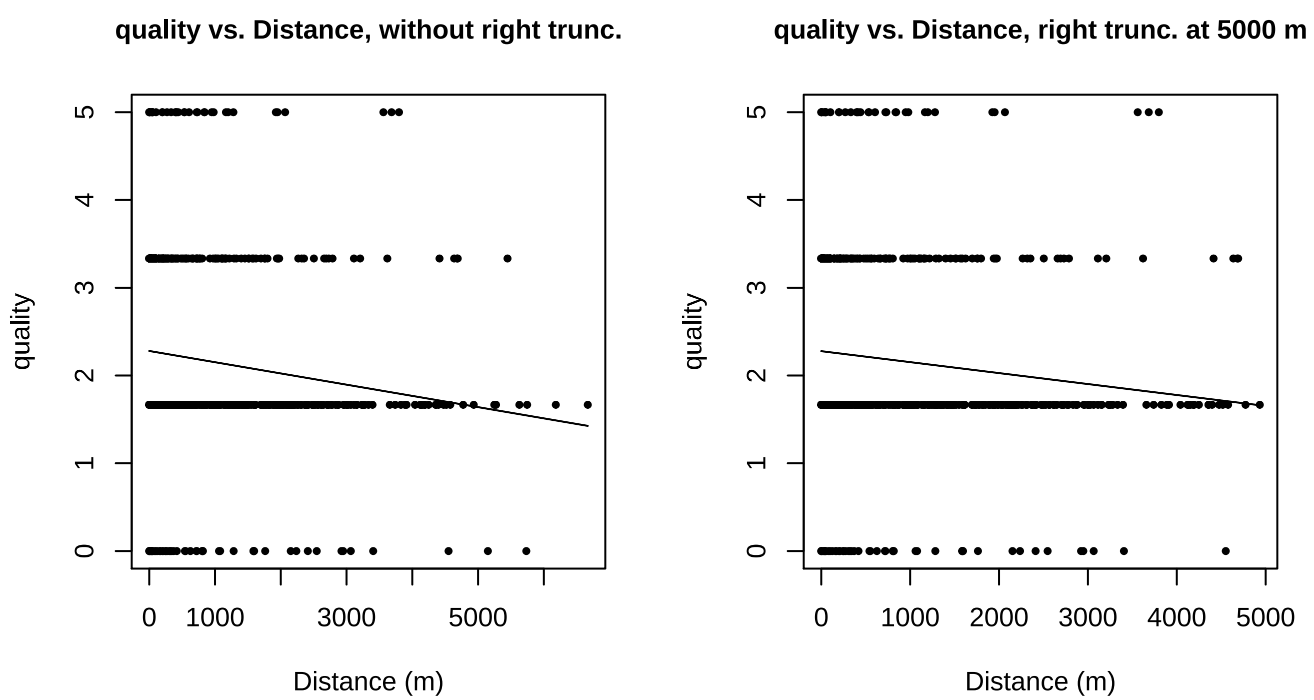

Figure 22: Scatterplots showing the relationship between the survey-specific index of the quality of observation conditions and perpendicular sighting distance, for all sightings (left) and only those not right truncated (right). Low values of the quality index correspond to better observation conditions. The line is a simple linear regression.

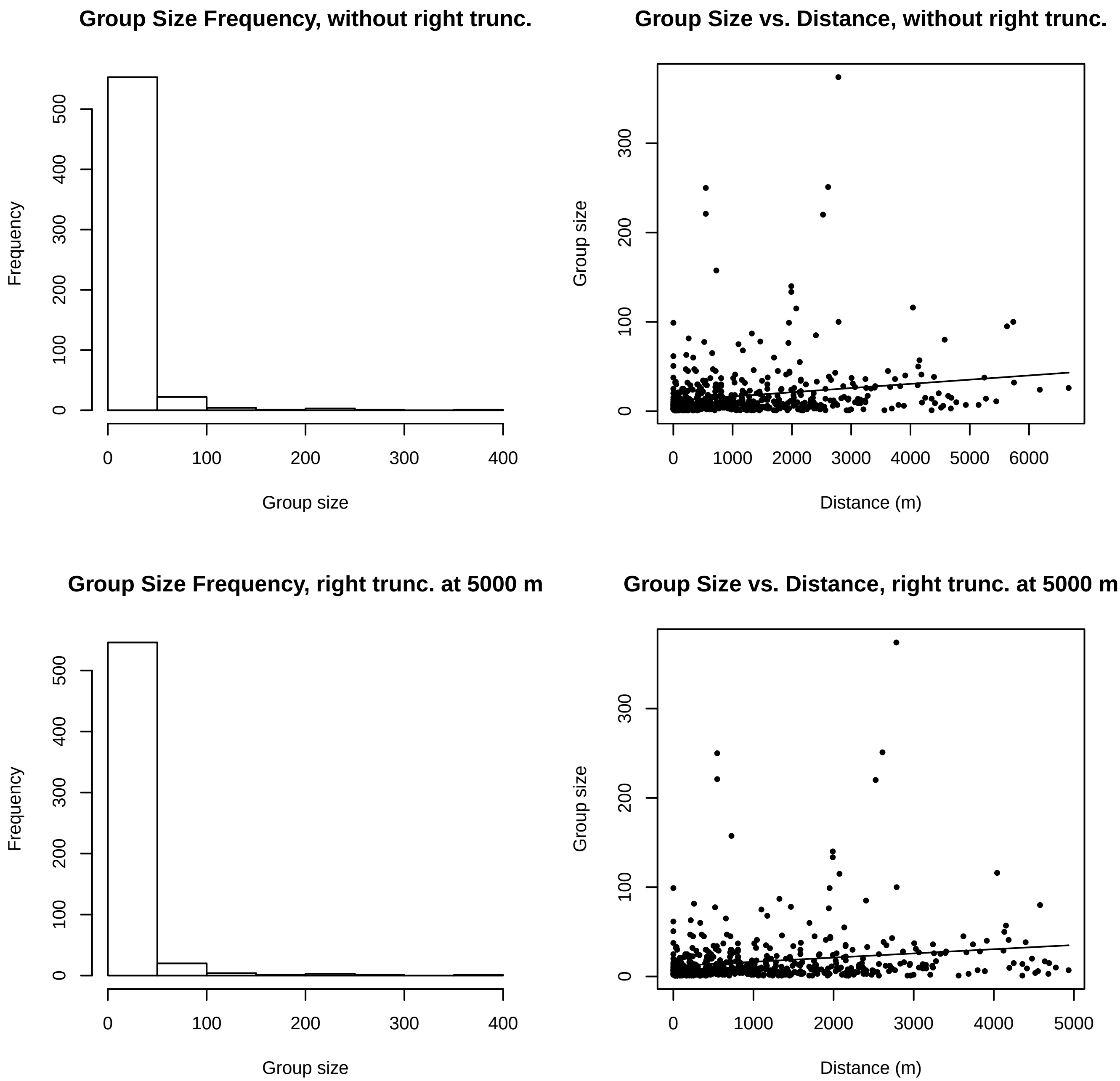

Figure 23: Histograms showing group size frequency and scatterplots showing the relationship between group size and perpendicular sighting distance, for all sightings (top row) and only those not right truncated (bottom row). In the scatterplot, the line is a simple linear regression.

Aerial Surveys

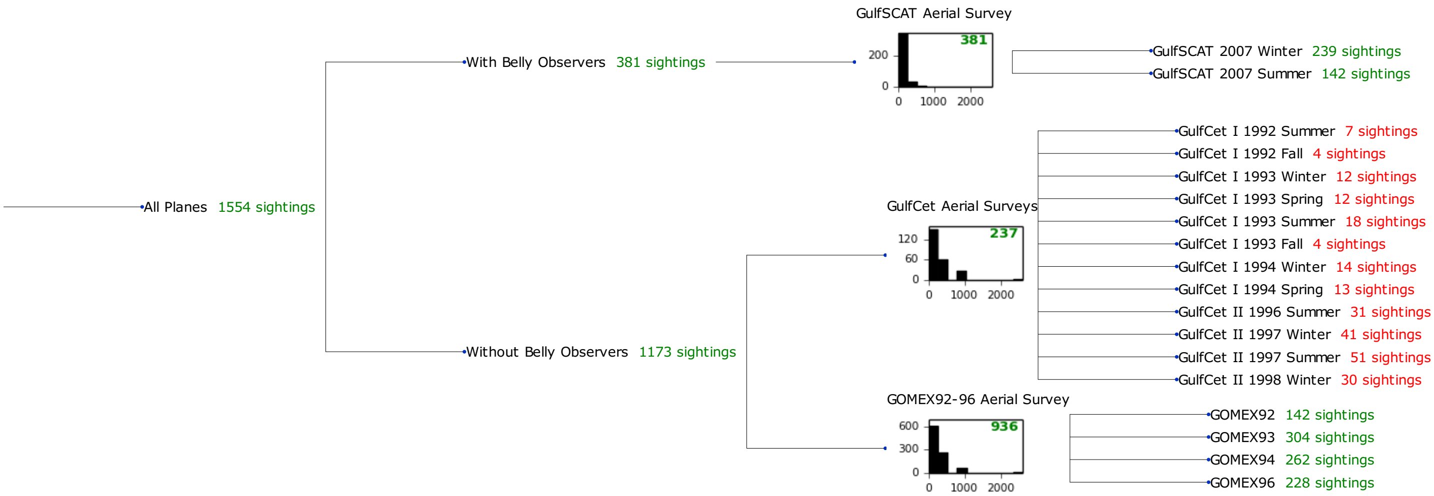

Figure 24: Detection hierarchy for aerial surveys

GulfSCAT Aerial Survey

The sightings were right truncated at 628m.

Covariate	Description
beaufort	Beaufort sea state.
quality	Survey-specific index of the quality of observation conditions, utilizing relevant factors other than Beaufort sea state (see methods).
size	Estimated size (number of individuals) of the sighted group.

Table 12: Covariates tested in candidate "multi-covariate distance sampling" (MCDS) detection functions.

Key	Adjustment	Order	Covariates	Succeeded	Δ AIC	Mean ESHW (m)
hn	cos	3		Yes	0.00	225
hr			size	Yes	0.57	237
hn				Yes	1.36	199
hr				Yes	1.61	237
hn	cos	2		Yes	1.70	214
hn	herm	4		Yes	1.83	215
hn			size	Yes	1.83	198
hr			beaufort, size	Yes	2.07	238
hr	poly	4		Yes	2.60	233
hn			beaufort	Yes	3.30	199
hr			beaufort	Yes	3.30	238
hr	poly	2		Yes	3.65	237

hn	beaufort, size	Yes	3.69	198
hr	quality	No		
hn	quality	No		
hr	beaufort, quality	No		
hn	beaufort, quality	No		
hr	quality, size	No		
hn	quality, size	No		
hr	beaufort, quality, size	No		
hn	beaufort, quality, size	No		

Table 13: Candidate detection functions for GulfSCAT Aerial Survey. The first one listed was selected for the density model.

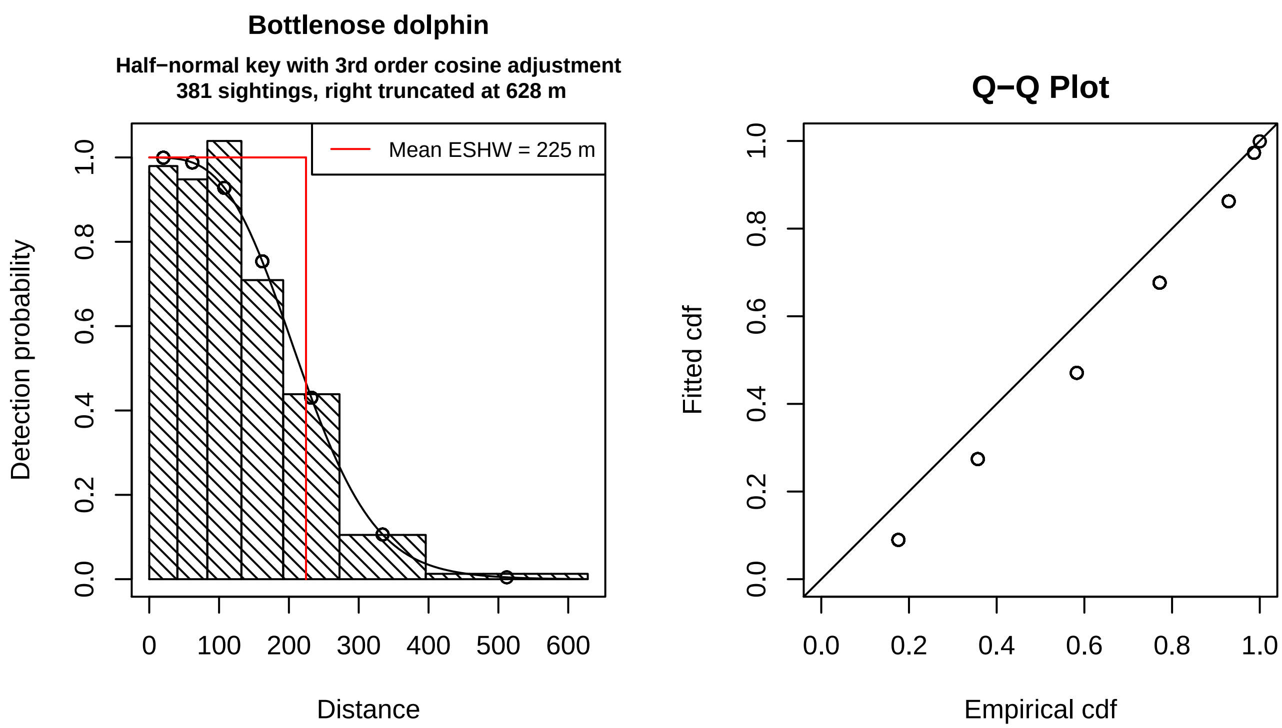

Figure 25: Detection function for GulfSCAT Aerial Survey that was selected for the density model

Statistical output for this detection function:

```
Summary for ds object
Number of observations :  381
Distance range         :  0  -  628
AIC                    :  1361.93

Detection function:
 Half-normal key function with cosine adjustment term of order 3

Detection function parameters
Scale Coefficients:
```

```
            estimate         se
(Intercept)  5.03541 0.03982634

Adjustment term parameter(s):
               estimate         se
cos, order 3 -0.1508097 0.08024846


Monotonicity constraints were enforced.
                        Estimate          SE         CV
Average p              0.3575448  0.02964342 0.08290827
N in covered region 1065.6007121 98.58974988 0.09252035

Monotonicity constraints were enforced.
```

Additional diagnostic plots:

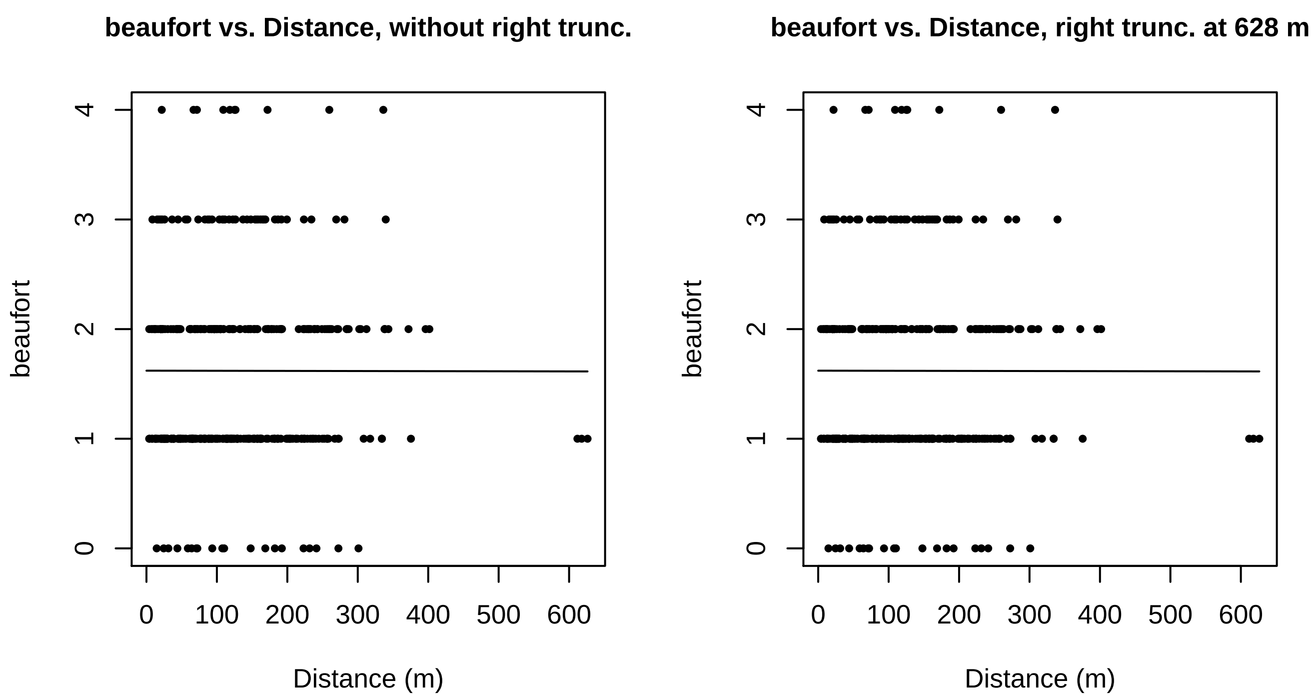

Figure 26: Scatterplots showing the relationship between Beaufort sea state and perpendicular sighting distance, for all sightings (left) and only those not right truncated (right). The line is a simple linear regression.

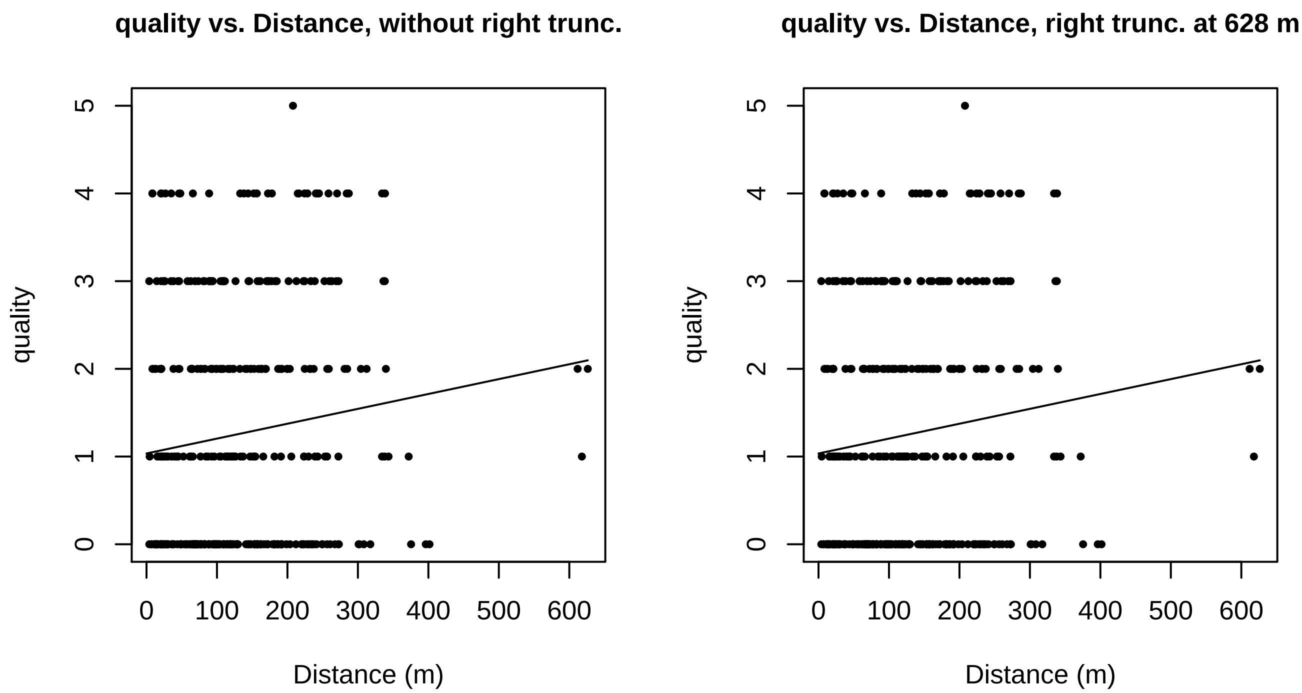

Figure 27: Scatterplots showing the relationship between the survey-specific index of the quality of observation conditions and perpendicular sighting distance, for all sightings (left) and only those not right truncated (right). Low values of the quality index correspond to better observation conditions. The line is a simple linear regression.

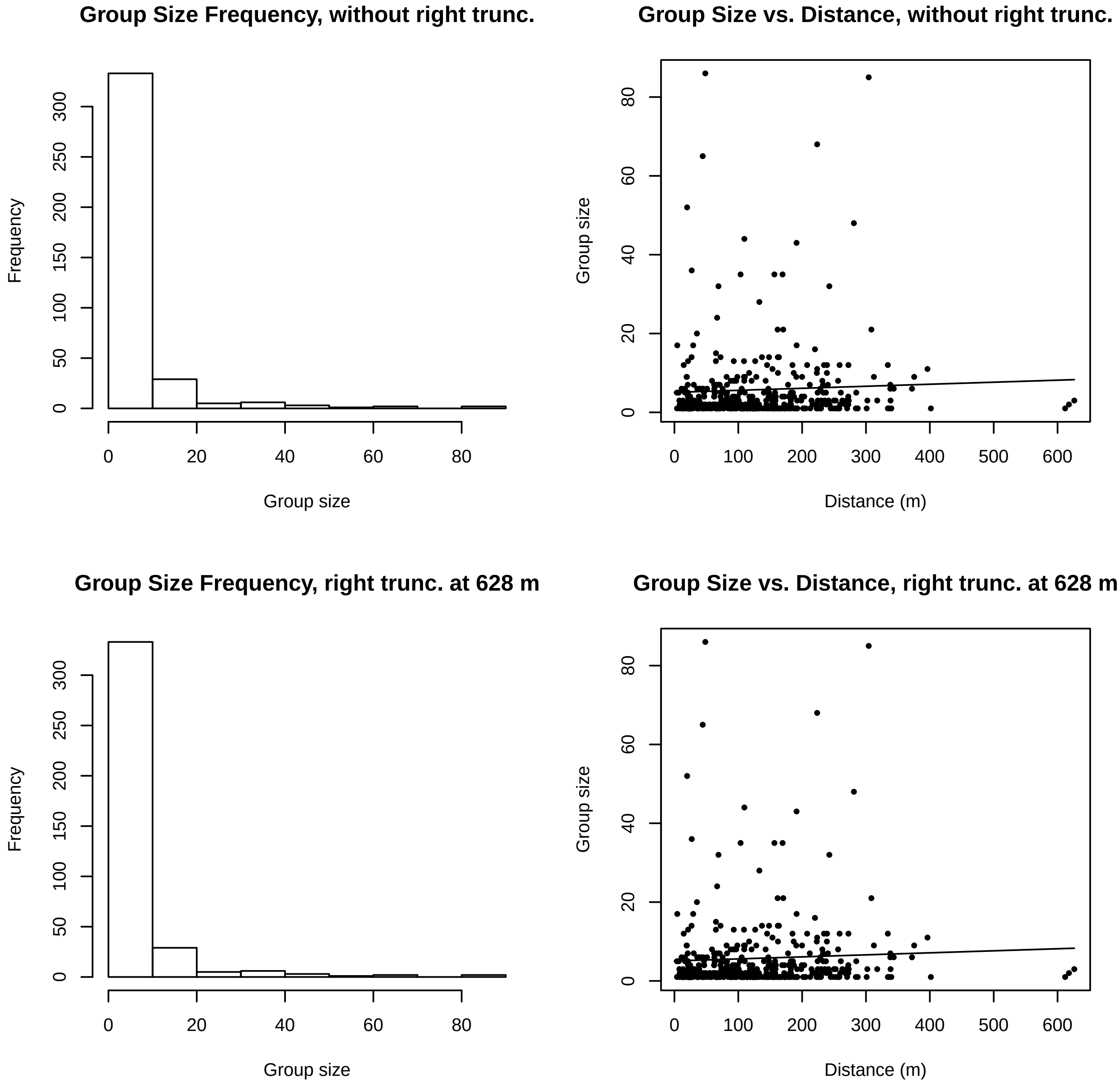

Figure 28: Histograms showing group size frequency and scatterplots showing the relationship between group size and perpendicular sighting distance, for all sightings (top row) and only those not right truncated (bottom row). In the scatterplot, the line is a simple linear regression.

GulfCet Aerial Surveys

The sightings were right truncated at 1296m. Due to a reduced frequency of sightings close to the trackline that plausibly resulted from the behavior of the observers and/or the configuration of the survey platform, the sightings were left truncted as well. Sightings closer than 40 m to the trackline were omitted from the analysis, and it was assumed that the the area closer to the trackline than this was not surveyed. This distance was estimated by inspecting histograms of perpendicular sighting distances.

Covariate	Description

beaufort	Beaufort sea state.
quality	Survey-specific index of the quality of observation conditions, utilizing relevant factors other than Beaufort sea state (see methods).
size	Estimated size (number of individuals) of the sighted group.

Table 14: Covariates tested in candidate "multi-covariate distance sampling" (MCDS) detection functions.

Key	Adjustment	Order	Covariates	Succeeded	Δ AIC	Mean ESHW (m)
hr			size	Yes	0.00	346
hn	cos	2		Yes	0.95	318
hr				Yes	1.73	333
hn	cos	3		Yes	3.66	278
hr	poly	2		Yes	3.73	333
hr	poly	4		Yes	4.20	317
hn			size	Yes	17.33	405
hn				Yes	21.19	404
hn	herm	4		Yes	23.06	404
hr			beaufort	No		
hn			beaufort	No		
hr			quality	No		
hn			quality	No		
hr			beaufort, quality	No		
hn			beaufort, quality	No		
hr			beaufort, size	No		
hn			beaufort, size	No		
hr			quality, size	No		
hn			quality, size	No		
hr			beaufort, quality, size	No		
hn			beaufort, quality, size	No		

Table 15: Candidate detection functions for GulfCet Aerial Surveys. The first one listed was selected for the density model.

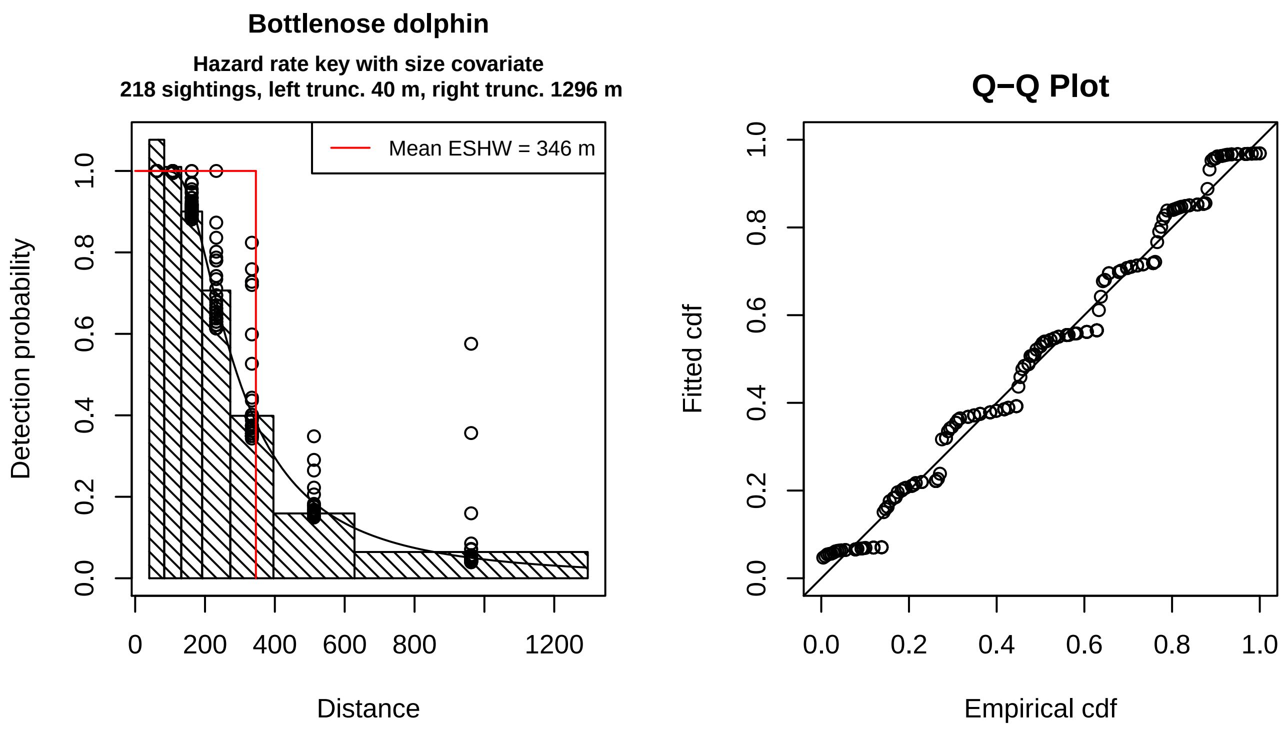

Figure 29: Detection function for GulfCet Aerial Surveys that was selected for the density model

Statistical output for this detection function:

```
Summary for ds object
Number of observations :  218
Distance range         :  40.30835  -  1296
AIC                    :  847.2577

Detection function:
 Hazard-rate key function

Detection function parameters
Scale Coefficients:
             estimate         se
(Intercept) 5.4148062 0.15146942
size        0.1832565 0.08934361

Shape parameters:
             estimate        se
(Intercept) 0.8065024 0.1166782

                       Estimate          SE         CV
Average p             0.2589319  0.02618002 0.1011078
N in covered region 841.9203026 98.39311604 0.1168675
```

Additional diagnostic plots:

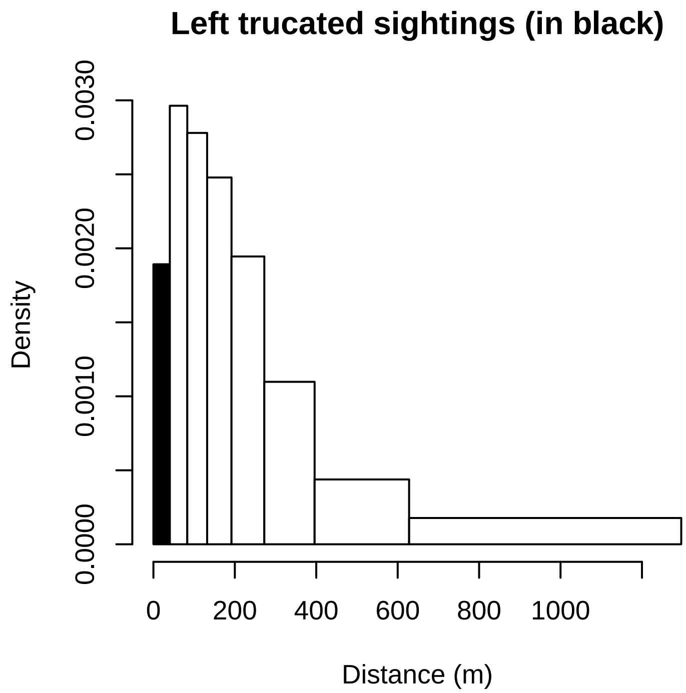

Figure 30: Density of sightings by perpendicular distance for GulfCet Aerial Surveys. Black bars on the left show sightings that were left truncated.

Figure 31: Scatterplots showing the relationship between Beaufort sea state and perpendicular sighting distance, for all sightings (left) and only those not right truncated (right). The line is a simple linear regression.

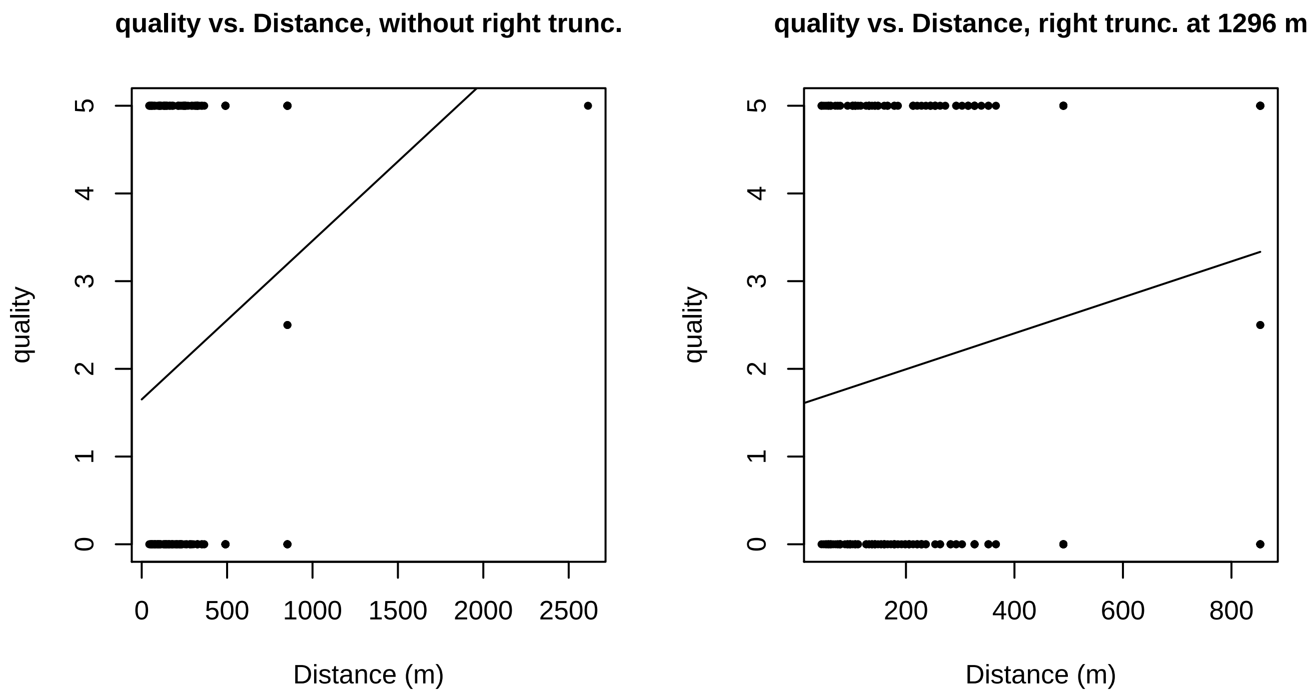

Figure 32: Scatterplots showing the relationship between the survey-specific index of the quality of observation conditions and perpendicular sighting distance, for all sightings (left) and only those not right truncated (right). Low values of the quality index correspond to better observation conditions. The line is a simple linear regression.

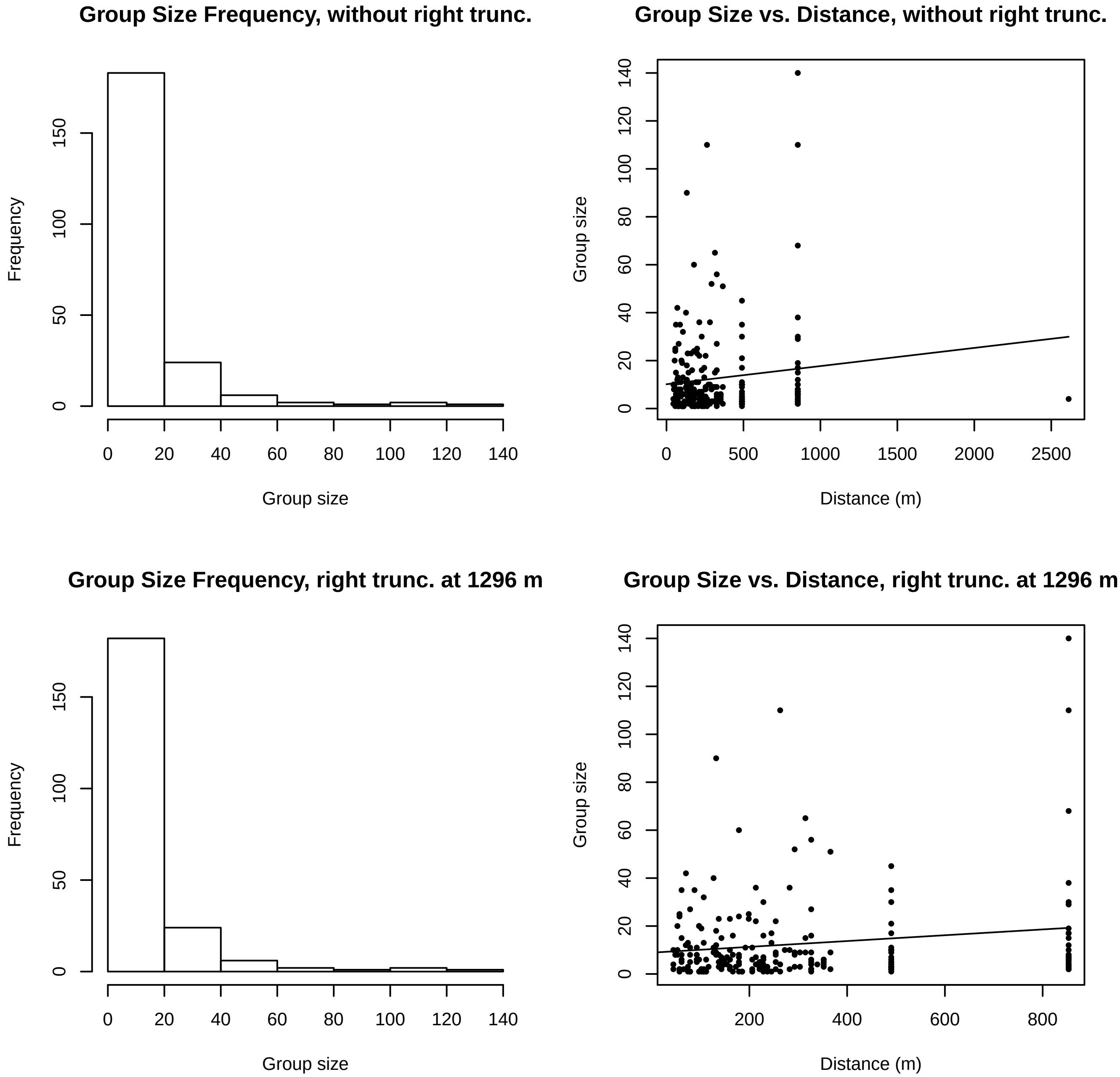

Figure 33: Histograms showing group size frequency and scatterplots showing the relationship between group size and perpendicular sighting distance, for all sightings (top row) and only those not right truncated (bottom row). In the scatterplot, the line is a simple linear regression.

GOMEX92-96 Aerial Survey

The sightings were right truncated at 1296m. Due to a reduced frequency of sightings close to the trackline that plausibly resulted from the behavior of the observers and/or the configuration of the survey platform, the sightings were left truncted as well. Sightings closer than 83 m to the trackline were omitted from the analysis, and it was assumed that the the area closer to the trackline than this was not surveyed. This distance was estimated by inspecting histograms of perpendicular sighting distances.

Covariate	Description

beaufort	Beaufort sea state.
quality	Survey-specific index of the quality of observation conditions, utilizing relevant factors other than Beaufort sea state (see methods).
size	Estimated size (number of individuals) of the sighted group.

Table 16: Covariates tested in candidate “multi-covariate distance sampling” (MCDS) detection functions.

Key	Adjustment	Order	Covariates	Succeeded	Δ AIC	Mean ESHW (m)
hr			size	Yes	0.00	280
hr				Yes	2.38	278
hn	cos	3		Yes	3.71	219
hr	poly	4		Yes	4.39	278
hr	poly	2		Yes	4.39	278
hn	cos	2		Yes	9.94	258
hn			size	Yes	40.32	306
hn				Yes	42.06	306
hn	herm	4		Yes	43.81	306
hr			beaufort	No		
hn			beaufort	No		
hr			quality	No		
hn			quality	No		
hr			beaufort, quality	No		
hn			beaufort, quality	No		
hr			beaufort, size	No		
hn			beaufort, size	No		
hr			quality, size	No		
hn			quality, size	No		
hr			beaufort, quality, size	No		
hn			beaufort, quality, size	No		

Table 17: Candidate detection functions for GOMEX92-96 Aerial Survey. The first one listed was selected for the density model.

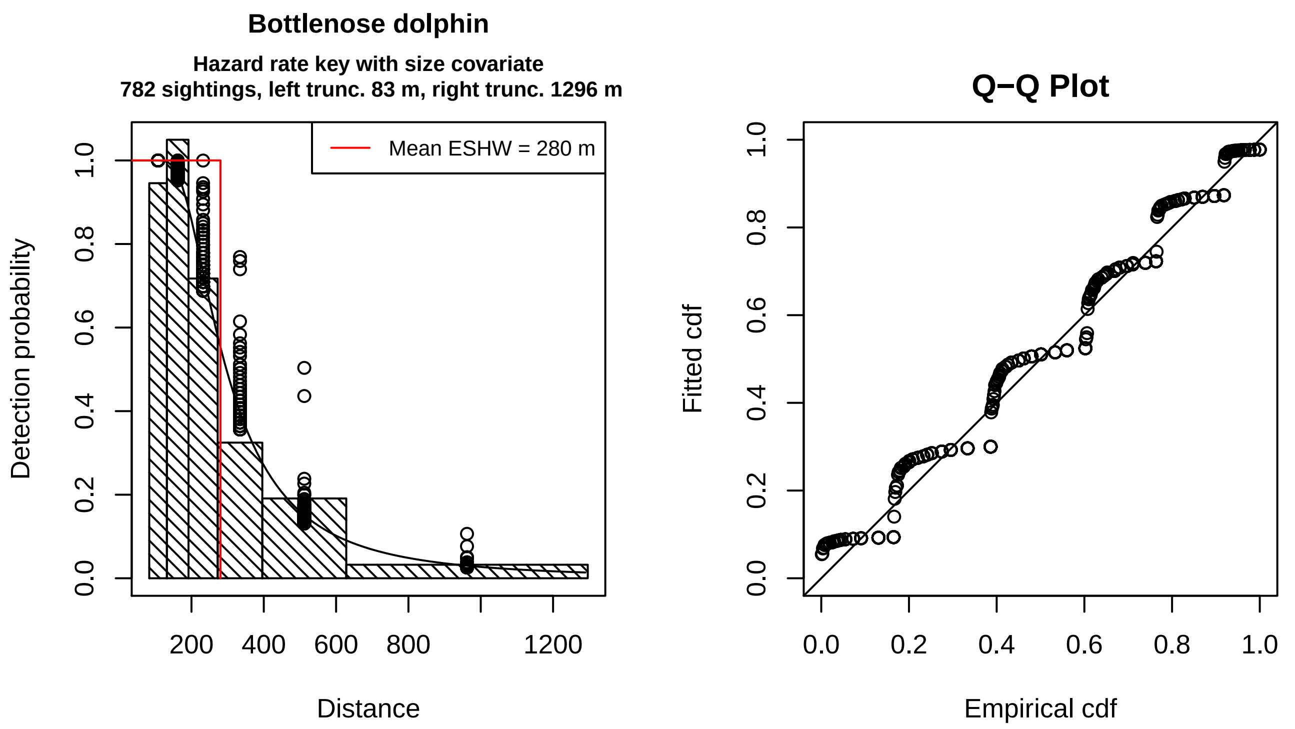

Figure 34: Detection function for GOMEX92-96 Aerial Survey that was selected for the density model

Statistical output for this detection function:

```
Summary for ds object
Number of observations :  782
Distance range         :  83.2036  -  1296
AIC                    :  2744.589

Detection function:
 Hazard-rate key function

Detection function parameters
Scale Coefficients:
              estimate         se
(Intercept) 5.49389431 0.06866783
size        0.08363174 0.03816366

Shape parameters:
             estimate         se
(Intercept) 0.9827602 0.05937892

                        Estimate           SE         CV
Average p              0.2140879   0.01175494 0.05490705
N in covered region 3652.7045766 231.66521158 0.06342293
```

Additional diagnostic plots:

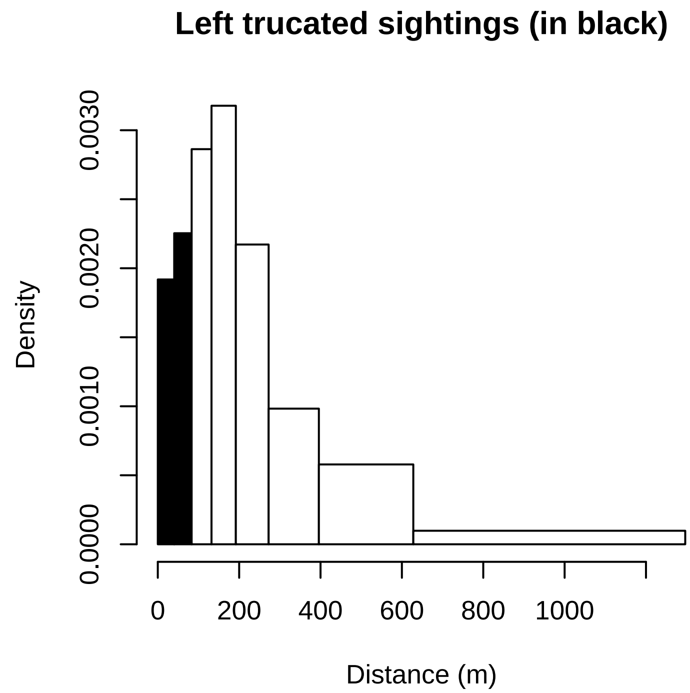

Figure 35: Density of sightings by perpendicular distance for GOMEX92-96 Aerial Survey. Black bars on the left show sightings that were left truncated.

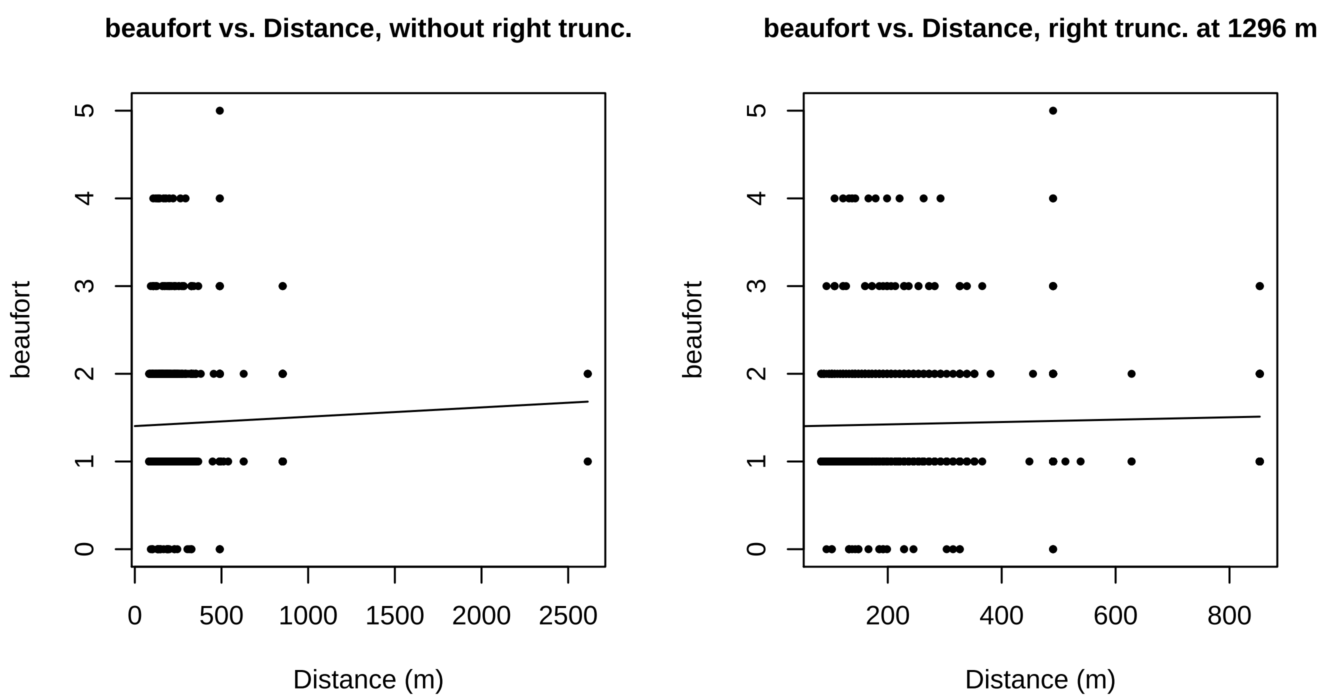

Figure 36: Scatterplots showing the relationship between Beaufort sea state and perpendicular sighting distance, for all sightings (left) and only those not right truncated (right). The line is a simple linear regression.

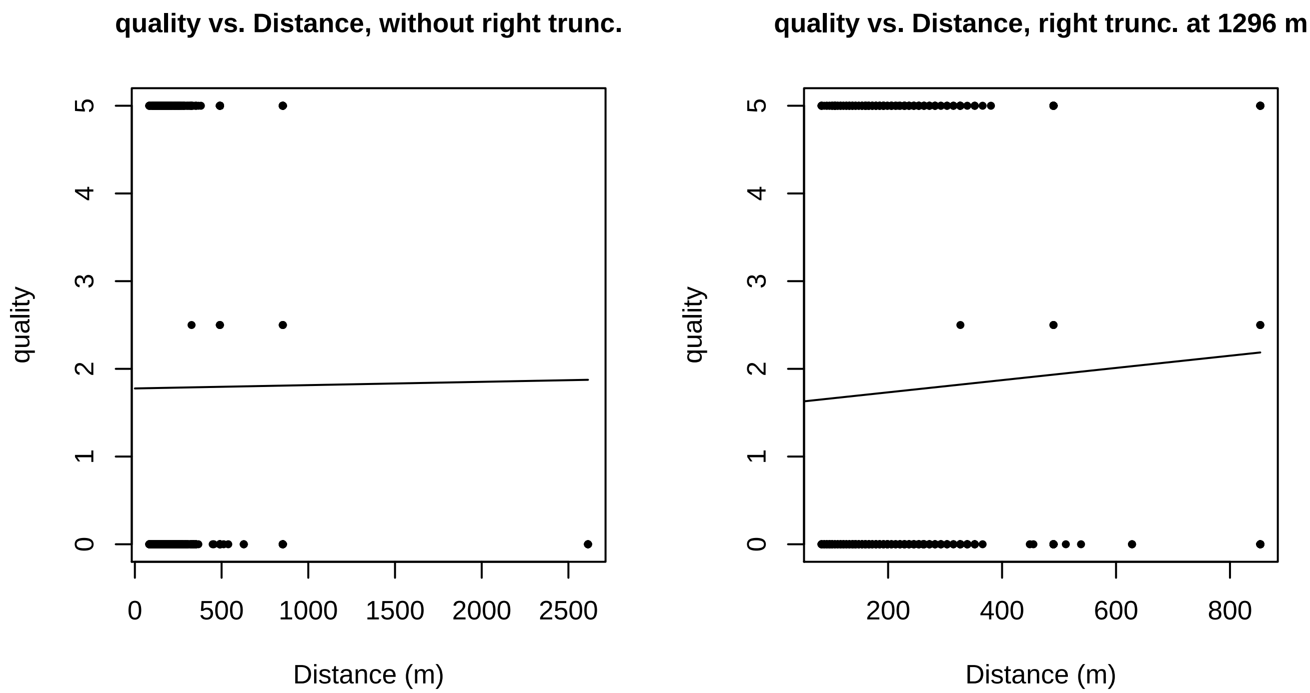

Figure 37: Scatterplots showing the relationship between the survey-specific index of the quality of observation conditions and perpendicular sighting distance, for all sightings (left) and only those not right truncated (right). Low values of the quality index correspond to better observation conditions. The line is a simple linear regression.

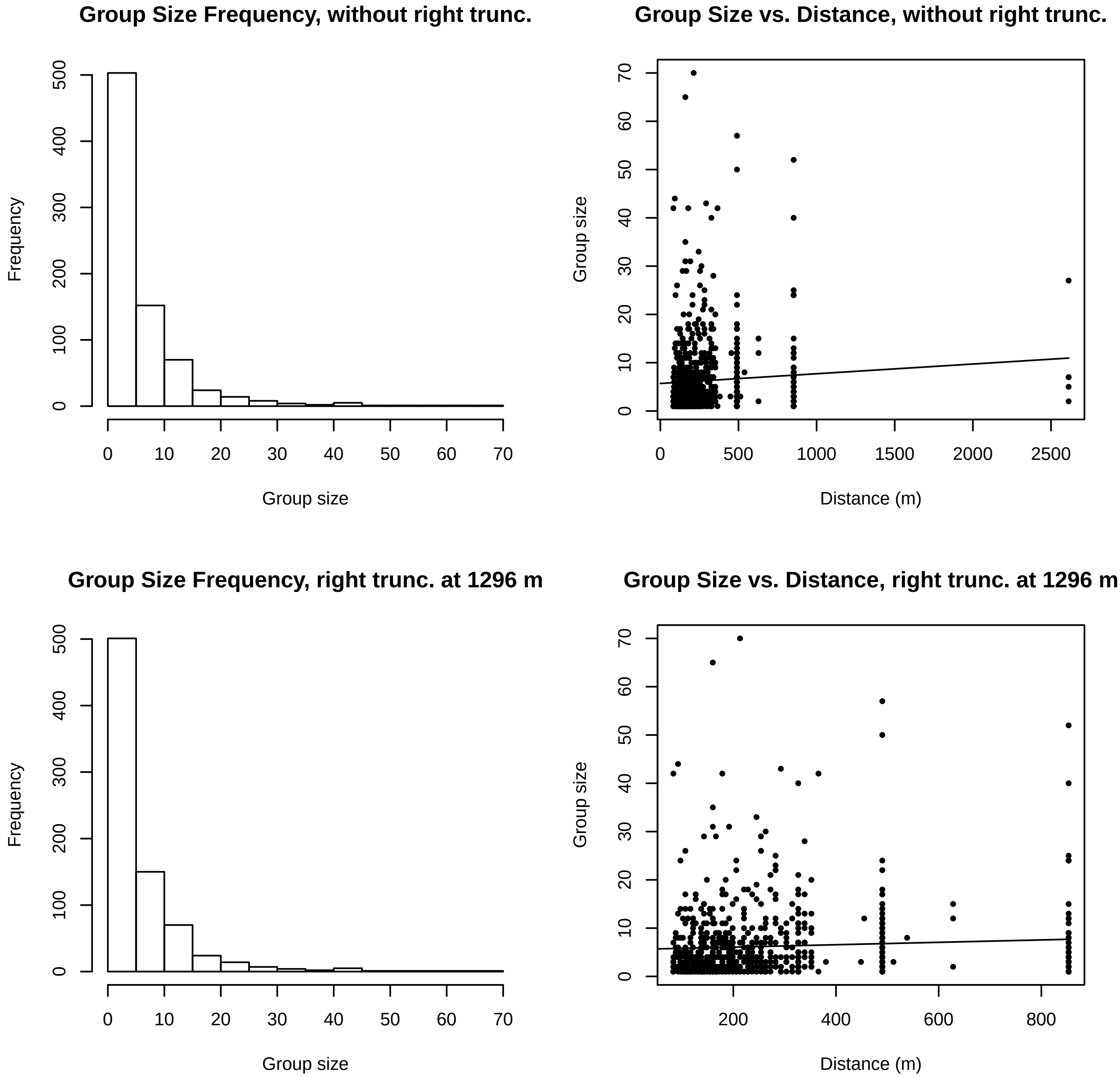

Figure 38: Histograms showing group size frequency and scatterplots showing the relationship between group size and perpendicular sighting distance, for all sightings (top row) and only those not right truncated (bottom row). In the scatterplot, the line is a simple linear regression.

g(0) Estimates

Platform	Surveys	Group Size	*g(0)*	Biases Addressed	Source
Shipboard	All	1-20	0.856	Perception	Barlow and Forney (2007)
		>20	0.970	Perception	Barlow and Forney (2007)
Aerial	All	1-5	0.43	Both	Palka (2006)
		>5	0.960	Both	Carretta et al. (2000)

Table 18: Estimates of *g(0)* used in this density model.

No g(0) estimates were published for any of the shipboard surveys available to us from this region. Instead, we utilized Barlow and Forney's (2007) estimates for delphinids, produced from several years of dual-team surveys that used bigeye binoculars and similar protocols to the surveys in our study. This study provided separate estimates for small and large groups, but pooled sightings of several species together to provide a generic estimate for all delphinids, due to sample-size limitations. To our knowledge, there is no species-specific shipboard g(0) estimate that treats small and large groups separately, so we believe Barlow and Forney (2007) provide the best general-purpose alternative. Their estimate accounted for perception bias but not availability bias; dive times for dolphins are short enough that availability bias is not expected to be significant for dolphins observed from shipboard surveys.

For aerial surveys, we were unable to locate species-specific g(0) estimates in the literature. For small groups, defined here as 1-5 individuals, we used Palka's (2006) estimate of g(0) for groups of 1-5 small cetaceans, estimated from two years of aerial surveys using the Hiby (1999) circle-back method. This estimate accounted for both availability and perception bias, but pooled sightings of several species together to provide a generic estimate for all delphinids, due to sample-size limitations. For large groups, defined here as greater than 5 individuals, Palka (2006) assumed that g(0) was 1. When we discussed this with NOAA SWFSC reviewers, they agreed that it was safe to assume that the availability bias component of g(0) was 1 but insisted that perception bias should be slightly less than 1, because it was possible to miss large groups. We agreed to take a conservative approach and obtained our g(0) for large groups from Carretta et al. (2000), who estimated g(0) for both small and large groups of delphinids. We used Carretta et al.'s g(0) estimate for groups of 1-25 individuals (0.960), rather than their larger one for more than 25 individuals (0.994), to account for the fact that we were using Palka's definition of large groups as those with more than 5 individuals.

Density Models

The common bottlenose dolphin is the most abundant cetacean in the northern Gulf of Mexico, with the possible exception of the pantropical spotted dolphin. Owing to its overall abundance and its distribution close to shore, the surveys used in our study reported more sightings of it than any other species–over 1800–allowing us to fit species-specific and survey-program-specific or vessel-specific detection functions (see Detection Functions section above).

Two morphologically and genetically distinct ecotypes of bottlenose dolphins, known as the coastal and offshore forms, inhabit the northern Gulf of Mexico (Vollmer and Rosel 2013). The offshore ecotype is larger and inhabits off-shelf, slope, and shelf-break waters, as well as outer portions of the continental shelf. The coastal ecotype is smaller and inhabits the inner portions of the continental shelf, bays, sounds, and estuaries. The spatiotemporal extents and dynamics of the distributions of the two ecotypes (e.g. how far they range from the shelf edge or the shore) are not fully determined and are a topic of active research (Waring et al. 2013).

Bottlenose dolphins exhibit the most complex population structure yet documented for any cetacean in the U.S. Atlantic or Gulf of Mexico. The U.S. Marine Mammal Protection Act (MMPA) requires that cetaceans be managed on a per "stock" basis, and defines a stock as "a group of marine mammals of the same species or smaller taxa in a common spatial arrangement, that interbreed when mature". The National Marine Fisheries Service (NMFS) is responsible for defining stocks and estimating their abundance, and periodically issues stock assessment reports that summarize the latest research and promulgate stock definitions and abundance estimates.

At the time of this writing, the most recent finalized stock assessment report defined 37 stocks in the northern Gulf of Mexico (Waring et al. 2013). In that report, NMFS delimited boundaries between the stocks using bathymetric and geographic limits. The oceanic stock, believed to consist exclusively of the oceanic ecotype, is defined as bottlenose dolphins inhabiting waters > 200 m deep within the U.S. Exclusive Economic Zone (EEZ). The continental shelf stock is defined as the dolphins inhabiting waters between 20 and 200 m depth, EEZ-wide, and is presumed to consist of a mix of the two ecotypes. Three "coastal" stocks are defined for waters that extend from the 20 m isobath to shore, barrier islands, or presumed outer bay boundaries. The eastern coastal stock extends from Key West, Florida to 84 W. The northern coastal stock extends from 84 W to the Mississippi River Delta. The western coastal stock extends from the Mississippi River Delta to the Texas-Mexico border. The three coastal stocks are presumed to consist mainly of the coastal ecotype, but the offshore ecotype could potentially occur in them (Waring et al. 2013). The remaining stocks are defined for specific bays, sounds, and estuaries scattered across the U.S. Gulf states. While these stock boundaries have an ecological basis, NMFS notes that they represent management boundaries rather than true ecological boundaries (Waring et al. 2013), that animals move across these boundaries, and that seasonal movements are generally poorly understood.

The focus of our study was to model cetaceans that occur outside of bays and estuaries. Accordingly, prior to analysis, we discarded all estuarine survey transects (in the Gulf of Mexico, most of these were part of the "SEFSC GOMEX92-96 Aerial Surveys"). Thus it is reasonable to assume that our model estimates the aggregate density of the coastal and offshore stocks and excludes the estuarine stocks (although some estuarine animals are known to range into coastal areas beyond their home estuaries; presumably some of these were sighted and we failed to discard them).

It stands to reason that the two ecotypes could exhibit different relationships to their environment, as could different "stocks" in the original MMPA sense. In situations like this, when differently-behaving groups of animals occupy different parts of the study area–as with right whales in winter, when some move to the calving grounds in the southeast U.S. while others remain in the Gulf of Maine to overwinter–our modeling strategy is to split the study area into geographic strata occupied by the different groups and model each stratum separately. But because the NMFS stock definitions represented management boundaries rather than ecotype or true MMPA stock boundaries, we did not define geographic modeling strata from them. Neither did we define seasonal strata, owing to the lack of information about seasonality in the Gulf of Mexico, as well as substantial spatial and seasonal biases in survey effort. Thus we modeled bottlenose dolphins in the Gulf of Mexico using a single "year-round" model of all survey segments.

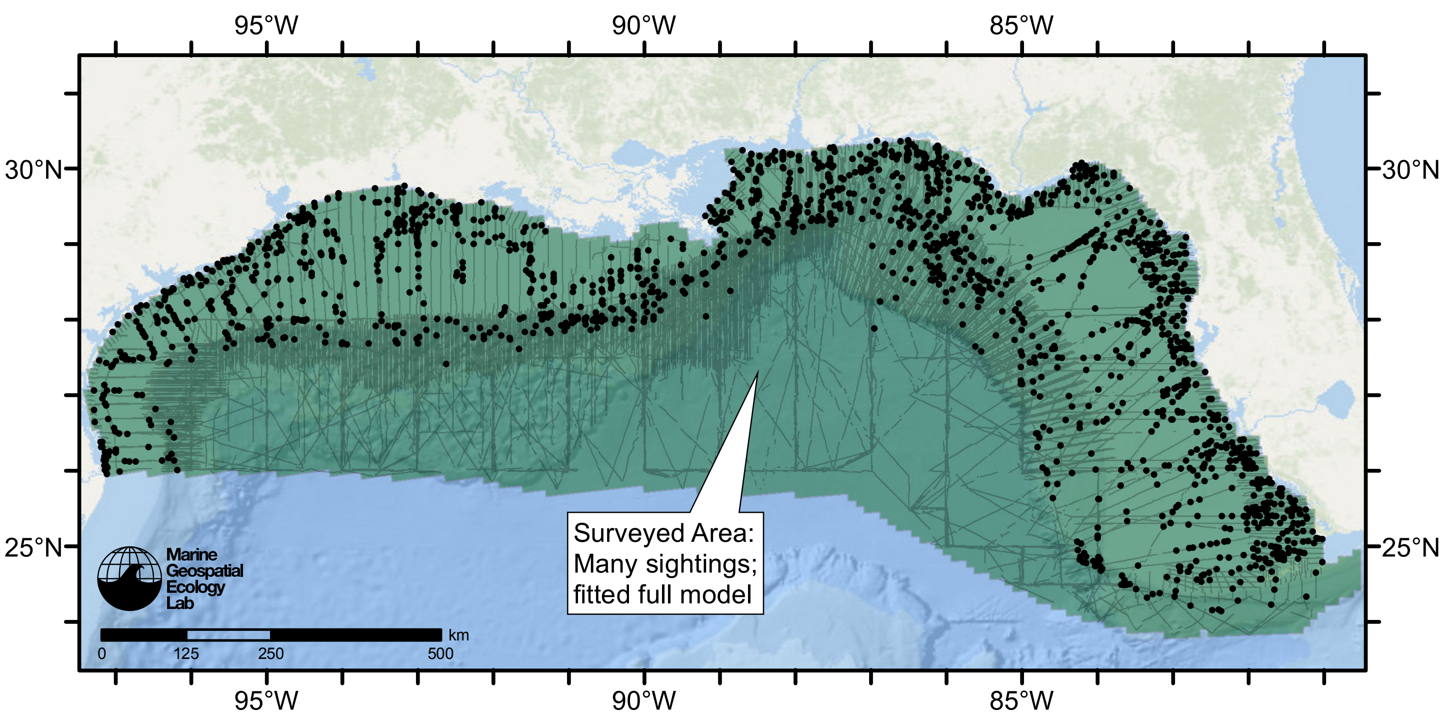

Figure 39: Bottlenose dolphin density model schematic. All on-effort sightings are shown, including those that were truncated when detection functions were fitted.

Climatological Model

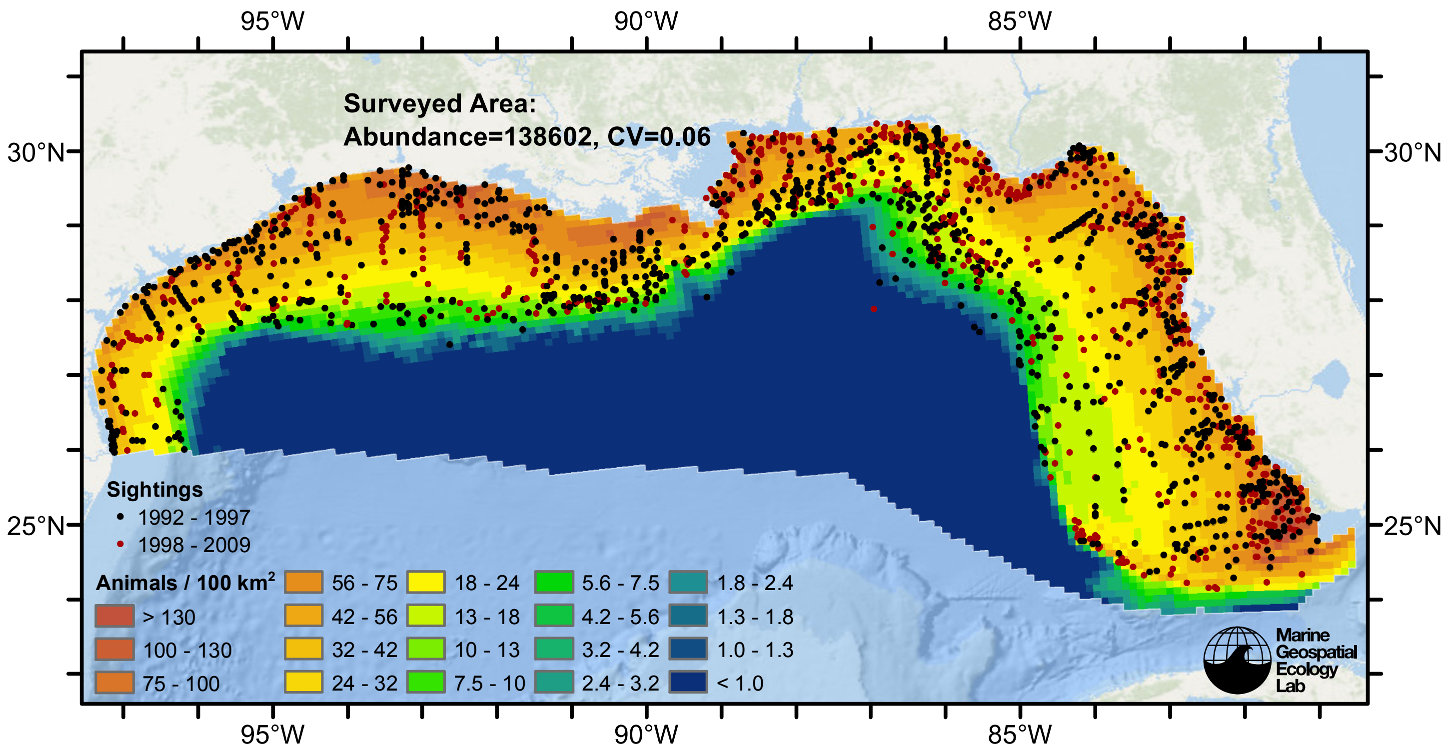

Figure 40: Bottlenose dolphin density predicted by the climatological model that explained the most deviance. Pixels are 10x10 km. The legend gives the estimated individuals per pixel; breaks are logarithmic. Abundance for each region was computed by summing the density cells occuring in that region.

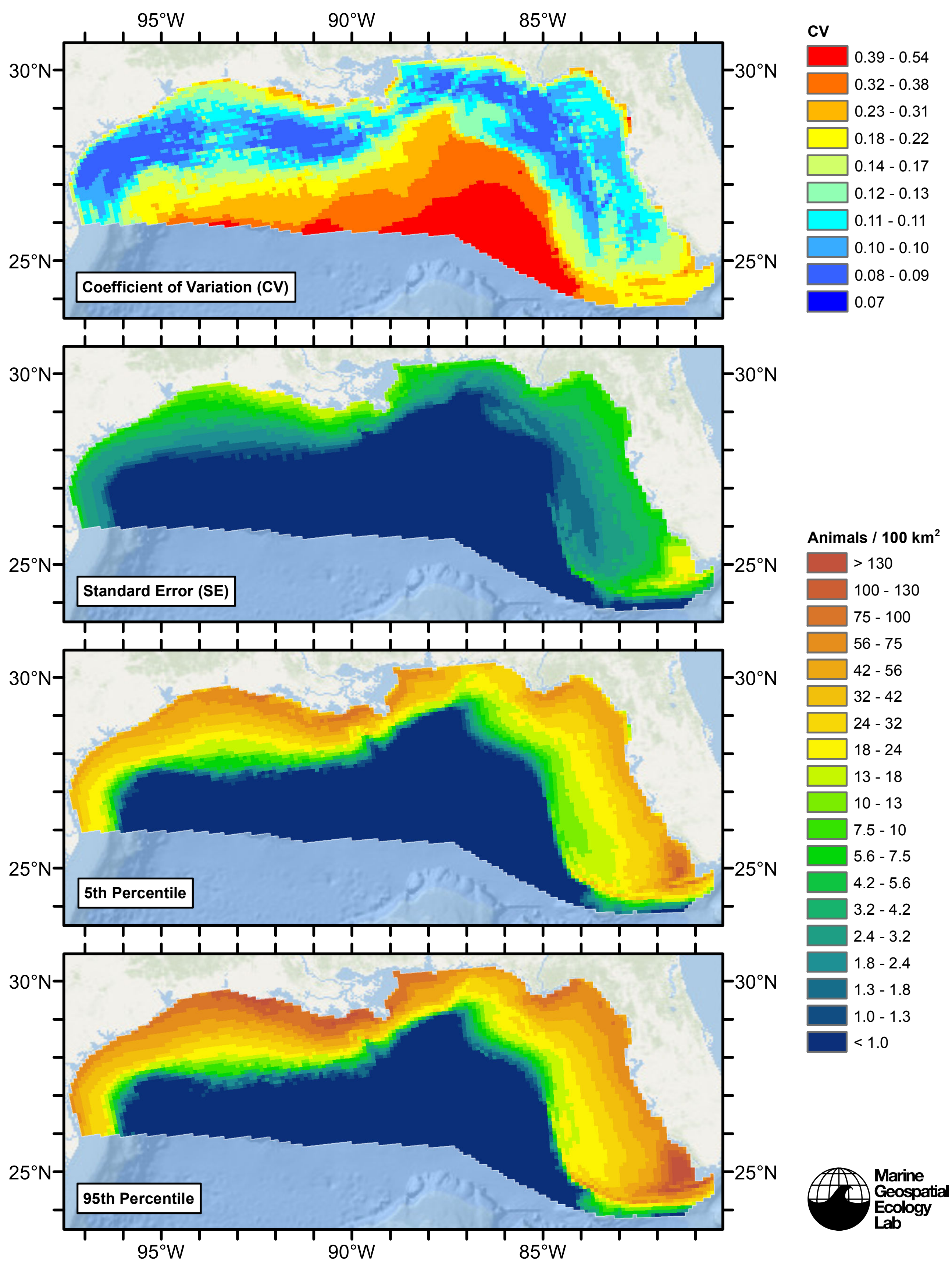

Figure 41: Estimated uncertainty for the climatological model that explained the most deviance. These estimates only incorporate the statistical uncertainty estimated for the spatial model (by the R mgcv package). They do not incorporate uncertainty in the detection functions, g(0) estimates, predictor variables, and so on.

Surveyed Area

Statistical output

```
Rscript.exe: This is mgcv 1.8-2. For overview type 'help("mgcv-package")'.


Family: Tweedie(p=1.398)
Link function: log

Formula:
abundance ~ offset(log(area_km2)) + s(log10(Depth), bs = "ts",
    k = 5) + s(log10(pmax(Slope, 1e-06)), bs = "ts", k = 5) +
    s(I(DistToShore/1000), bs = "ts", k = 5) + s(ClimSST, bs = "ts",
    k = 5) + s(pmin(I(ClimDistToFront3/1000), 1000), bs = "ts",
    k = 5) + s(log10(pmax(ClimEKE, 0.001)), bs = "ts", k = 5) +
    s(log10(pmax(ClimPkPB, 0.01)), bs = "ts", k = 5)

Parametric coefficients:
            Estimate Std. Error t value Pr(>|t|)
(Intercept) -3.43783    0.06647  -51.72   <2e-16 ***
---
Signif. codes:  0 '***' 0.001 '**' 0.01 '*' 0.05 '.' 0.1 ' ' 1

Approximate significance of smooth terms:
                                         edf Ref.df       F  p-value
s(log10(Depth))                        3.958      4 122.272  < 2e-16 ***
s(log10(pmax(Slope, 1e-06)))           3.843      4  12.821 6.29e-11 ***
s(I(DistToShore/1000))                 1.063      4   4.369 1.32e-05 ***
s(ClimSST)                             3.295      4  20.777  < 2e-16 ***
s(pmin(I(ClimDistToFront3/1000), 1000)) 3.027      4  14.470 4.17e-14 ***
s(log10(pmax(ClimEKE, 0.001)))         3.274      4  10.518 4.23e-10 ***
s(log10(pmax(ClimPkPB, 0.01)))         1.493      4   6.266 2.29e-07 ***
---
Signif. codes:  0 '***' 0.001 '**' 0.01 '*' 0.05 '.' 0.1 ' ' 1

R-sq.(adj) =  0.0714   Deviance explained = 32.9%
-REML =  11940  Scale est. = 47.124    n = 19881

All predictors were significant. This is the final model.
Creating term plots.
Diagnostic output from gam.check():

Method: REML   Optimizer: outer newton
full convergence after 9 iterations.
Gradient range [-0.0025201,0.00098885]
(score 11940.46 & scale 47.1244).
Hessian positive definite, eigenvalue range [0.1888911,3245.402].
Model rank =  29 / 29

Basis dimension (k) checking results. Low p-value (k-index<1) may
indicate that k is too low, especially if edf is close to k'.

                                          k'   edf k-index p-value
s(log10(Depth))                        4.000 3.958   0.737    0.00
s(log10(pmax(Slope, 1e-06)))           4.000 3.843   0.765    0.52
s(I(DistToShore/1000))                 4.000 1.063   0.758    0.28
s(ClimSST)                             4.000 3.295   0.758    0.28
s(pmin(I(ClimDistToFront3/1000), 1000)) 4.000 3.027   0.760    0.42
```

s(log10(pmax(ClimEKE, 0.001)))	4.000	3.274	0.721	0.00
s(log10(pmax(ClimPkPB, 0.01)))	4.000	1.493	0.782	0.96

Predictors retained during the model selection procedure: Depth, Slope, DistToShore, ClimSST, ClimDistToFront3, ClimEKE, ClimPkPB

Predictors dropped during the model selection procedure:

Model term plots

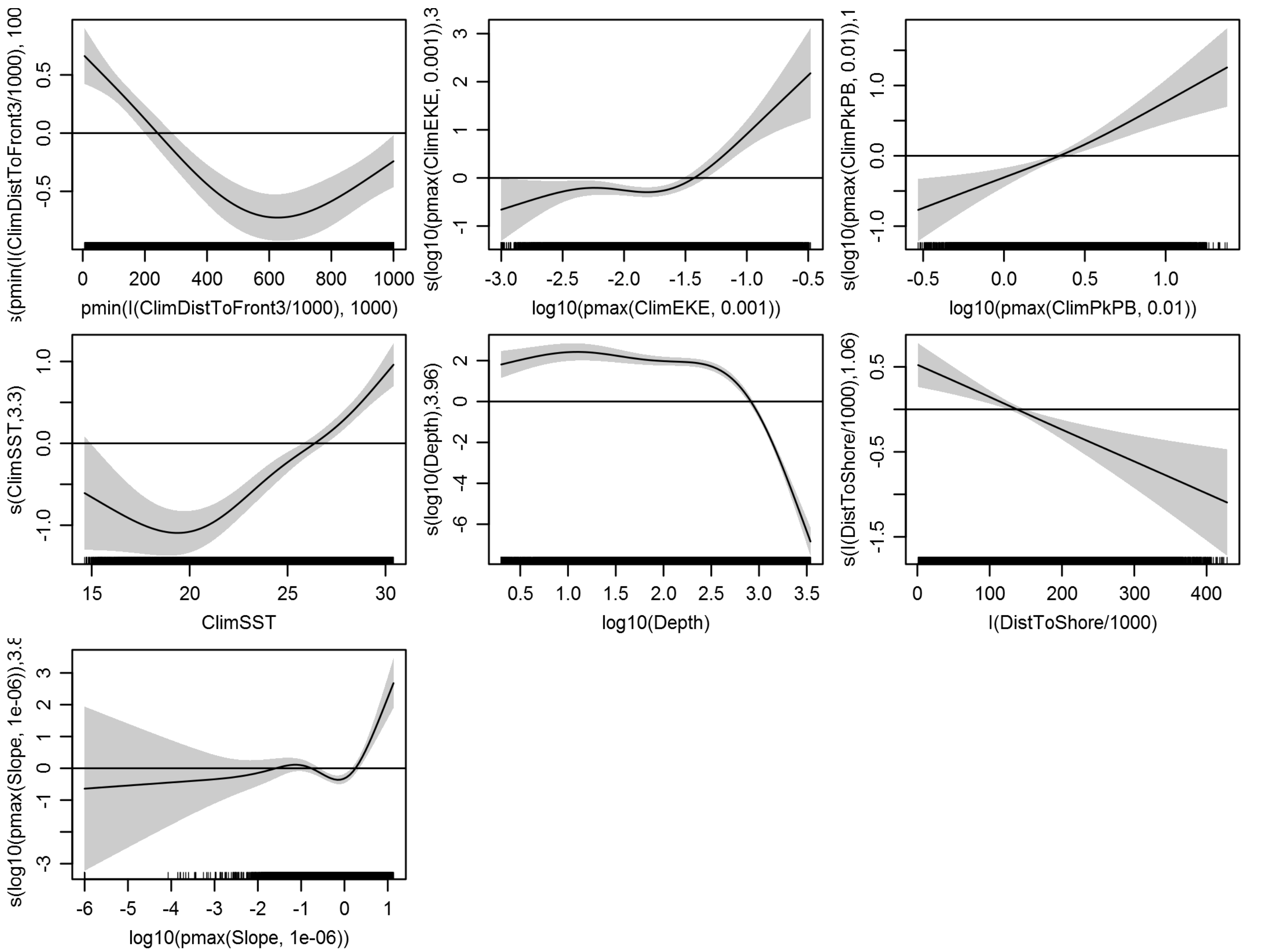

Diagnostic plots

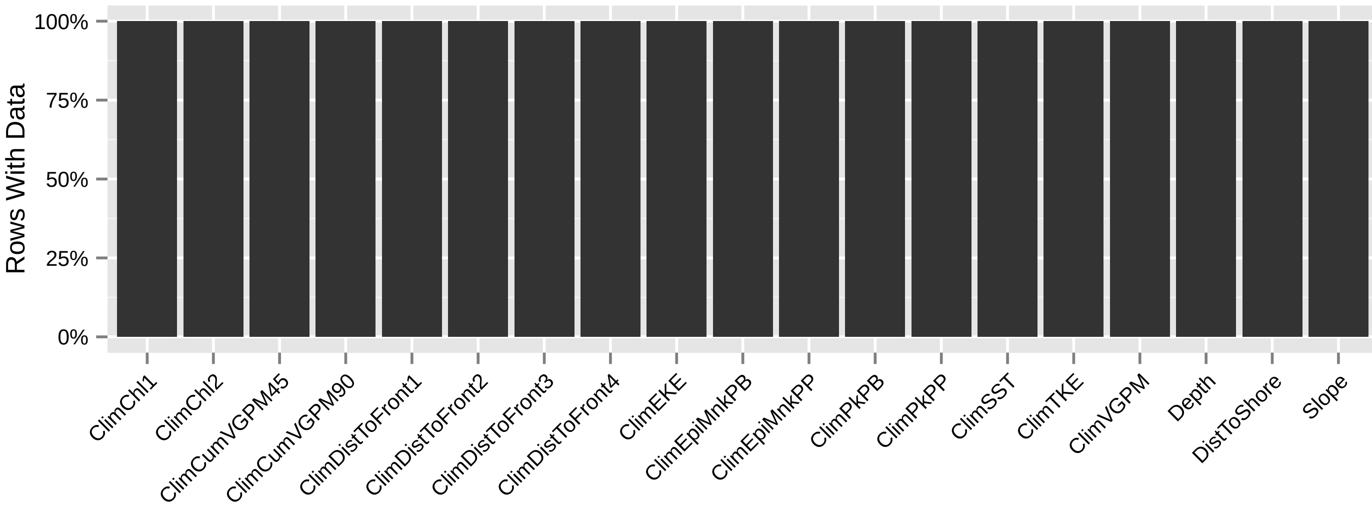

Figure 42: Segments with predictor values for the Bottlenose dolphin Climatological model, Surveyed Area. This plot is used to assess how many segments would be lost by including a given predictor in a model.

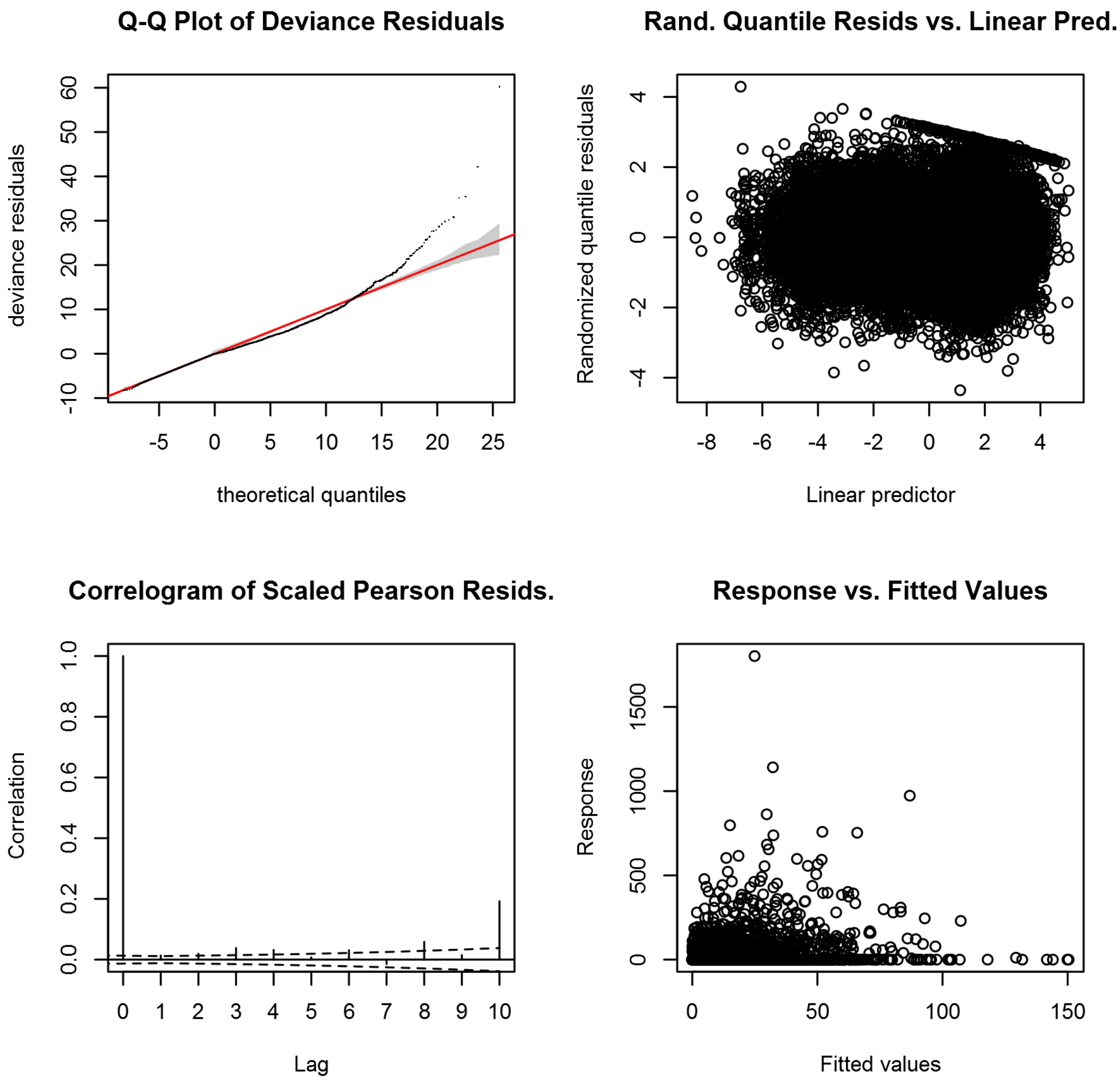

Figure 43: Statistical diagnostic plots for the Bottlenose dolphin Climatological model, Surveyed Area.

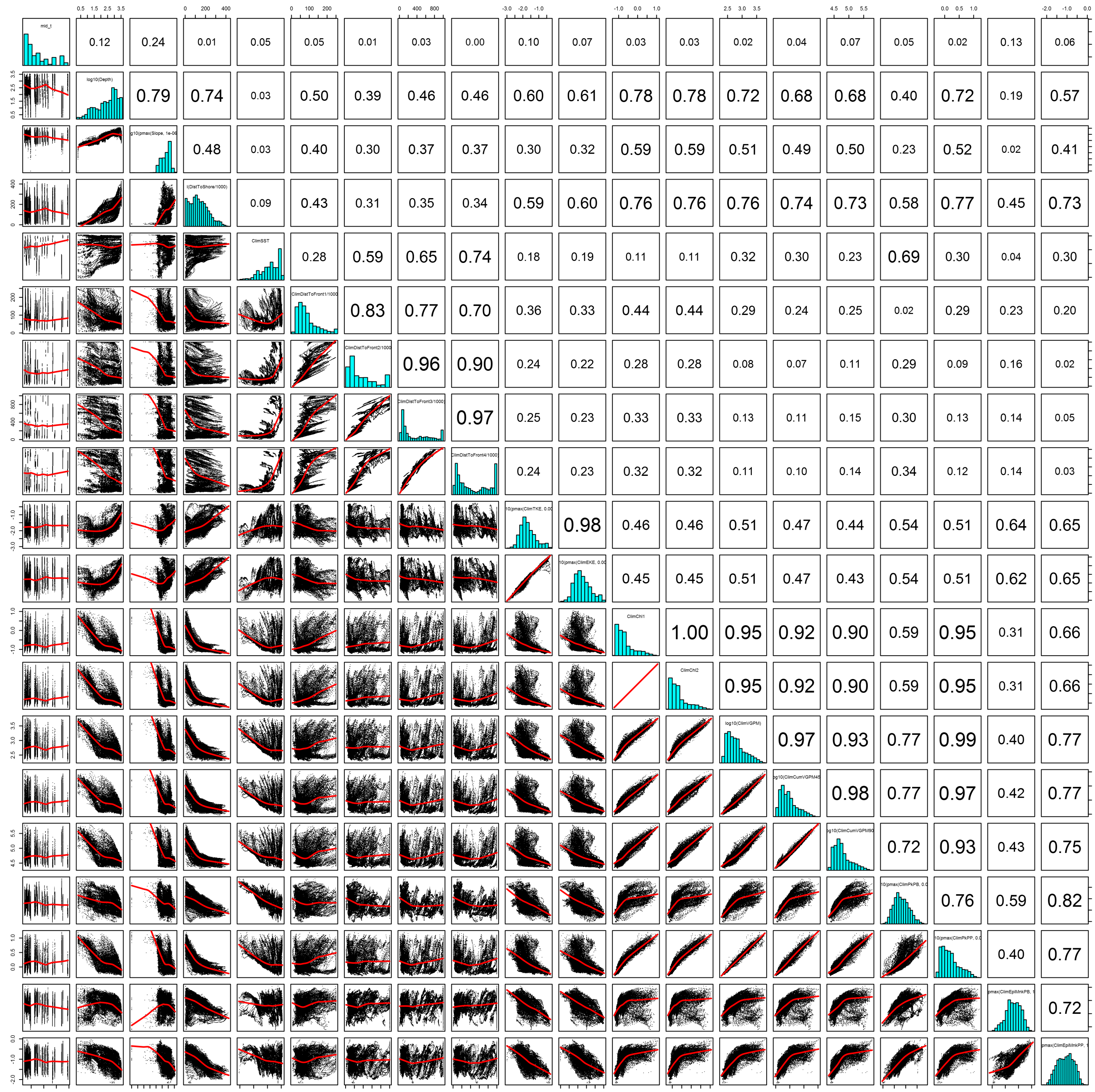

Figure 44: Scatterplot matrix for the Bottlenose dolphin Climatological model, Surveyed Area. This plot is used to inspect the distribution of predictors (via histograms along the diagonal), simple correlation between predictors (via pairwise Pearson coefficients above the diagonal), and linearity of predictor correlations (via scatterplots below the diagonal). This plot is best viewed at high magnification.

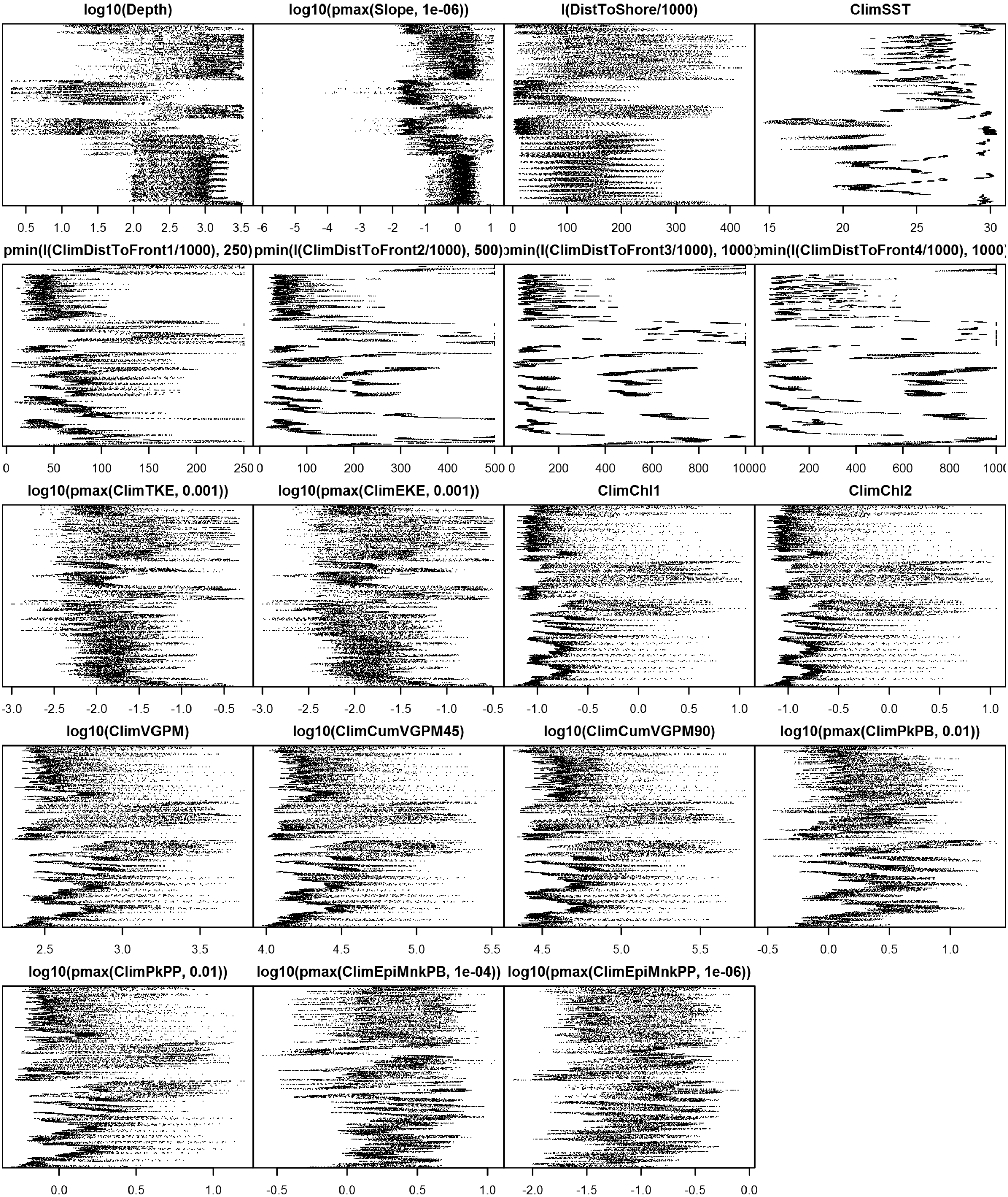

Figure 45: Dotplot for the Bottlenose dolphin Climatological model, Surveyed Area. This plot is used to check for suspicious patterns and outliers in the data. Points are ordered vertically by transect ID, sequentially in time.

Contemporaneous Model

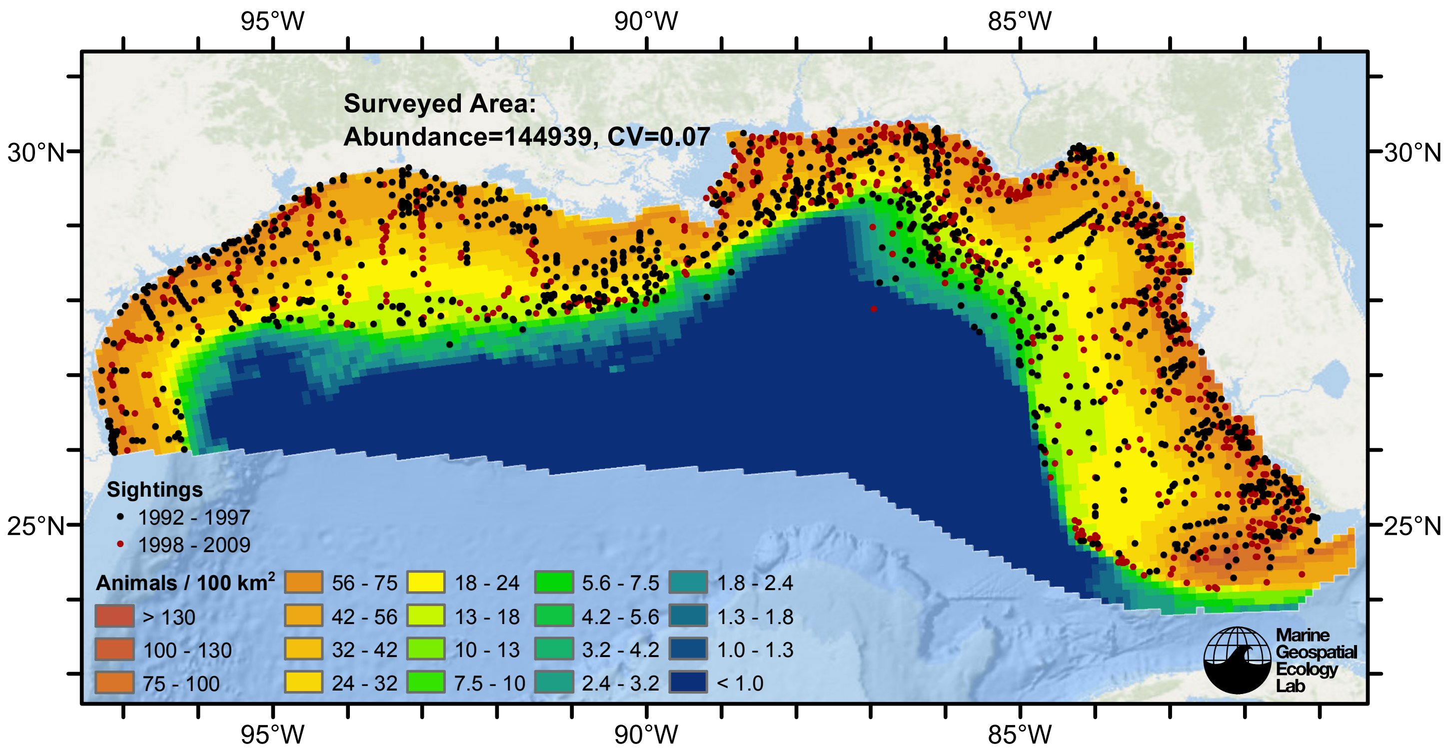

Figure 46: Bottlenose dolphin density predicted by the contemporaneous model that explained the most deviance. Pixels are 10x10 km. The legend gives the estimated individuals per pixel; breaks are logarithmic. Abundance for each region was computed by summing the density cells occuring in that region.

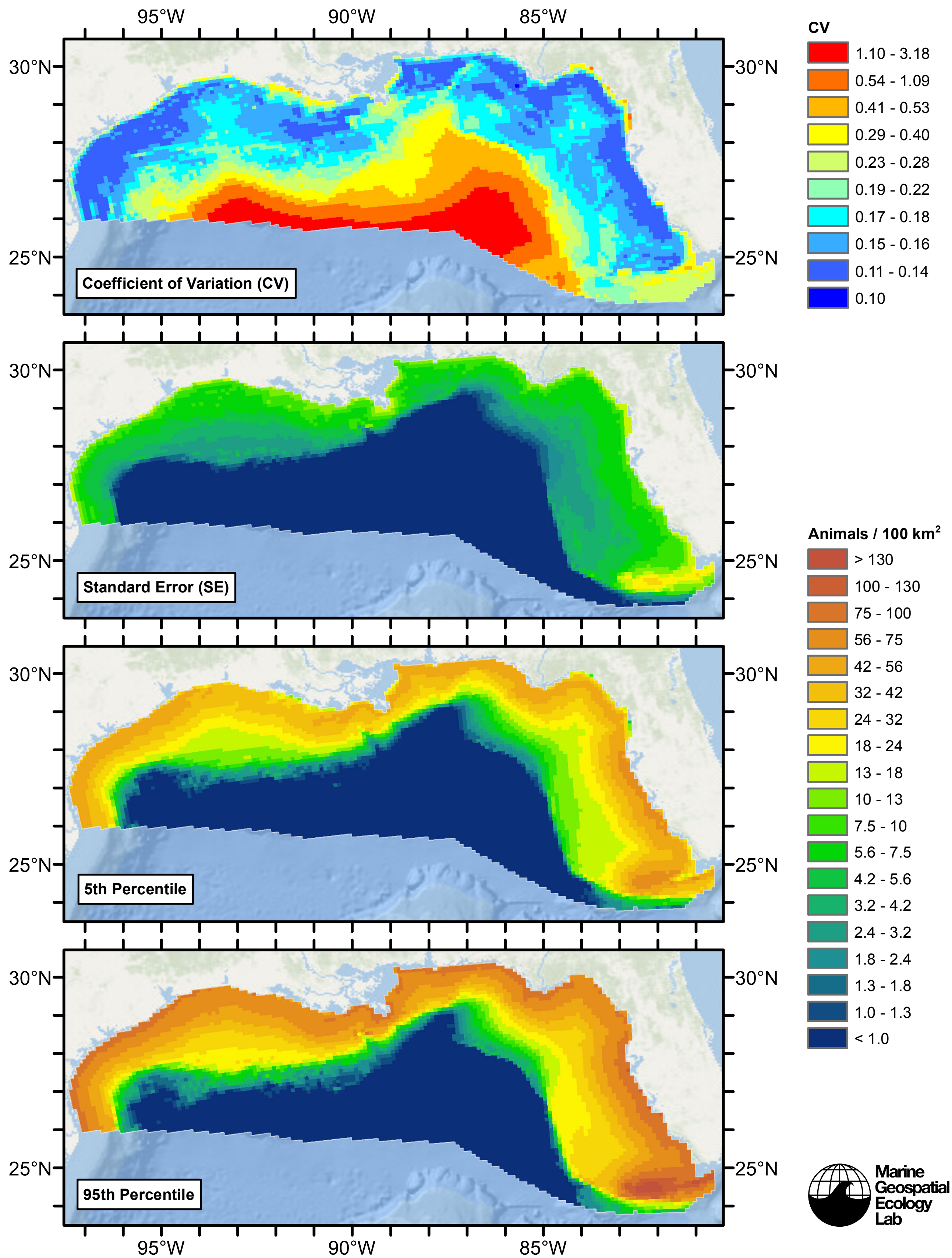

Figure 47: Estimated uncertainty for the contemporaneous model that explained the most deviance. These estimates only incorporate the statistical uncertainty estimated for the spatial model (by the R mgcv package). They do not incorporate uncertainty in the detection functions, g(0) estimates, predictor variables, and so on.

Surveyed Area

Statistical output

```
Rscript.exe: This is mgcv 1.8-2. For overview type 'help("mgcv-package")'.


Family: Tweedie(p=1.458)
Link function: log

Formula:
abundance ~ offset(log(area_km2)) + s(log10(Depth), bs = "ts",
    k = 5) + s(log10(pmax(Slope, 1e-06)), bs = "ts", k = 5) +
    s(I(DistToShore/1000), bs = "ts", k = 5) + s(pmin(I(DistToFront4/1000),
    1000), bs = "ts", k = 5) + s(log10(pmax(PkPB, 0.01)), bs = "ts",
    k = 5)

Parametric coefficients:
            Estimate Std. Error t value Pr(>|t|)
(Intercept)  -3.6380     0.1475  -24.67   <2e-16 ***
---
Signif. codes:  0 '***' 0.001 '**' 0.01 '*' 0.05 '.' 0.1 ' ' 1

Approximate significance of smooth terms:
                                   edf Ref.df      F  p-value
s(log10(Depth))                 3.7787      4 43.837  < 2e-16 ***
s(log10(pmax(Slope, 1e-06)))    3.3562      4  5.708 2.32e-05 ***
s(I(DistToShore/1000))          3.5987      4  9.089 4.67e-08 ***
s(pmin(I(DistToFront4/1000), 1000)) 0.9337      4  2.212  0.00144 **
s(log10(pmax(PkPB, 0.01)))      0.9561      4  2.287  0.00127 **
---
Signif. codes:  0 '***' 0.001 '**' 0.01 '*' 0.05 '.' 0.1 ' ' 1

R-sq.(adj) =  0.0889   Deviance explained = 31.9%
-REML = 4851.2  Scale est. = 42.684    n = 6420

All predictors were significant. This is the final model.
Creating term plots.
Diagnostic output from gam.check():

Method: REML   Optimizer: outer newton
full convergence after 12 iterations.
Gradient range [-2.68444e-07,3.789692e-09]
(score 4851.238 & scale 42.68401).
Hessian positive definite, eigenvalue range [0.3800128,1174.845].
Model rank =  21 / 21

Basis dimension (k) checking results. Low p-value (k-index<1) may
indicate that k is too low, especially if edf is close to k'.

                                       k'   edf k-index p-value
s(log10(Depth))                     4.000 3.779   0.643    0.00
s(log10(pmax(Slope, 1e-06)))        4.000 3.356   0.706    0.48
s(I(DistToShore/1000))              4.000 3.599   0.659    0.00
s(pmin(I(DistToFront4/1000), 1000)) 4.000 0.934   0.695    0.14
s(log10(pmax(PkPB, 0.01)))          4.000 0.956   0.719    0.94

Predictors retained during the model selection procedure: Depth, Slope, DistToShore, DistToFront4,
PkPB
```

```
Predictors dropped during the model selection procedure: SST, TKE
```

Model term plots

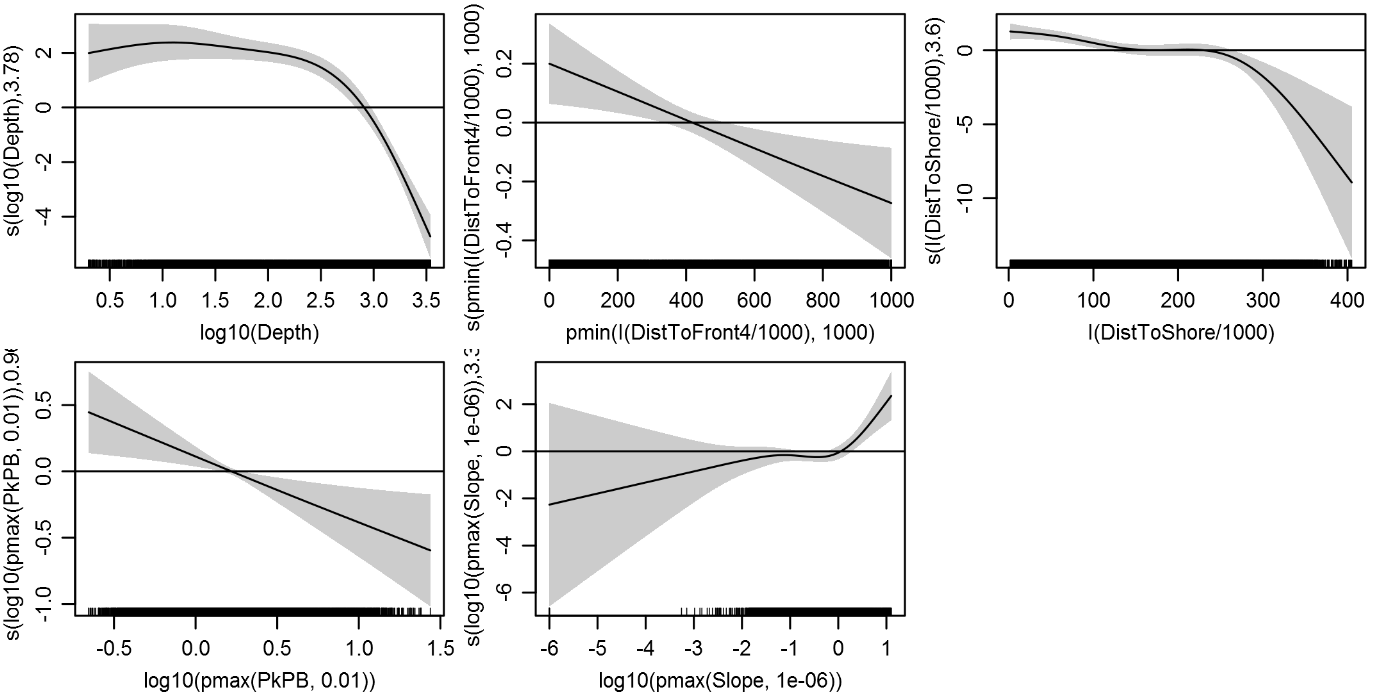

Diagnostic plots

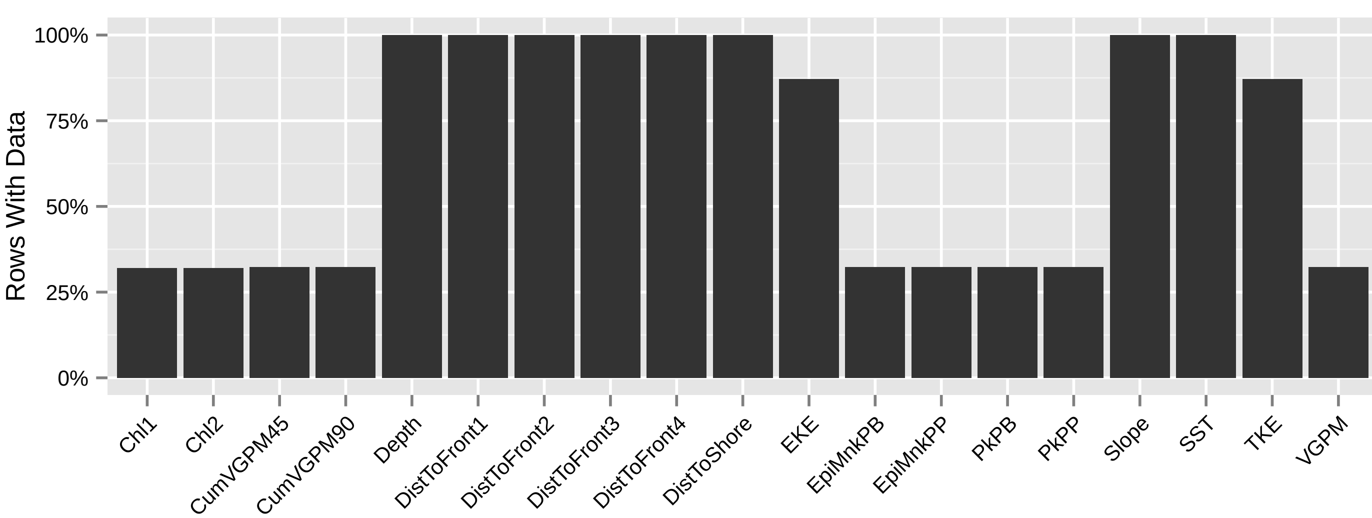

Figure 48: Segments with predictor values for the Bottlenose dolphin Contemporaneous model, Surveyed Area. This plot is used to assess how many segments would be lost by including a given predictor in a model.

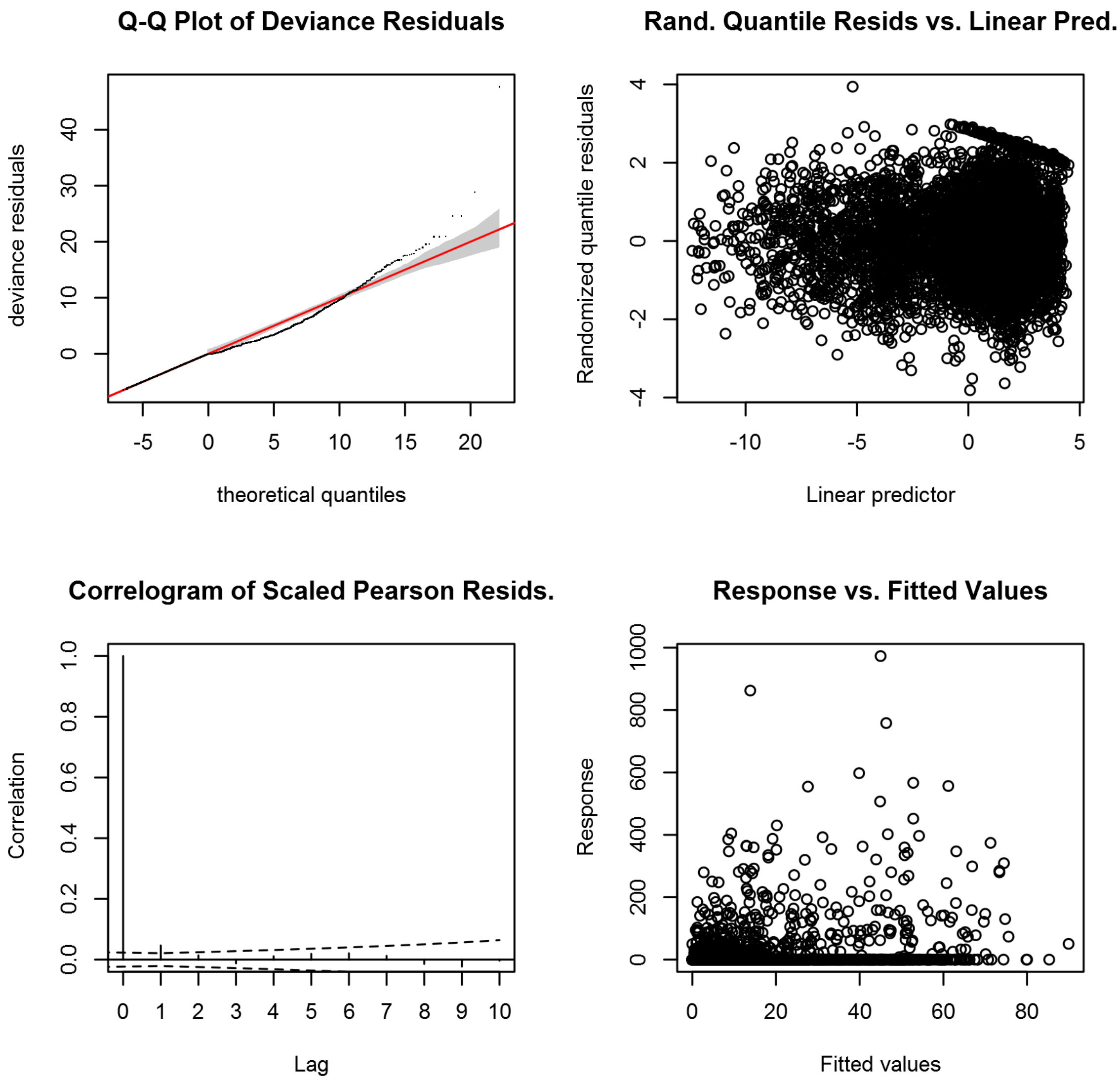

Figure 49: Statistical diagnostic plots for the Bottlenose dolphin Contemporaneous model, Surveyed Area.

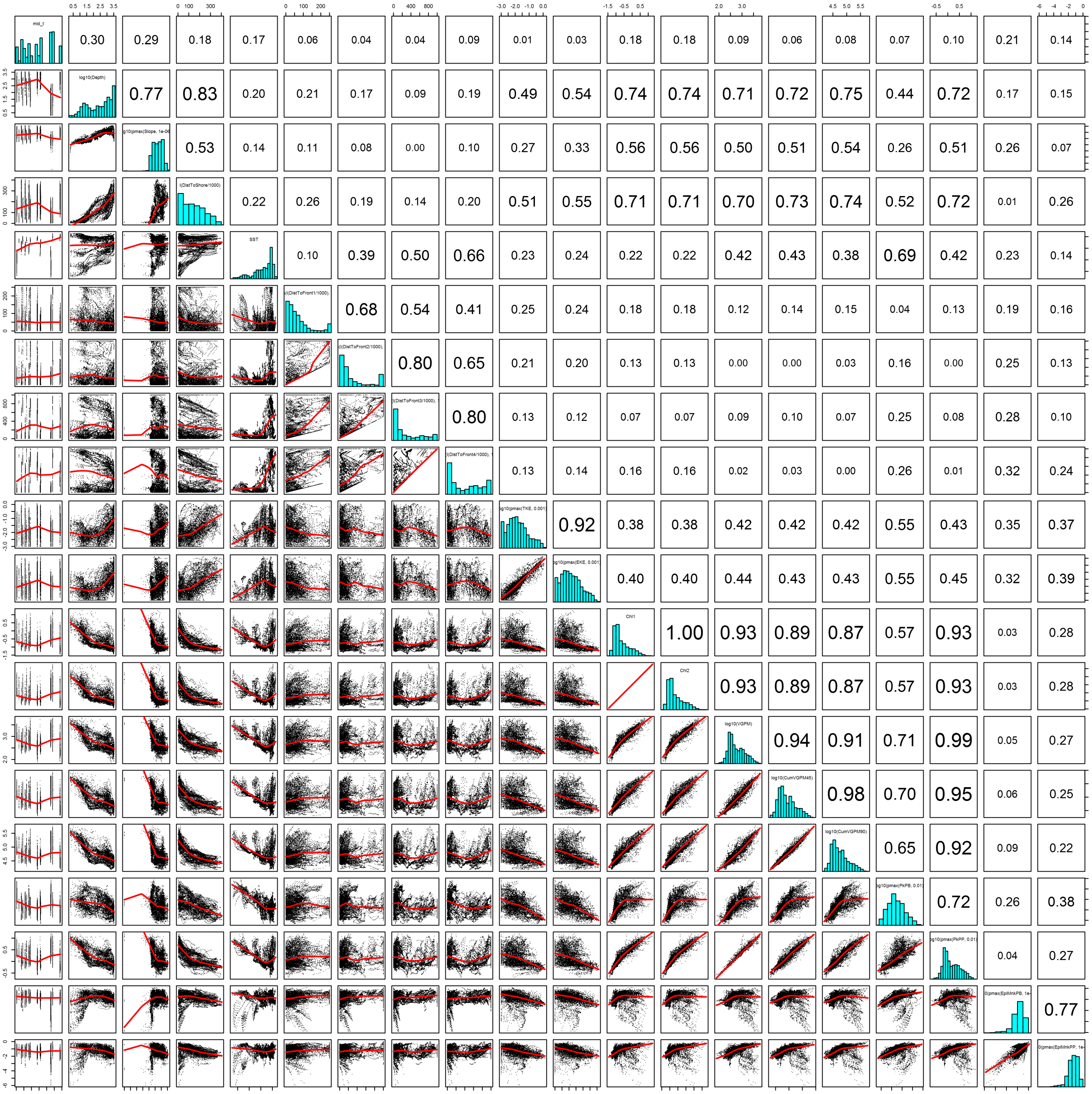

Figure 50: Scatterplot matrix for the Bottlenose dolphin Contemporaneous model, Surveyed Area. This plot is used to inspect the distribution of predictors (via histograms along the diagonal), simple correlation between predictors (via pairwise Pearson coefficients above the diagonal), and linearity of predictor correlations (via scatterplots below the diagonal). This plot is best viewed at high magnification.

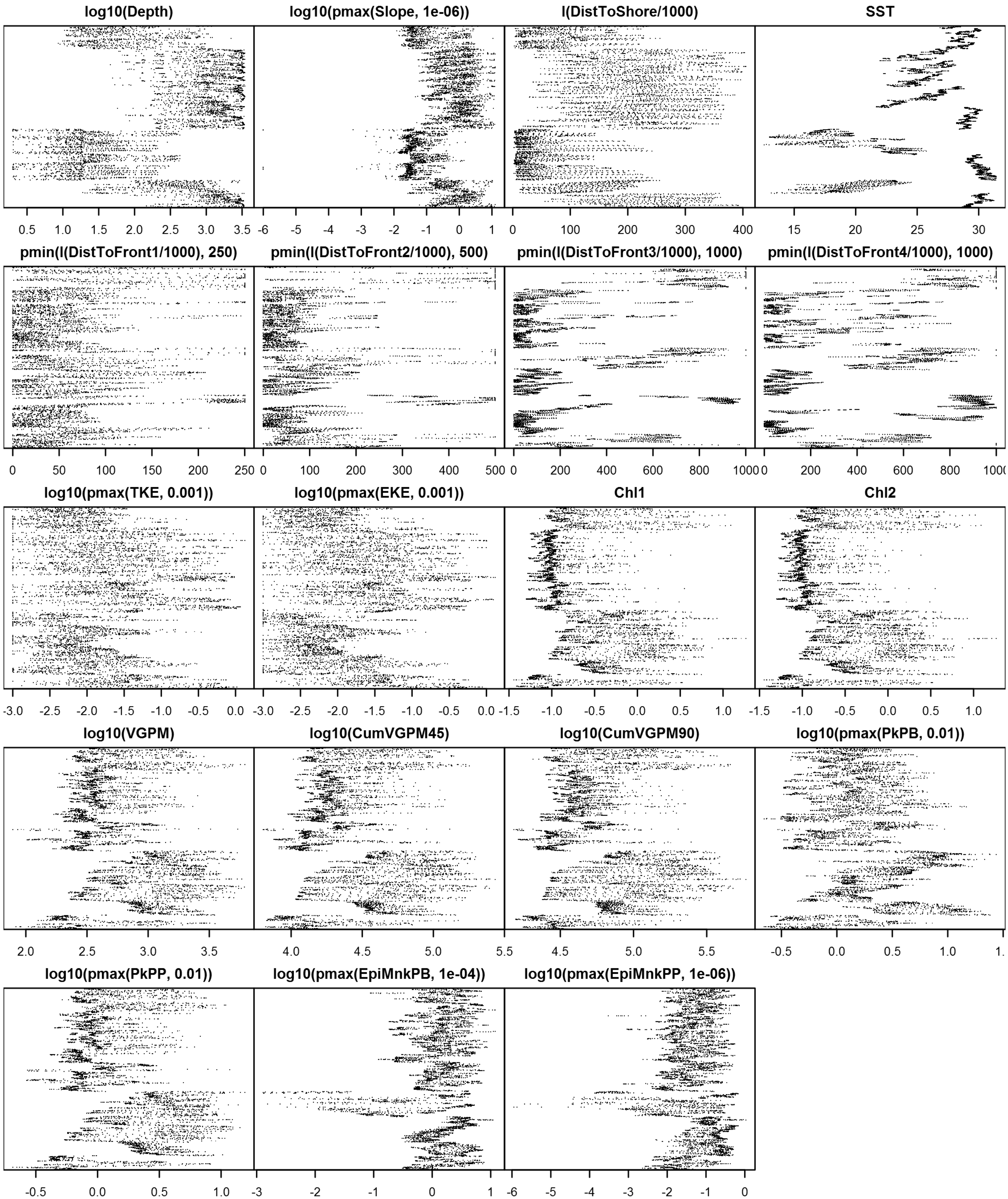

Figure 51: Dotplot for the Bottlenose dolphin Contemporaneous model, Surveyed Area. This plot is used to check for suspicious patterns and outliers in the data. Points are ordered vertically by transect ID, sequentially in time.

Climatological Same Segments Model

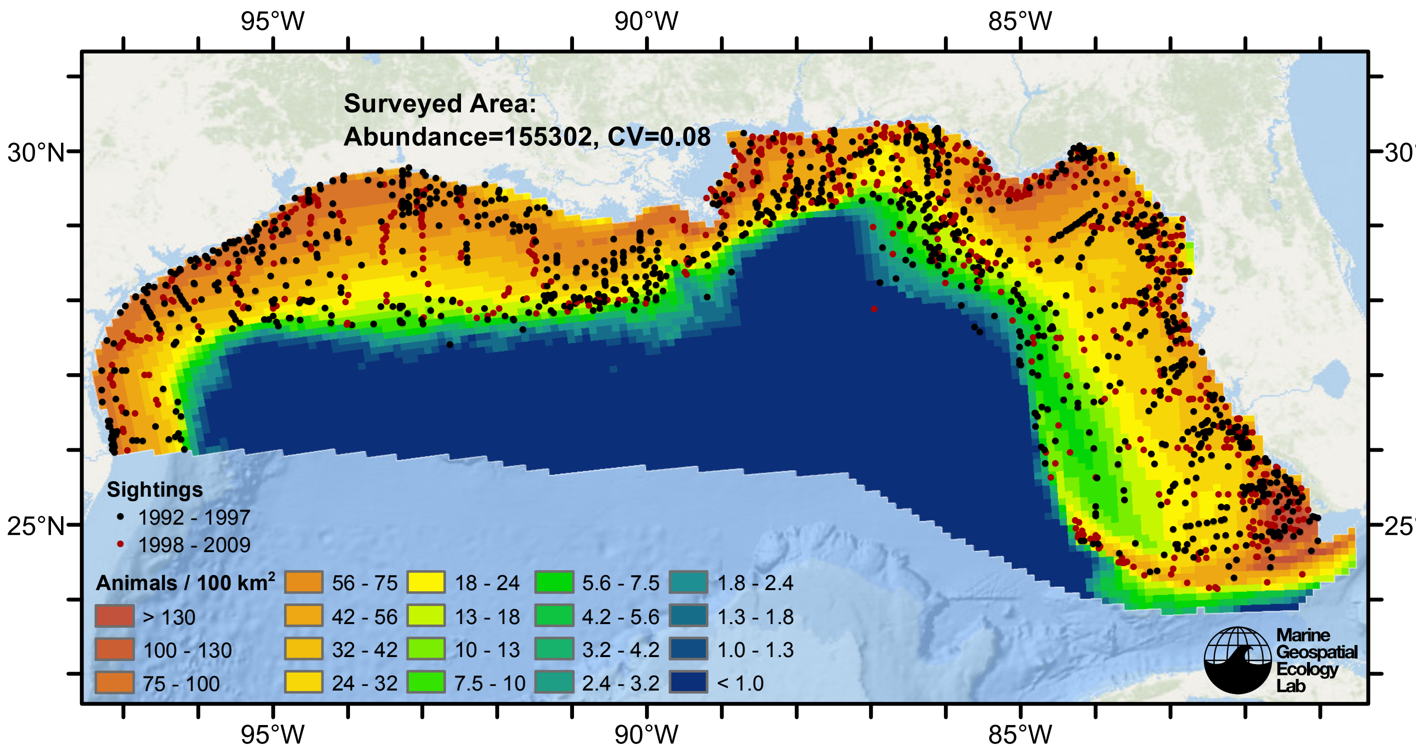

Figure 52: Bottlenose dolphin density predicted by the climatological same segments model that explained the most deviance. Pixels are 10x10 km. The legend gives the estimated individuals per pixel; breaks are logarithmic. Abundance for each region was computed by summing the density cells occuring in that region.

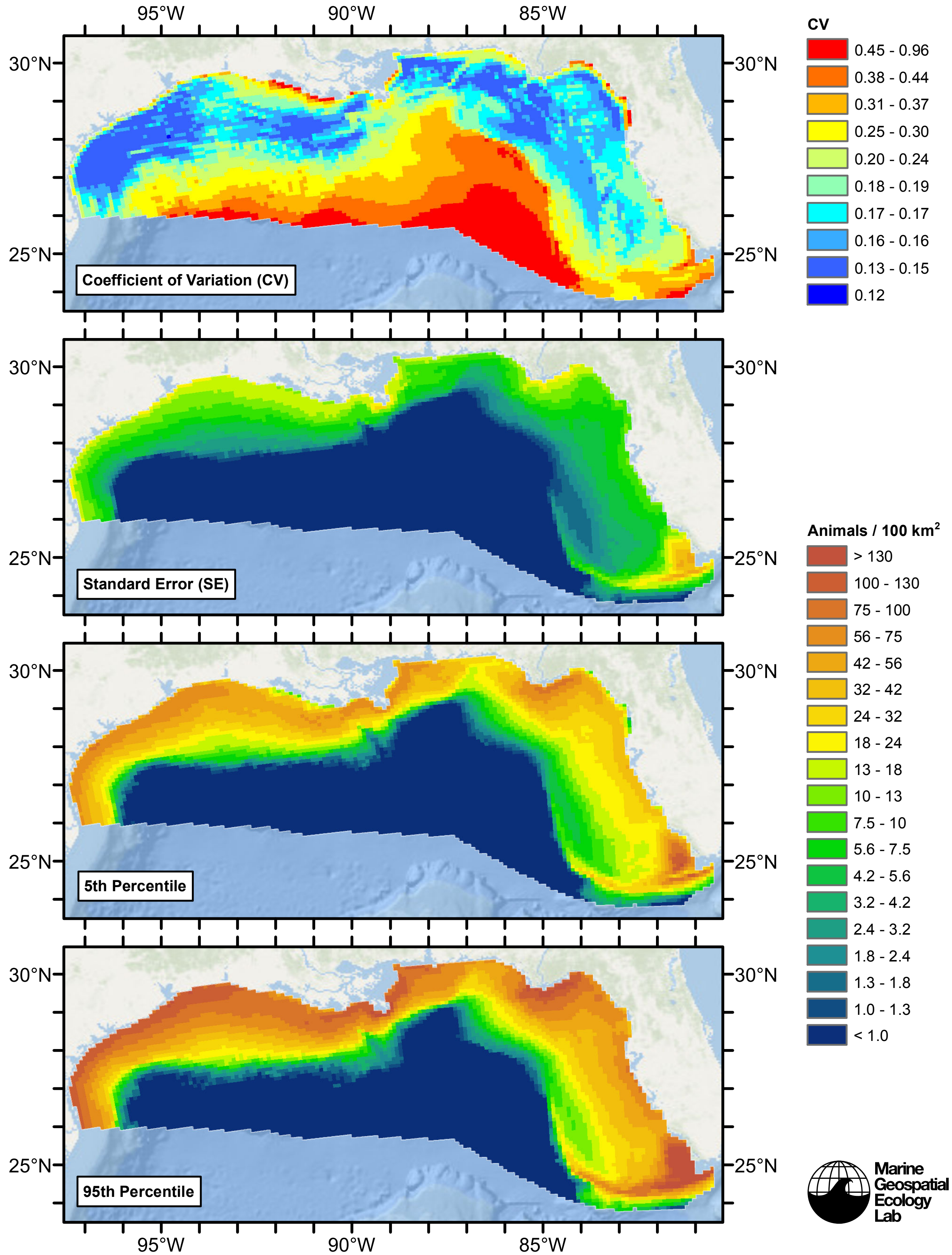

Figure 53: Estimated uncertainty for the climatological same segments model that explained the most deviance. These estimates only incorporate the statistical uncertainty estimated for the spatial model (by the R mgcv package). They do not incorporate uncertainty in the detection functions, g(0) estimates, predictor variables, and so on.

Surveyed Area

Statistical output

```
Rscript.exe: This is mgcv 1.8-2. For overview type 'help("mgcv-package")'.


Family: Tweedie(p=1.442)
Link function: log

Formula:
abundance ~ offset(log(area_km2)) + s(log10(Depth), bs = "ts",
    k = 5) + s(log10(pmax(Slope, 1e-06)), bs = "ts", k = 5) +
    s(I(DistToShore/1000), bs = "ts", k = 5) + s(pmin(I(ClimDistToFront3/1000),
    1000), bs = "ts", k = 5) + s(log10(pmax(ClimEKE, 0.001)),
    bs = "ts", k = 5) + s(log10(pmax(ClimEpiMnkPB, 1e-04)), bs = "ts",
    k = 5)

Parametric coefficients:
            Estimate Std. Error t value Pr(>|t|)
(Intercept) -3.42189    0.09839  -34.78   <2e-16 ***
---
Signif. codes:  0 '***' 0.001 '**' 0.01 '*' 0.05 '.' 0.1 ' ' 1

Approximate significance of smooth terms:
                                      edf Ref.df      F  p-value
s(log10(Depth))                     3.854      4 55.365  < 2e-16 ***
s(log10(pmax(Slope, 1e-06)))        3.082      4  4.469  0.00019 ***
s(I(DistToShore/1000))              1.074      4  3.637 5.73e-05 ***
s(pmin(I(ClimDistToFront3/1000), 1000)) 2.603      4  3.000  0.00279 **
s(log10(pmax(ClimEKE, 0.001)))      3.592      4 14.314 4.63e-13 ***
s(log10(pmax(ClimEpiMnkPB, 1e-04)))     2.933      4  5.086 3.55e-05 ***
---
Signif. codes:  0 '***' 0.001 '**' 0.01 '*' 0.05 '.' 0.1 ' ' 1

R-sq.(adj) =  0.103   Deviance explained = 34.5%
-REML = 4832.3  Scale est. = 41.767    n = 6420

All predictors were significant. This is the final model.
Creating term plots.
Diagnostic output from gam.check():

Method: REML   Optimizer: outer newton
full convergence after 11 iterations.
Gradient range [-0.0003335767,5.237629e-05]
(score 4832.275 & scale 41.76662).
Hessian positive definite, eigenvalue range [0.3314811,1202.707].
Model rank =  25 / 25

Basis dimension (k) checking results. Low p-value (k-index<1) may
indicate that k is too low, especially if edf is close to k'.

                                           k'   edf k-index p-value
s(log10(Depth))                         4.000 3.854   0.691    0.00
s(log10(pmax(Slope, 1e-06)))            4.000 3.082   0.709    0.04
s(I(DistToShore/1000))                  4.000 1.074   0.686    0.00
s(pmin(I(ClimDistToFront3/1000), 1000)) 4.000 2.603   0.737    0.90
s(log10(pmax(ClimEKE, 0.001)))          4.000 3.592   0.703    0.02
s(log10(pmax(ClimEpiMnkPB, 1e-04)))     4.000 2.933   0.713    0.12
```

```
Predictors retained during the model selection procedure: Depth, Slope, DistToShore,
ClimDistToFront3, ClimEKE, ClimEpiMnkPB

Predictors dropped during the model selection procedure: ClimSST
```

Model term plots

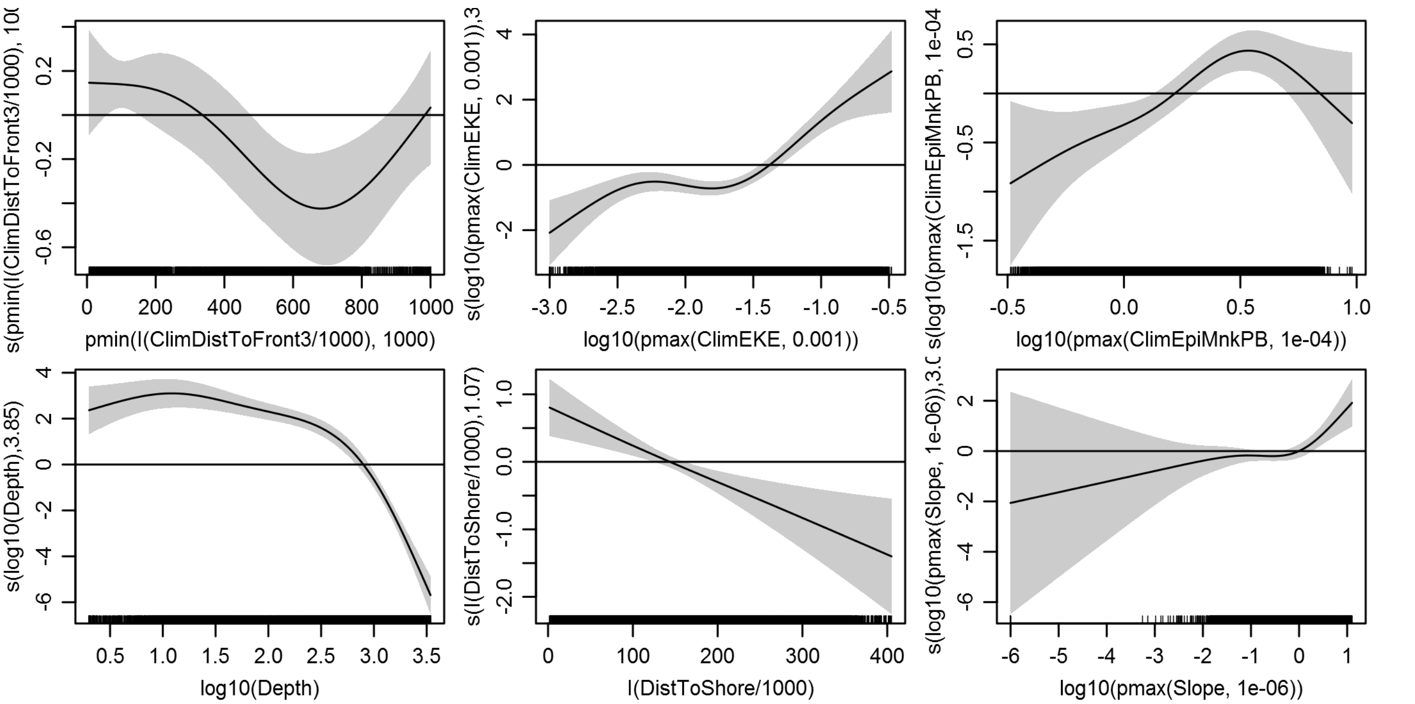

Diagnostic plots

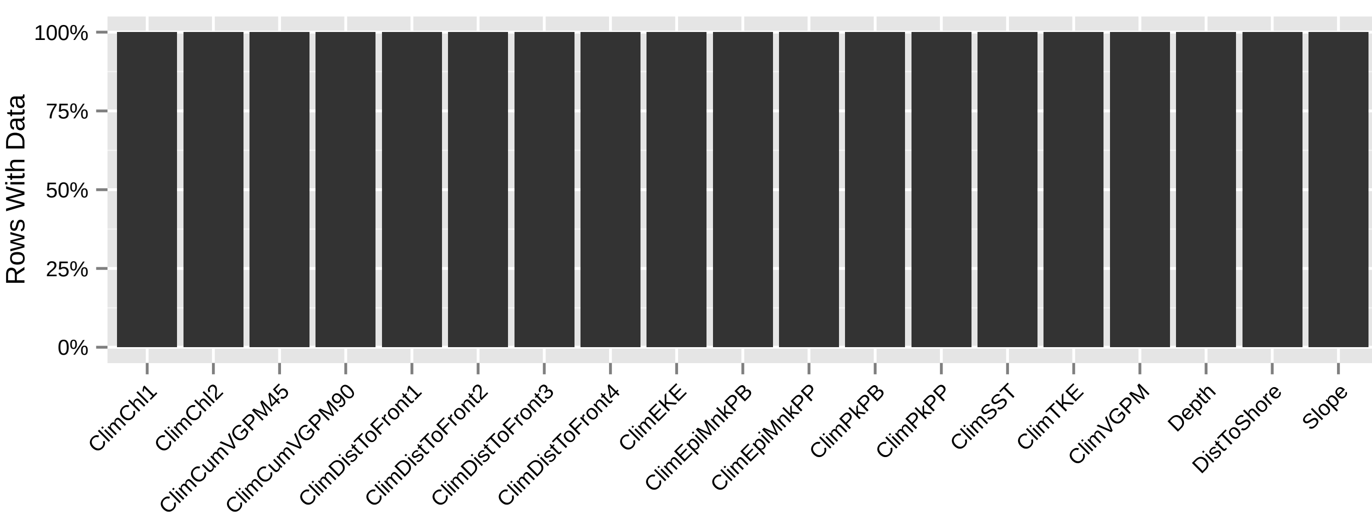

Figure 54: Segments with predictor values for the Bottlenose dolphin Climatological model, Surveyed Area. This plot is used to assess how many segments would be lost by including a given predictor in a model.

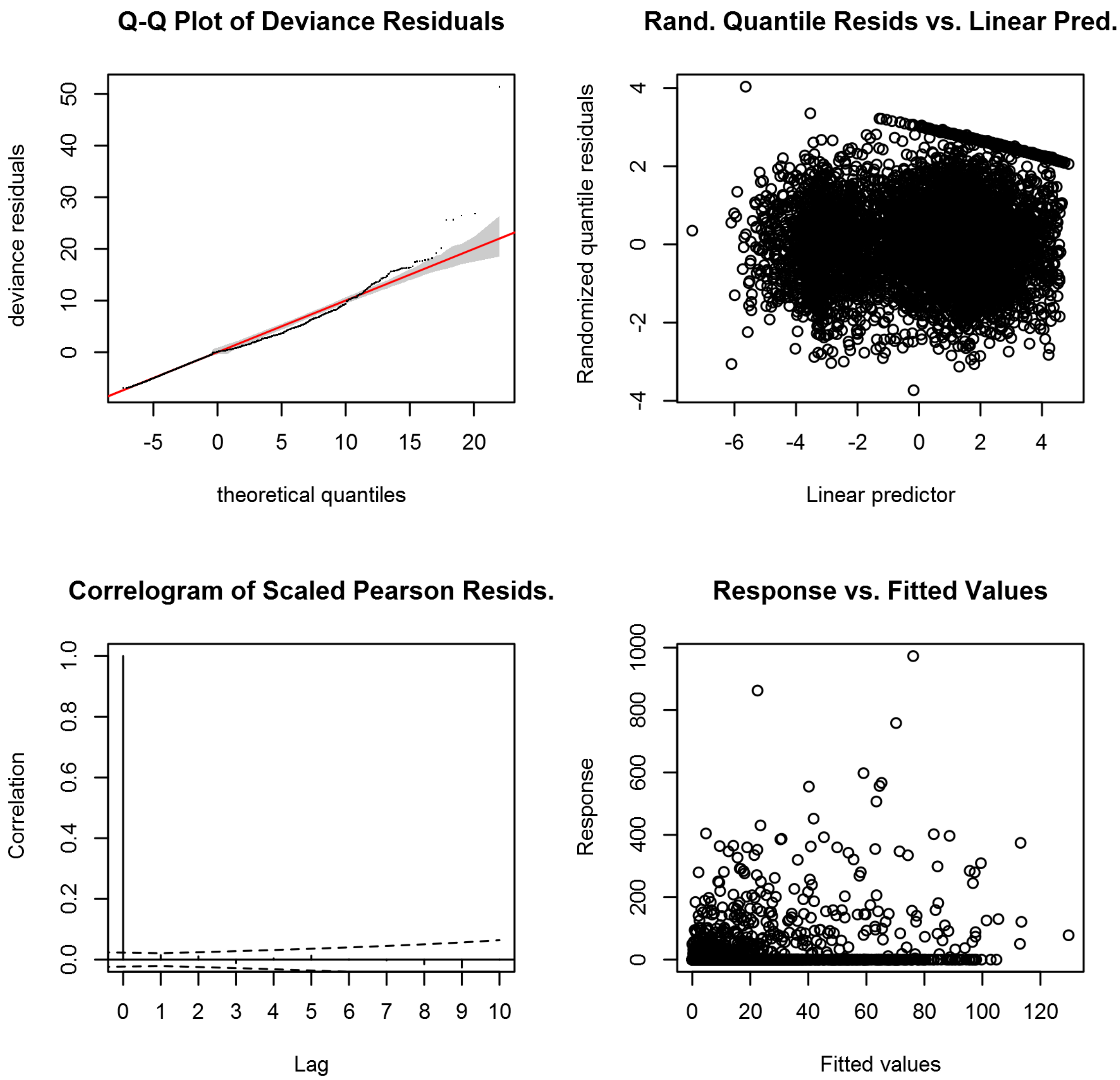

Figure 55: Statistical diagnostic plots for the Bottlenose dolphin Climatological model, Surveyed Area.

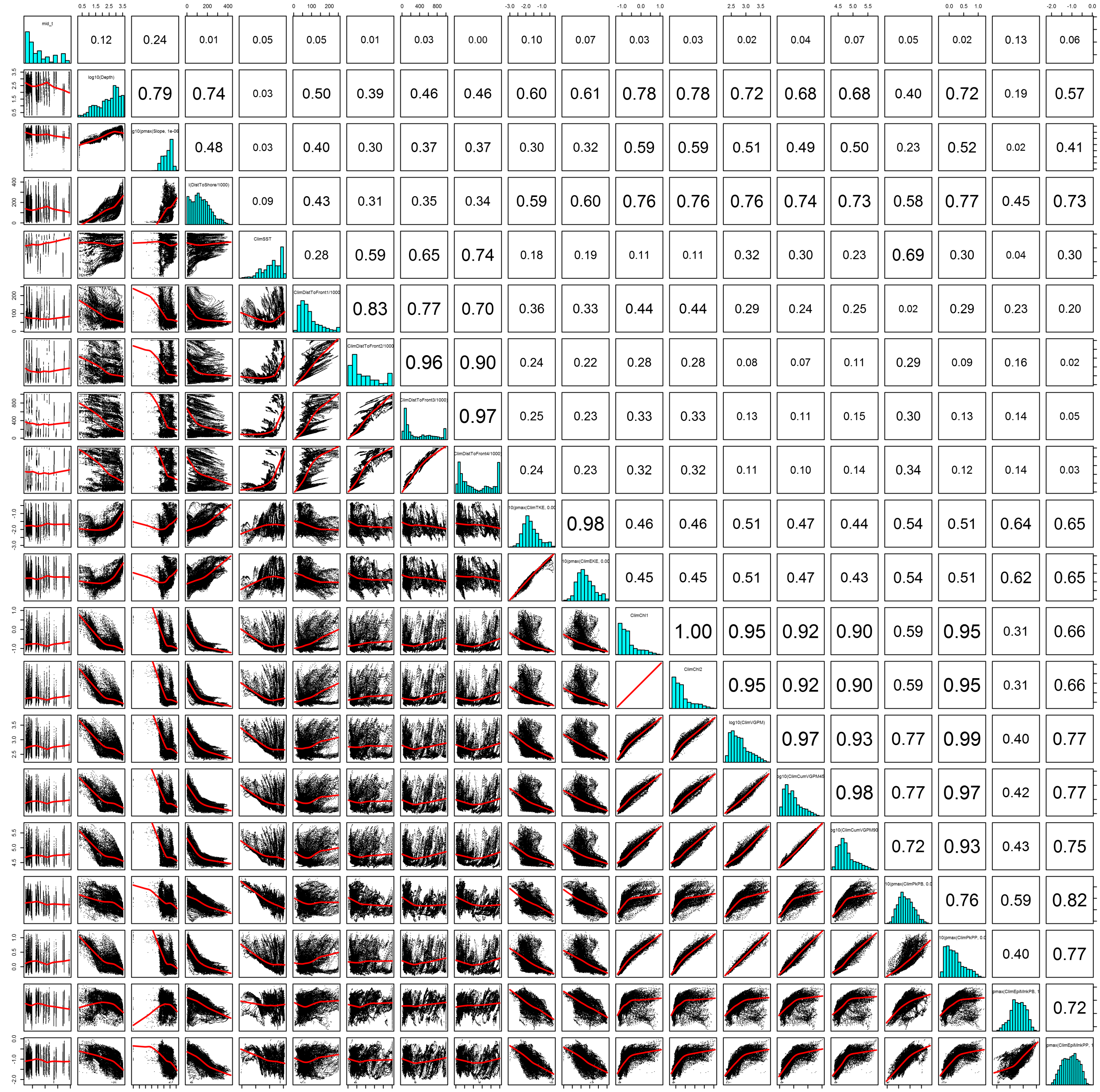

Figure 56: Scatterplot matrix for the Bottlenose dolphin Climatological model, Surveyed Area. This plot is used to inspect the distribution of predictors (via histograms along the diagonal), simple correlation between predictors (via pairwise Pearson coefficients above the diagonal), and linearity of predictor correlations (via scatterplots below the diagonal). This plot is best viewed at high magnification.

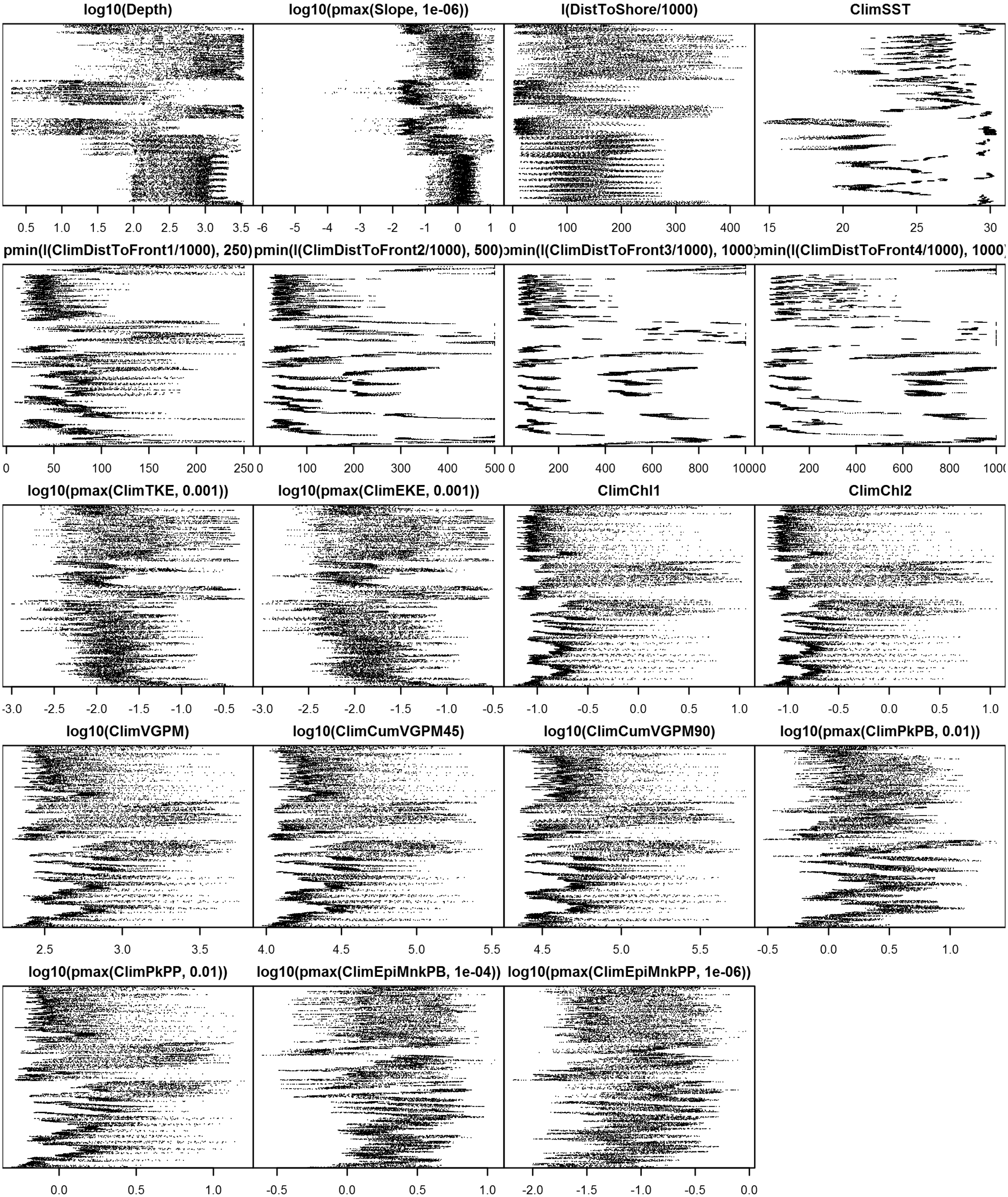

Figure 57: Dotplot for the Bottlenose dolphin Climatological model, Surveyed Area. This plot is used to check for suspicious patterns and outliers in the data. Points are ordered vertically by transect ID, sequentially in time.

Model Comparison

Spatial Model Performance

The table below summarizes the performance of the candidate spatial models that were tested. The first model contained only physiographic predictors. Subsequent models added additional suites of predictors of based on when they became available via remote sensing.

For each model, three versions were fitted; the % Dev Expl columns give the % deviance explained by each one. The "climatological" models were fitted to 8-day climatologies of the environmental predictors. Because the environmental predictors were always available, no segments were lost, allowing these models to consider the maximal amount of survey data. The "contemporaneous" models were fitted to day-of-sighting images of the environmental predictors; these were smoothed to reduce data loss due to clouds, but some segments still failed to retrieve environmental values and were lost. Finally, the "climatological same segments" models fitted climatological predictors to the segments retained by the contemporaneous model, so that the explantory power of the two types of predictors could be directly compared. For each of the three models, predictors were selected independently via shrinkage smoothers; thus the three models did not necessarily utilize the same predictors.

Predictors derived from ocean currents first became available in January 1993 after the launch of the TOPEX/Poseidon satellite; productivity predictors first became available in September 1997 after the launch of the SeaWiFS sensor. Contemporaneous and climatological same segments models considering these predictors usually suffered data loss. Date Range shows the years spanned by the retained segments. The Segments column gives the number of segments retained; % Lost gives the percentage lost.

Predictors	Climatol % Dev Expl	Contemp % Dev Expl	Climatol Same Segs % Dev Expl	Segments	% Lost	Date Range
Phys	30.6			19881		1992-2009
Phys+SST	32.1	30.8	32.1	19881	0.0	1992-2009
Phys+SST+Curr	32.6	30.8	32.6	19881	0.0	1992-2009
Phys+SST+Curr+Prod	32.9	31.9	34.5	6420	67.7	1998-2009

Table 19: Deviance explained by the candidate density models.

Abundance Estimates

The table below shows the estimated mean abundance (number of animals) within the study area, for the models that explained the most deviance for each model type. Mean abundance was calculated by first predicting density maps for a series of time steps, then computing the abundance for each map, and then averaging the abundances. For the climatological models, we used 8-day climatologies, resulting in 46 abundance maps. For the contemporaneous models, we used daily images, resulting in 365 predicted abundance maps per year that the prediction spanned. The Dates column gives the dates to which the estimates apply. For our models, these are the years for which both survey data and remote sensing data were available.

The Assumed g(0)=1 column specifies whether the abundance estimate assumed that detection was certain along the survey trackline. Studies that assumed this did not correct for availability or perception bias, and therefore underestimated abundance. The In our models column specifies whether the survey data from the study was also used in our models. If not, the study provides a completely independent estimate of abundance.

Dates	Model or study	Estimated abundance	CV	Assumed g(0)=1	In our models
1992-2009	Climatological model*	138602	0.06	No	
1998-2009	Contemporaneous model	144939	0.07	No	
1992-2009	Climatological same segments model	155302	0.08	No	

2009	Oceanic stock (Waring et al. 2013)	5806	0.39	Yes	Yes
2011-2012	Continental shelf stock (Waring et al. 2015)	51192	0.10	No	No
2011-2012	Eastern coastal stock (Waring et al. 2015)	12388	0.13	No	No
2011-2012	Northern coastal stock (Waring et al. 2015)	7185	0.21	No	No
2011-2012	Western coastal stock (Waring et al. 2015)	20161	0.17	No	No
2009-2012	All stocks, combined	96732	0.07		
1992-2007	Spatiotemporal mismatches in earlier surveys confound production of an “All stocks, combined” estimate from earlier surveys				

Table 20: Estimated mean abundance within the study area. We selected the model marked with * as our best estimate of the abundance and distribution of this taxon. For comparison, independent abundance estimates from NOAA technical reports and/or the scientific literature are shown. Please see the Discussion section below for our evaluation of our models compared to the other estimates. Note that our abundance estimates are averaged over the whole year, while the other studies may have estimated abundance for specific months or seasons. Our coefficients of variation (CVs) underestimate the true uncertainty in our estimates, as they only incorporated the uncertainty of the GAM stage of our models. Other sources of uncertainty include the detection functions and g(0) estimates. It was not possible to incorporate these into our CVs without undertaking a computationally-prohibitive bootstrap; we hope to attempt that in a future version of our models.

Density Maps

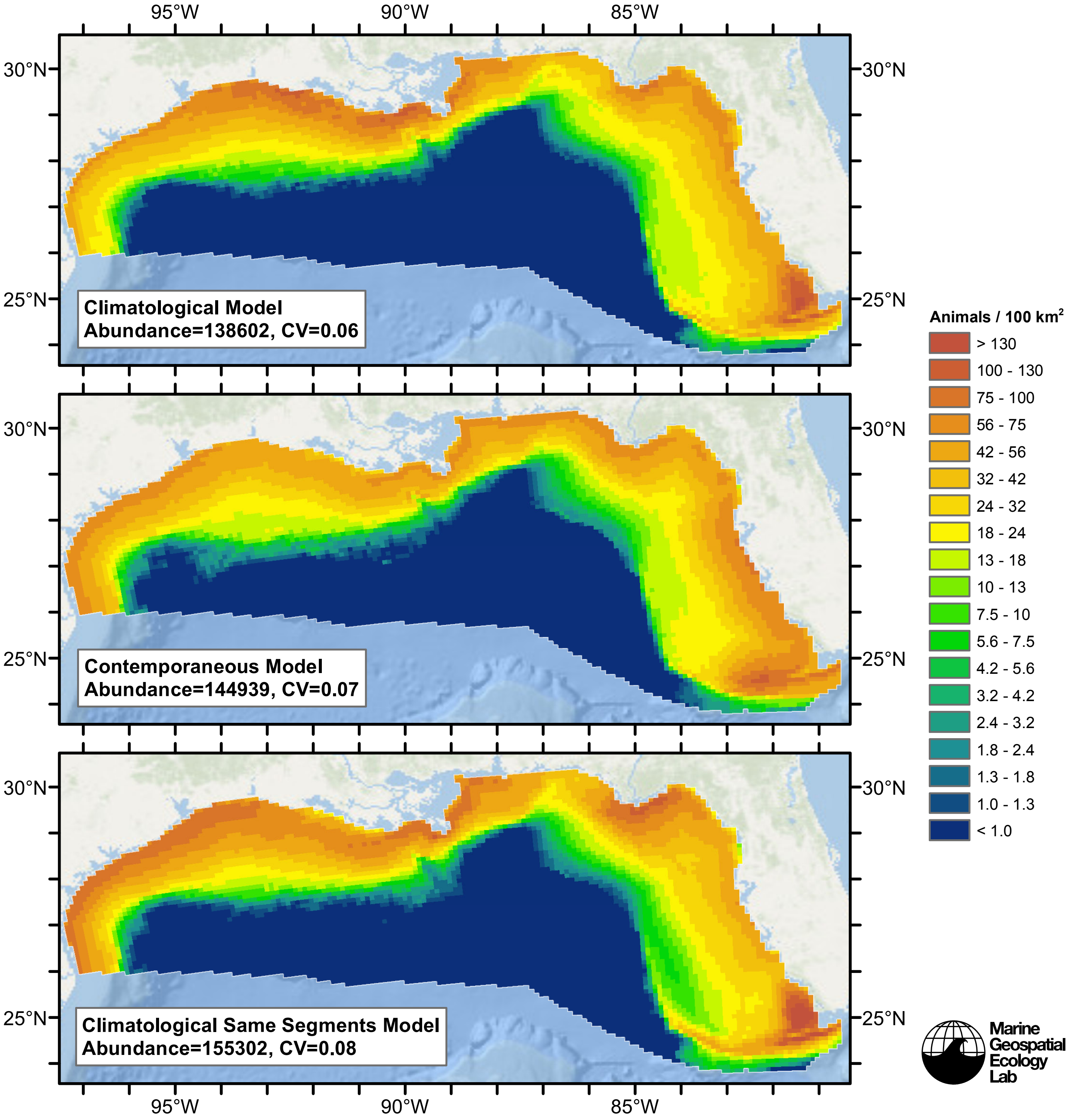

Figure 58: Bottlenose dolphin density and abundance predicted by the models that explained the most deviance. Regions inside the study area (white line) where the background map is visible are areas we did not model (see text).

Temporal Variability

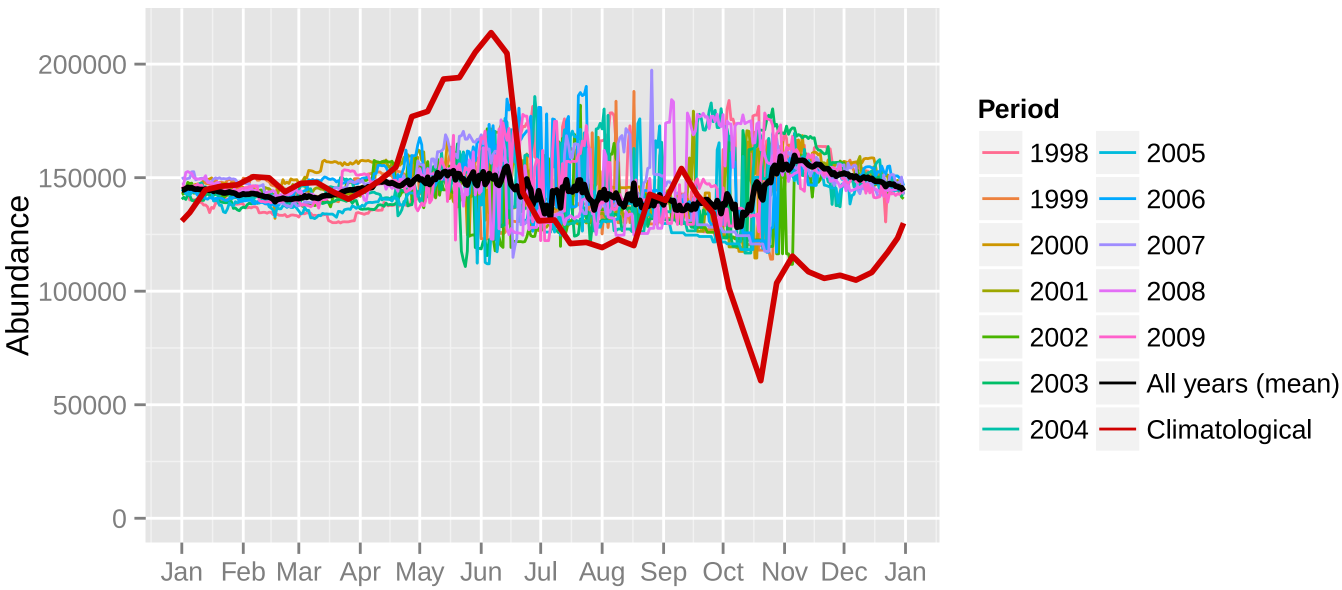

Figure 59: Comparison of Bottlenose dolphin abundance predicted at a daily time step for different time periods. Individual years were predicted using contemporaneous models. "All years (mean)" averages the individual years, giving the mean annual abundance of the contemporaneous model. "Climatological" was predicted using the climatological model. The results for the climatological same segments model are not shown.

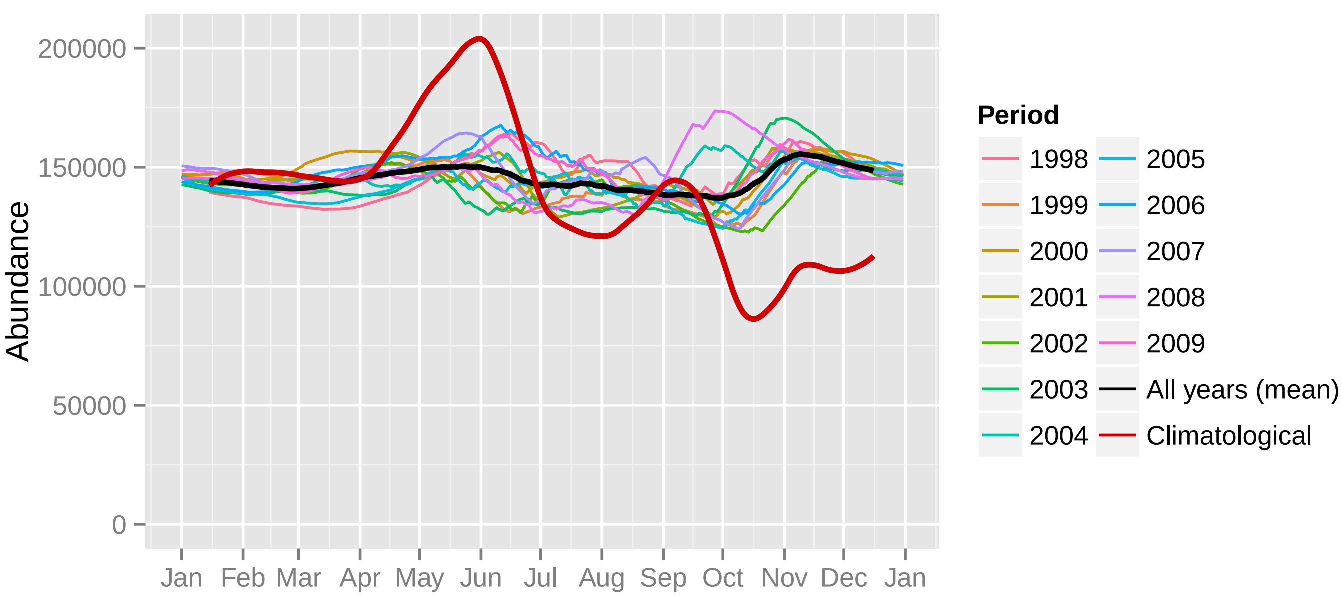

Figure 60: The same data as the preceding figure, but with a 30-day moving average applied.

Climatological Model

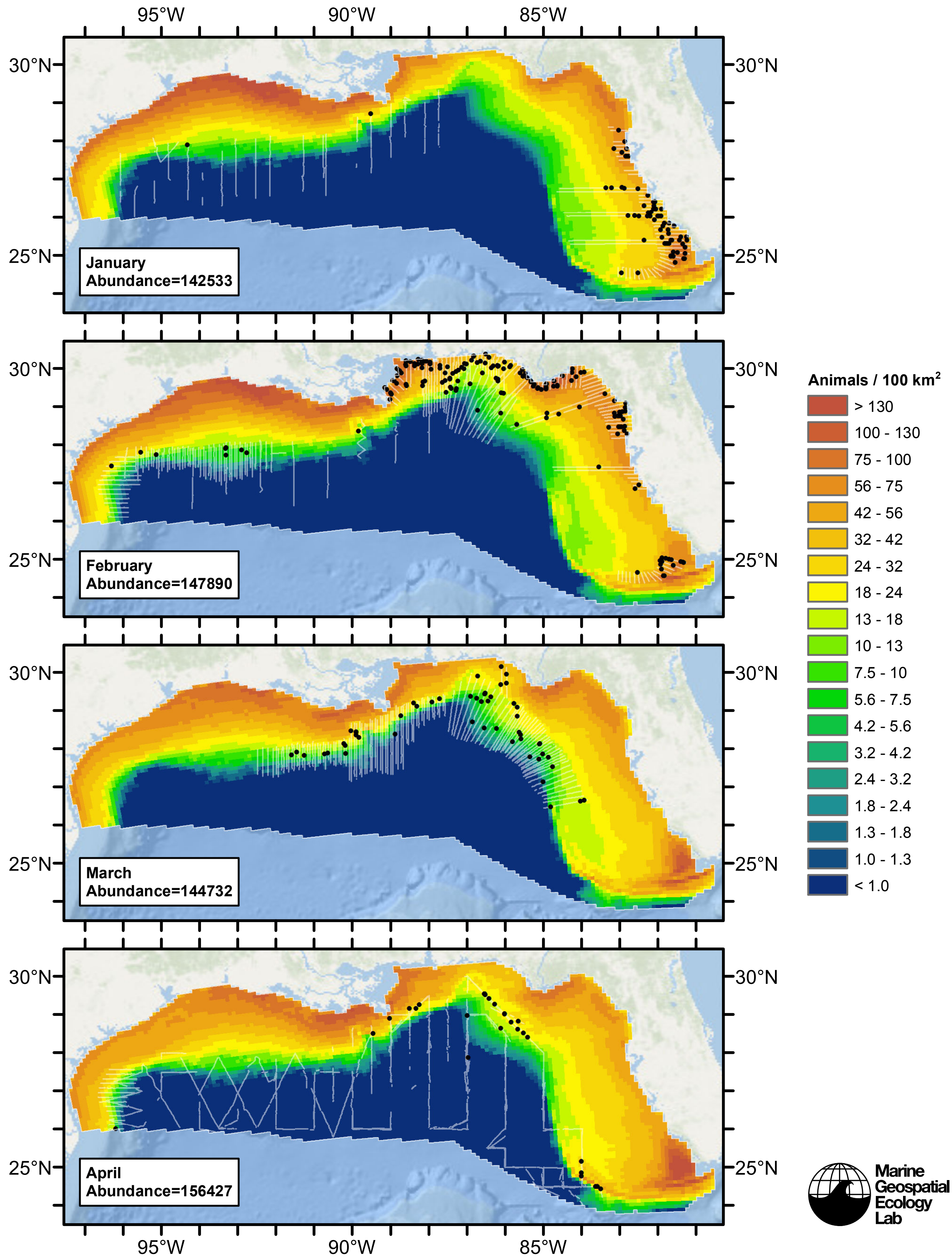

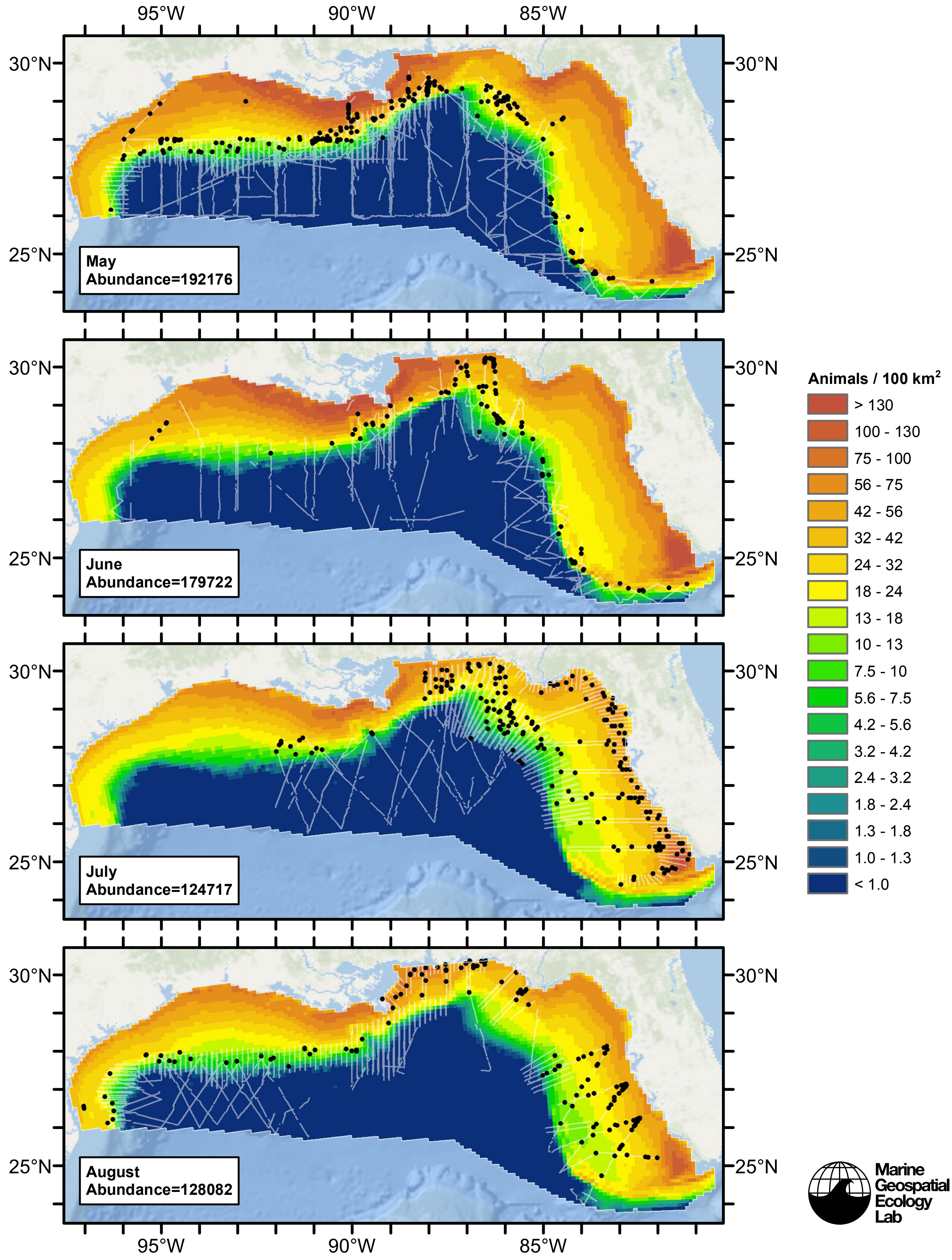
95°W
90°W
85°W
30°N
25°N
May
Abundance=192176
June
Abundance=179722
July
Abundance=124717
August
Abundance=128082
Animals / 100 km²
> 130
100 - 130
75 - 100
56 - 75
42 - 56
32 - 42
24 - 32
18 - 24
13 - 18
10 - 13
7.5 - 10
5.6 - 7.5
4.2 - 5.6
3.2 - 4.2
2.4 - 3.2
1.8 - 2.4
1.3 - 1.8
1.0 - 1.3
< 1.0
Marine Geospatial Ecology Lab

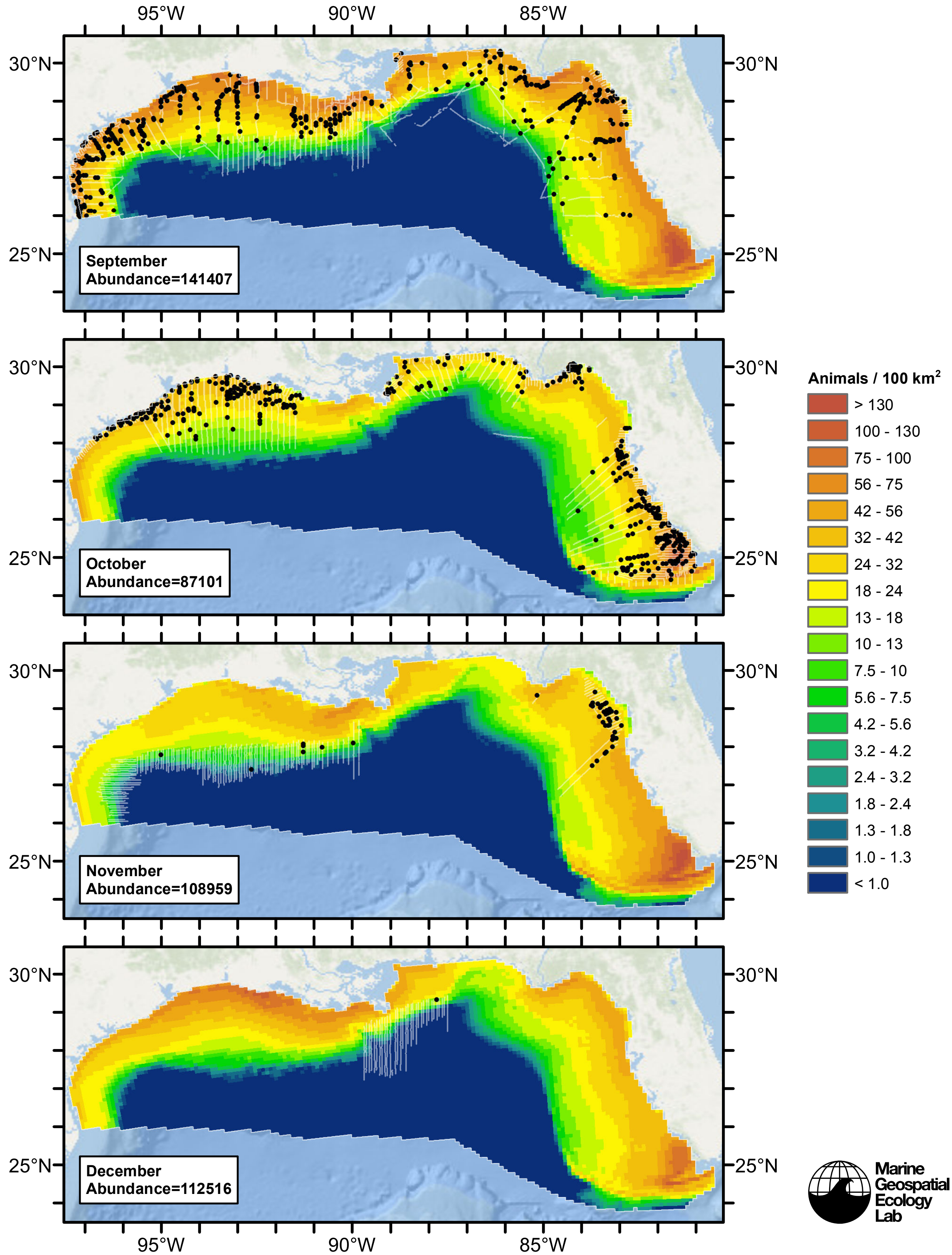

95°W
90°W
85°W
30°N
25°N
September
Abundance=141407
October
Abundance=87101
November
Abundance=108959
December
Abundance=112516
Animals / 100 km²
> 130
100 - 130
75 - 100
56 - 75
42 - 56
32 - 42
24 - 32
18 - 24
13 - 18
10 - 13
7.5 - 10
5.6 - 7.5
4.2 - 5.6
3.2 - 4.2
2.4 - 3.2
1.8 - 2.4
1.3 - 1.8
1.0 - 1.3
< 1.0
Marine Geospatial Ecology Lab

Contemporaneous Model

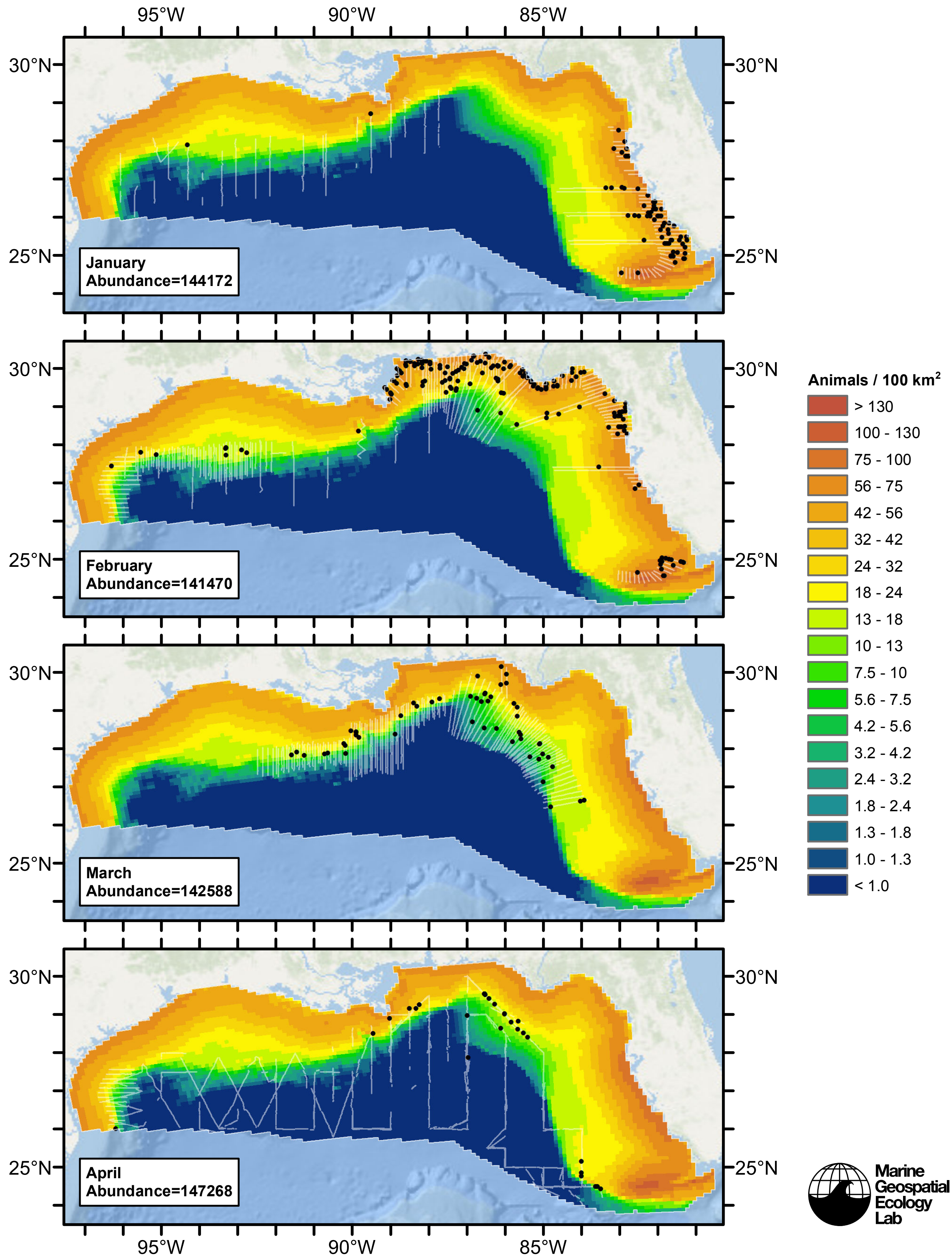

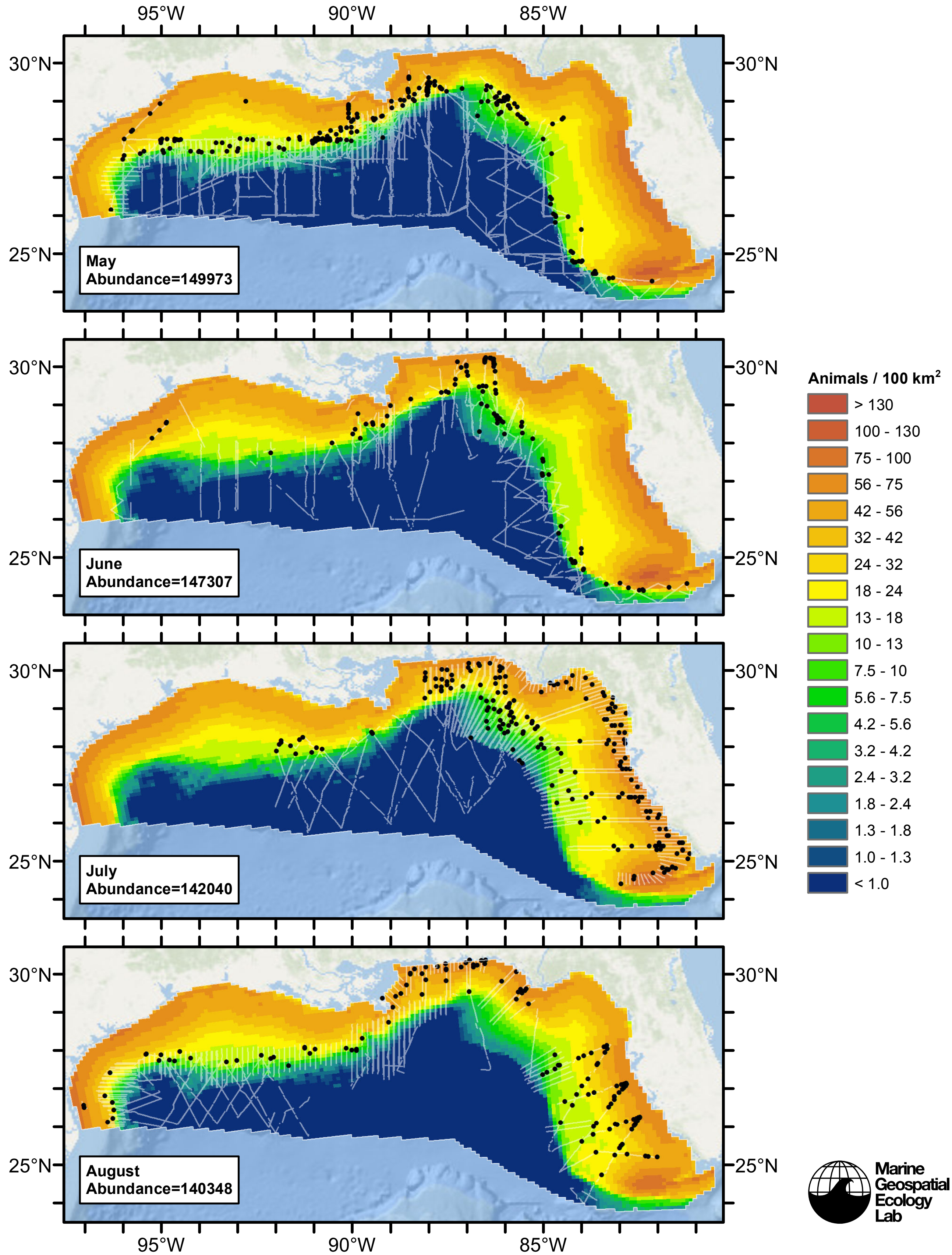
95°W
90°W
85°W
30°N
25°N
May
Abundance=149973
June
Abundance=147307
July
Abundance=142040
August
Abundance=140348
Animals / 100 km^2
> 130
100 - 130
75 - 100
56 - 75
42 - 56
32 - 42
24 - 32
18 - 24
13 - 18
10 - 13
7.5 - 10
5.6 - 7.5
4.2 - 5.6
3.2 - 4.2
2.4 - 3.2
1.8 - 2.4
1.3 - 1.8
1.0 - 1.3
< 1.0
Marine Geospatial Ecology Lab

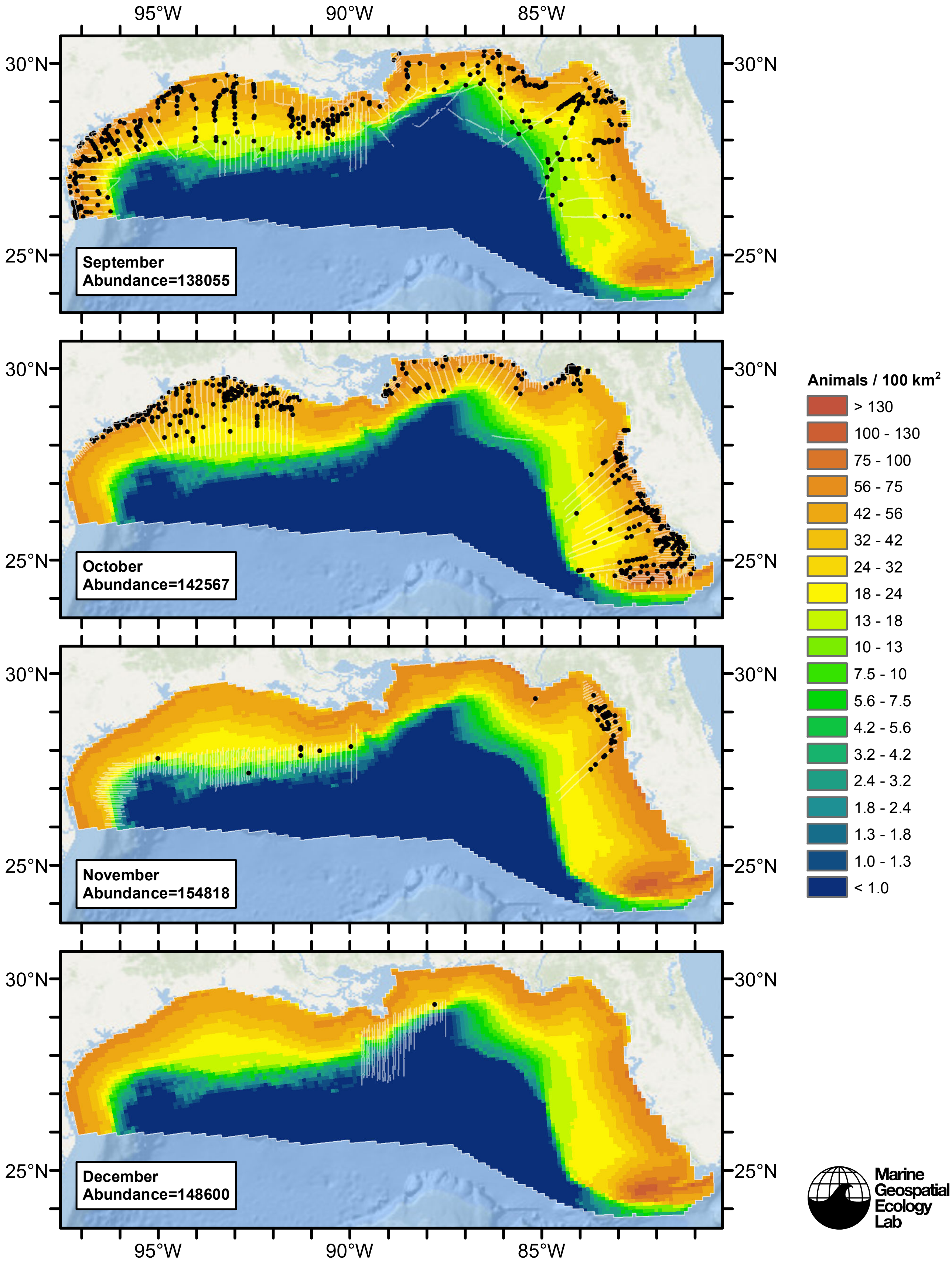
95°W
90°W
85°W
30°N
25°N
September
Abundance=138055
October
Abundance=142567
November
Abundance=154818
December
Abundance=148600
Animals / 100 km²
> 130
100 - 130
75 - 100
56 - 75
42 - 56
32 - 42
24 - 32
18 - 24
13 - 18
10 - 13
7.5 - 10
5.6 - 7.5
4.2 - 5.6
3.2 - 4.2
2.4 - 3.2
1.8 - 2.4
1.3 - 1.8
1.0 - 1.3
< 1.0
Marine
Geospatial
Ecology
Lab

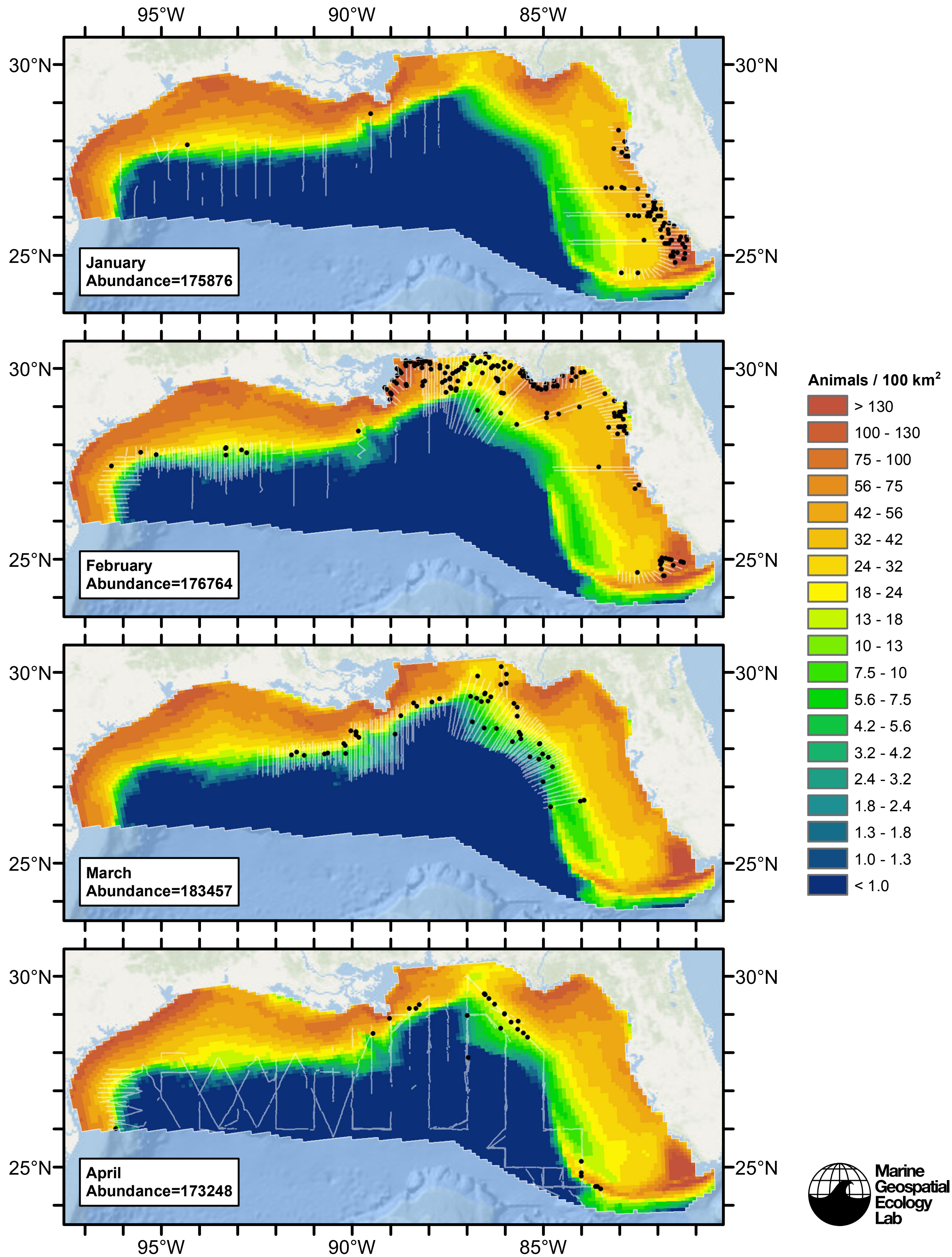
95°W
90°W
85°W
30°N
25°N
January
Abundance=175876
February
Abundance=176764
March
Abundance=183457
April
Abundance=173248
Animals / 100 km²
> 130
100 - 130
75 - 100
56 - 75
42 - 56
32 - 42
24 - 32
18 - 24
13 - 18
10 - 13
7.5 - 10
5.6 - 7.5
4.2 - 5.6
3.2 - 4.2
2.4 - 3.2
1.8 - 2.4
1.3 - 1.8
1.0 - 1.3
< 1.0
Marine Geospatial Ecology Lab

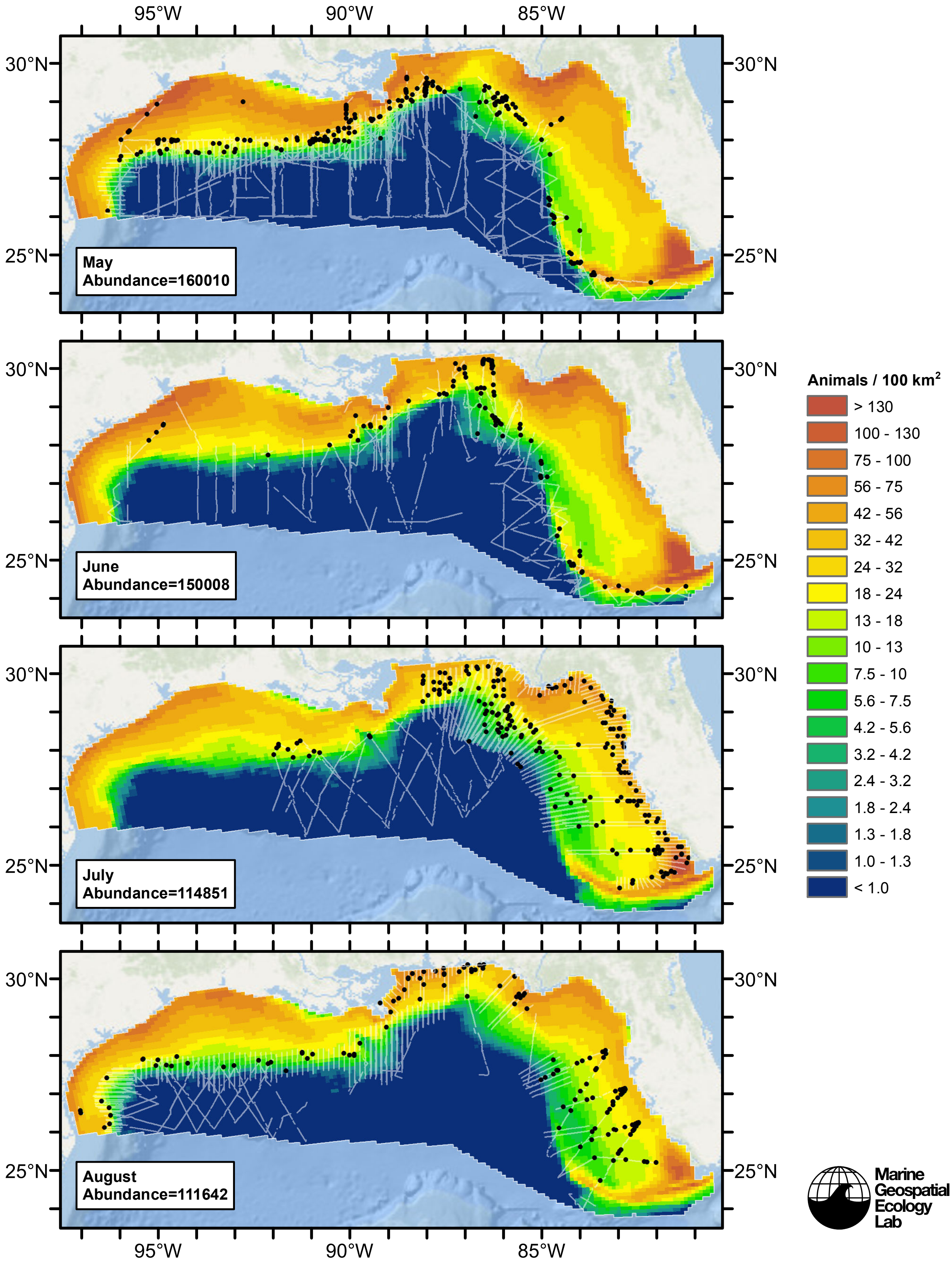

Marine Geospatial Ecology Lab

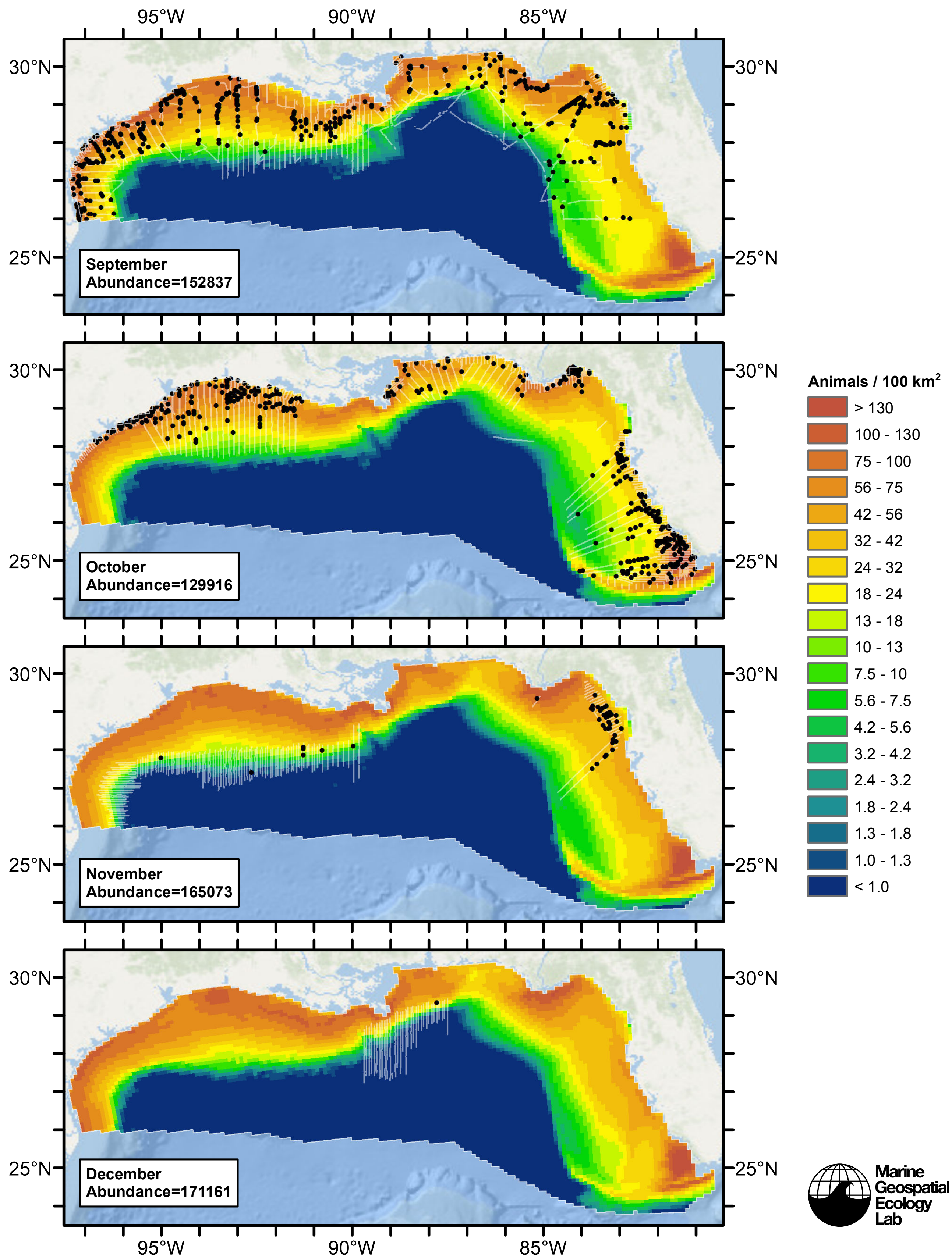
95°W
90°W
85°W
30°N
25°N
September
Abundance=152837
October
Abundance=129916
November
Abundance=165073
December
Abundance=171161
Animals / 100 km²
> 130
100 - 130
75 - 100
56 - 75
42 - 56
32 - 42
24 - 32
18 - 24
13 - 18
10 - 13
7.5 - 10
5.6 - 7.5
4.2 - 5.6
3.2 - 4.2
2.4 - 3.2
1.8 - 2.4
1.3 - 1.8
1.0 - 1.3
< 1.0
Marine Geospatial Ecology Lab

Discussion

Models fitted with climatological estimates of dynamic predictors consistently explained more deviance than models fitted with contemporaneous estimates (Table 19). However, the best climatological models and the best contemporaneous model predicted very similar spatial distributions (Fig. 58) and mean abundances estimates fell within 10% of each other (Table 20). Because the contemporaneous model selected a productivity-related covariate (zooplankton potential biomass, PkPB) that was only available after the launch of the SeaWiFS satellite in late 1997, 67% of the survey segments were lost from the model because they did not have a value for this covariate. Because climatological covariates offered more explanatory power and did not result in loss of survey data, we selected the climatological model that was fitted to all segments as our best estimate of bottlenose dolphin distribution and abundance in the northern Gulf of Mexico.

The survey effort used as input to our models was biased toward spring and summer and was spatiotemporally patchy (see maps in the Temporal Variability section above), thus we were not confident that any of our models could produce realistic predictions at a monthly temporal resolution. This effort bias problem affected all species that we modeled in the Gulf of Mexico, and we recommend that year-round average predictions be used for all Gulf of Mexico species.

At the time of this writing, NMFS's most recent abundance estimates for the three coastal stocks and the continental shelf stock were available in the draft 2015 stock assessment report (Waring et al. 2015), which was still under formal public review. These estimates came from an EEZ-wide aerial survey conducted in spring, summer, and fall of 2011 and winter of 2012. This survey was not available from NMFS to be incorporated into our models, thus it offers completely independent estimates. Although this survey covered all four seasons, NMFS produced year-round average estimates, explaining: "Due to the uncertainty in stock movements and apparent seasonal variability in the abundance of the [stocks], a weighted average of these seasonal estimates was taken where the weighting was the inverse of the CV." (Waring et al. 2015). Adding these four estimates to the most recent oceanic stock estimate, from a shipboard survey in 2009 (Waring et al. 2013) gives a total abundance of 96,732 (Table 20). From NMFS's per-stock CVs, we estimated the CV of the aggregate abundance to be 0.07 (assuming independence and adding standard errors in quadrature).

In comparison, our climatological model estimated a total abundance of 138,602, also with a low CV of 0.06. Initially, it would appear that our estimate and NMFS's are significantly different. To consider this question in more detail, we shall focus on the coastal and continental-shelf stocks, which contain nearly all of the total abundance. Waring et al. (2015) stated that NMFS estimated variance by bootstrap resampling. Although no more details were provided, we presume the bootstrap accounted for uncertainty in both the detection functions, the correction for perception bias, and the abundance estimator. In comparison, our model only accounted for uncertainty in the abundance estimation stage (specifically, in the GAM parameter estimates). By not accounting for uncertainty in the detection functions or the g(0) estimate that corrected for perception bias, we underestimated uncertainty.

As noted in our paper, extant statistical methods did not provide a way to estimate uncertainty for models as complex as ours except via bootstrapping, but we lacked the computational resources to attempt a bootstrap for our large and complex model in the time available for the project. But in the case of this bottlenose dolphin model, we can offer a rough alternative. The detection functions utilized in this model had CVs ranging from 0.124-0.136 for shipboard surveys and 0.055-0.101 for aerial surveys. Most of the sightings were of small groups; the CVs of the g(0) estimates for small groups were 0.056 for shipboard sightings and 0.37 for aerial sightings. Using the delta method for combining uncertainties (Buckland et al. 2001), CVs that account for all three modeling stages would be roughly 0.15-0.16 for shipboard surveys and 0.39-0.40 for aerial surveys. The CV of our final abundance estimate likely falls between the shipboard and aerial CV estimates. Even if it fell closer to the shipboard CV than the aerial CV, the resulting lower 95% confidence interval would probably still enclose NMFS's abundance estimate, suggesting that our estimate was not significantly different from theirs.

We intend to secure the computational resources necessary to run a bootstrap in the next scheduled major revision of our model. At that point we will be able to discuss the differences between our result and NMFS's with greater confidence and precision. Ideally, we would also incorporate NMFS's 2011-2012 surveys into our revision. One potentially important consideration between our current estimate and NMFS's is that the surveys used in our model were all conducted prior to the Deepwater Horizon oil spill while the survey used in NMFS's was conducted after it. Evidence suggests this event had a substantial deleterious effect on at least one estuarine bottlenose dolphin stock (Schwacke et al. 2014). To our knowledge, the effects of the event on the coastal and oceanic stocks of bottlenose dolphins are unknown. We speculate that the oil spill likely resulted in mortalities in some of those stocks, but without more study we cannot guess whether this would explain some of the difference between pre-spill abundance estimates (such as ours) and post-spill estimates (such as NMFS's).

In any case, at the time of this writing we consider our predicted density surface to be the best available map of bottlenose dolphin density suitable for marine spatial planning applications in the northern Gulf of Mexico. While our model does not directly provide per-stock estimates, NOAA defines stock boundaries based on specific bathymetric and geographic limits, allowing per-stock density surfaces to be obtained from our single surface by splitting it up using a GIS.

References

Barlow J, Forney KA (2007) Abundance and density of cetaceans in the California Current ecosystem. Fish. Bull. 105: 509-526.

Carretta JV, Lowry MS, Stinchcomb CE, Lynn MS, Cosgrove RE (2000) Distribution and abundance of marine mammals at San Clemente Island and surrounding offshore waters: results from aerial and ground surveys in 1998 and 1999. Administrative Report LJ-00-02, available from Southwest Fisheries Science Center, P.O. Box 271, La Jolla, CA USA 92038. 44 p.

Hiby L (1999) The objective identification of duplicate sightings in aerial survey for porpoise. In: Marine Mammal Survey and Assessment Methods (Garner GW, Amstrup SC, Laake JL, Manly BFJ, McDonald LL, Robertson DG, eds.). Balkema, Rotterdam, pp. 179-189.

Palka DL (2006) Summer Abundance Estimates of Cetaceans in US North Atlantic Navy Operating Areas. US Dept Commer, Northeast Fish Sci Cent Ref Doc. 06-03: 41 p.

Schwacke LH, Smith CR, Townsend FI, Wells RS, Hart LB, et al. (2014) Health of bottlenose dolphins (Tursiops truncatus) in Barataria Bay, Louisiana following the Deepwater Horizon oil spill. Environ. Sci. Technol. 48(1): 93-103.

Vollmer NL, Rosel PE (2013) A Review of Common Bottlenose Dolphins (Tursiops truncatus truncatus) in the Northern Gulf of Mexico: Population Biology, Potential Threats, and Management. Southeastern Naturalist 12: 1-43.

Waring GT, Josephson E, Maze-Foley K, Rosel PE, eds. (2013) U.S. Atlantic and Gulf of Mexico Marine Mammal Stock Assessments – 2012. NOAA Tech Memo NMFS NE 223; 419 p.

Waring GT, Josephson E, Maze-Foley K, Rosel PE, eds. (2015) U.S. Atlantic and Gulf of Mexico Marine Mammal Stock Assessments – 2015: Atlantic, Gulf, and Caribbean Draft Report. Available at: http://www.nmfs.noaa.gov/pr/sars/draft.htm. Accessed October 8, 2015.